AD-A087 426   AIR FORCE WRIGHT AERONAUTICAL LABS WRIGHT-PATTERSON AFB OH   F/6 1/2
IN-FLIGHT EVALUATION OF A SEVERE WEATHER AVOIDANCE SYSTEM FOR A--ETC(U)
MAY 80   R K BAUM, T J SEYMOUR   FAA/ARD-740

UNCLASSIFIED   AFWAL-TR-80-3022   NL

1 2

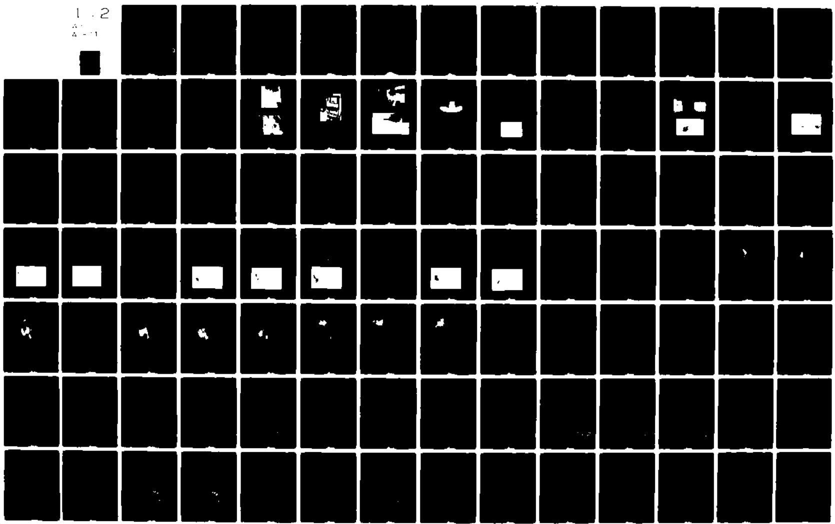

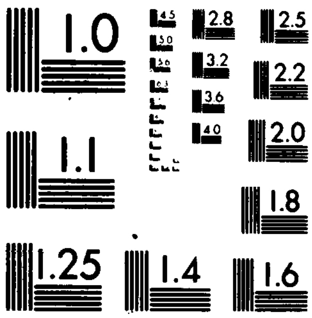

MICROCOPY RESOLUTION TEST CHART
NATIONAL BUREAU OF STANDARDS 1963-A

JL

AFWAL-TR-80-3022

LEVEL II

(2)

ADA087426

IN-FLIGHT EVALUATION OF A SEVERE WEATHER AVOIDANCE SYSTEM FOR AIRCRAFT

ROBERT K. BAUM, CAPTAIN, USAF
TIMOTHY J. SEYMOUR

FLIGHT VEHICLE PROTECTION BRANCH
VEHICLE EQUIPMENT DIVISION

MAY 1980

Approved for public release; distribution unlimited.

FLIGHT DYNAMICS LABORATORY
AIR FORCE WRIGHT AERONAUTICAL LABORATORIES
AIR FORCE SYSTEMS COMMAND
WRIGHT-PATTERSON AIR FORCE BASE, OHIO 45433

80 8 1 091

NOTICE

When Government drawings, specifications, or other data are used for any purpose other than in connection with a definitely related Government procurement operation, the United States Government thereby incurs no responsibility nor any obligation whatsoever; and the fact that the Government may have formulated, furnished, or in any way supplied the said drawings, specifications, or other data, is not to be regarded by implication or otherwise as in any manner licensing the holder or any other person or corporation, or conveying any rights or permission to manufacture, use, or sell any patented invention that may in any way be related thereto.

This report has been reviewed by the Office of Public Affairs (ASD/PAS) and is releasable to the National Technical Information Service (NTIS). At NTIS, it will be available to the general public, including foreign nations.

This technical report has been reviewed and is approved for publication.

The Air Force does not sanction or advertise the product used in the test described herein.

Timothy J. Seymour

TIMOTHY J. SEYMOUR
Test Engineer
Atmospheric Electricity Hazards Group

Gary A. Dubro

GARY A. DUBRO, Chief
Atmospheric Electricity
Hazards Group

Ambrose B. Nutt

AMBROSE B. NUTT
Director
Vehicle Equipment Division

Copies of this report should not be returned unless return is required by security considerations, contractual obligations, or notice on a specific document.

SECURITY CLASSIFICATION OF THIS PAGE (When Data Entered)

REPORT DOCUMENTATION PAGE

READ INSTRUCTIONS BEFORE COMPLETING FORM

1. REPORT NUMBER: 14 AFWAL-TR-80-3022	2. GOVT ACCESSION NO.: AD87426
3. RECIPIENT'S CATALOG NUMBER	
4. TITLE (and Subtitle): 6 IN-FLIGHT EVALUATION OF A SEVERE WEATHER AVOIDANCE SYSTEM FOR AIRCRAFT,	5. TYPE OF REPORT & PERIOD COVERED: 9 Final rept.,
	6. PERFORMING ORG. REPORT NUMBER
7. AUTHOR(s): 10 Robert K. Baum, Captain, USAF Timothy J. Seymour	8. CONTRACT OR GRANT NUMBER(s)
9. PERFORMING ORGANIZATION NAME AND ADDRESS: Flight Dynamics Laboratory (AFWAL/FIES) AF Wright Aeronautical Laboratories Wright-Patterson AFB, OH 45433	10. PROGRAM ELEMENT, PROJECT, TASK AREA & WORK UNIT NUMBERS: 16 Program Element 62201F Project 2402 Task 240202 Work Unit 24020223
11. CONTROLLING OFFICE NAME AND ADDRESS: Flight Dynamics Laboratory (AFWAL/FIE) AF Wright Aeronautical Laboratories Wright-Patterson AFB, OH 45433	12. REPORT DATE: 11 May 1980 17
	13. NUMBER OF PAGES: 128
14. MONITORING AGENCY NAME & ADDRESS (if different from Controlling Office): 15 FAA/ARD-740 12 128	15. SECURITY CLASS. (of this report): Unclassified
	15a. DECLASSIFICATION/DOWNGRADING SCHEDULE

16. DISTRIBUTION STATEMENT (of this Report)

Approved for public release; distribution unlimited.

17. DISTRIBUTION STATEMENT (of the abstract entered in Block 20, if different from Report)

18. SUPPLEMENTARY NOTES

19. KEY WORDS (Continue on reverse side if necessary and identify by block number)

Severe weather	LDAR
Thunderstorm	RF radiation
Lightning	Radar

Since there is increased

20. ABSTRACT (Continue on reverse side if necessary and identify by block number)

An increased awareness of the number of flight mishaps attributable to lightning and thunderstorms has produced interest in severe weather avoidance systems to augment conventional radar. ~~A~~ joint flight program was ~~therefore~~ undertaken ~~by FDL, 4950th TW, and FAA~~ to evaluate the Ryan Stormscope as a thunderstorm avoidance tool. Comparisons were made between Stormscope electrical activity areas and precipitation contours from both on-board and ground weather radar displays. Strongest correlation between Radar and Stormscope

DD FORM 1 JAN 73 1473 EDITION OF 1 NOV 65 IS OBSOLETE

SECURITY CLASSIFICATION OF THIS PAGE (When Data Entered)

392662

(cont)

was found in regions of high precipitation gradients (i.e., first-third level interface boundaries). Comparisons were also made between Stormscope and a ground-based Lightning Detection and Ranging System (LDAR) to determine range and azimuth accuracy of the electrical activity displayed on Stormscope. Because of inherent differences ~~between~~ among these systems (i.e., type and rate of data acquisition), corresponding groups of electrical activity areas were compared rather than a point-by-point comparison made. Items compared were group area ratios, group overlap areas and group centroid locations. In general, Stormscope groups were larger than corresponding LDAR groups (150% on the average). Additionally, Stormscope group centroid locations differed an average of 15 NM in range and 11 deg~~rees~~ in azimuth from those on the LDAR system. This margin of error ~~however,~~ is acceptable for in-flight thunderstorm avoidance.

FOREWORD

This report was prepared by the Atmospheric Electricity Hazards Group, Flight Vehicle Protection Branch, Vehicle Equipment Division, Air Force Flight Dynamics Laboratory, Wright Patterson Air Force Base, Ohio. The experimental program was conducted under work unit number 24020223, "Atmospheric Electricity Hazards to Aircraft". Partial funding was provided by the Federal Aviation Administration by an addition to interagency agreement ARD-740, between the FAA and the AFFDL.

The tests were performed during July, 1978 at Patrick AFB, Florida under the direction of Timothy J. Seymour, Program Manager, and Lt. Robert K. Baum, Test Engineer. Equipment installation and test support were provided by the 4950th Test Wing, Wright-Patterson AFB, under the direction of Larry A. Roberts, Flight Test Engineer, and Capt. Lee O. Singer, Chief of Operations Plans Branch.

Contract support was provided by Jean Reazer and Martin D. Risley of Technology/Scientific Services, Incorporated.

The authors would particularly like to thank Angelo Taiani, Project coordinator for TRIP-78, Carl Lennon, Chief, Launch Systems Operation Section, Kennedy Space Center, and Jesse Gullick and James Nicholson of the Kennedy Space Center Weather Station for their assistance during this program.

TABLE OF CONTENTS

LIST OF ILLUSTRATIONS

FIGURE		PAGE
B-8	Comparison of LDAR and Stormscope Electrical Activity, Run 4, 26 July 1978	
	a. LDAR Electrical Activity	102
	b. Centroids of LDAR Electrical Activity	103
	c. Stormscope Electrical Activity	104
	d. Centroids of Stormscope Electrical Activity	105
C-1	Overlap Areas - LDAR vs Stormscope Run 1, 25 July 1978	107
C-2	Overlap Areas - LDAR vs Stormscope Run 2, 25 July 1978	108
C-3	Overlap Areas - LDAR vs Stormscope Run 3, 25 July 1978	109
C-4	Overlap Areas - LDAR vs Stormscope Run 4, 25 July 1978	110
C-5	Overlap Areas - LDAR vs Stormscope Run 1, 26 July 1978	111
C-6	Overlap Areas - LDAR vs Stormscope Run 2, 26 July 1978	112
C-7	Overlap Areas - LDAR vs Stormscope Run 3, 26 July 1978	113
C-8	Overlap Areas - LDAR vs Stormscope Run 4, 26 July 1978	114
	ADDENDUM	
A	Stormscope, Radar, and Time Code Generator Displays Prior to Corona Condition	115
B	Effect of Corona on Stormscope, Radar, and Time Code Generator Displays	115
C	Effect of Corona on Stormscope, Radar, and Time Code Generator Displays	116
D	Effect of Corona on Stormscope, Radar, and Time Code Generator Displays	116
E	Strip Chart from Flight Recorder	116

LIST OF TABLES

SECTION I

INTRODUCTION

1. Purpose

The Ryan Stormscope^{TM} was evaluated to determine its capability to identify thunderstorm activity with sufficient accuracy to permit use as an inflight lightning and severe weather avoidance system. Stormscope^{TM} is a registered trademark of Ryan Stormscope, Columbus, Ohio.

2. Scope

The Stormscope was evaluated for 1) range and azimuth accuracy of discharge location, and 2) correlation between the displayed regions of electrical activity and turbulent weather formations. Range and azimuth accuracy were evaluated by comparing (numerically and visually) Stormscope vs. LDAR location of activity region boundaries and centroids. Turbulent weather correlation was accomplished by visually comparing Stormscope activity regions to the time behavior of precipitation contours displayed on ground and airborne weather radar.

SECTION II

BACKGROUND

Records indicate that during the five year period from 1970 to 1975, weather related flight mishaps resulted in a total economic loss to the Air Force of approximately $15 million (see Table 1).

CAUSES AND COSTS OF USAF WEATHER MISHAPS, 1970-75

Causes	%	Resources (K)
Lightning	55	7300
Hail	9	200
Icing	8	7800
Turbulence	8	63
Rain	5	20
Other	15	

Table 1. Causes and Costs of USAF Weather Mishaps

Perhaps even more unsettling is the fact that this mishap rate shows a steady increase over the same period, starting in 1970 with 1 mishap/64000 flight hours and climbing to 1 mishap/20000 flight hours in 1975 (see Figure 1)[1]. Although declining since, the rate is still approximately 1 mishap/33000 flight hours.

Lightning is by far the most frequent cause of significant weather mishaps, accounting for more than one-half of the total recorded incidents. Frequently, the occurrence of lightning in a weather formation indicates the presence of other violent atmospheric conditions such as hail, icing and turbulence[2], all of which pose significant threats to the safety of flight.

Detection of hazardous atmospheric conditions cannot, at present, be accomplished with absolute certainty. There are, however, certain remote observations which can provide limited severe weather avoidance capability, the most familiar of which is the precipitation contour mapping provided by weather radar. This observation technique is far from perfect however, being

influenced by many atmospheric aberrations and requiring substantial training for proper operation and display interpretation.

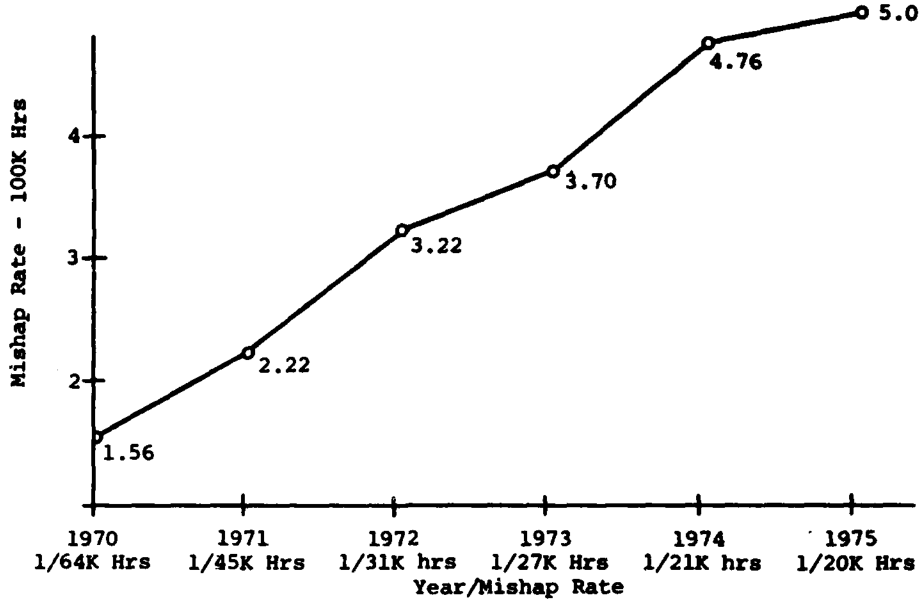

Figure 1. Weather Related Mishap Rate-USAF Aircraft

Another example of observable phenomena indicative of severe weather is atmospheric electrical activity. A turbulent atmosphere tends to cause electrical charge separation which can result in air breakdown and electrical discharge.[7] These electrical discharges emit broadband electromagnetic radiation of sufficient intensity for remote detection. The Lightning Detection and Ranging (LDAR) system at Kennedy Space Center (KSC) detects this type of radiation at four widely separated stations and, by measuring wavefront time-of-arrival at each station, determines location of the discharge.

The Ryan Stormscope[3], which recently became available, also detects electromagnetic radiation as does LDAR but at a much lower frequency. It uses automatic direction finding (ADF) and sense antennas along with some waveform processing techniques to determine the position of the discharge relative to the aircraft.

This system is unique among the several lightning detection devices available in that it was developed specifically for airborne application. Because of Stormscope's possible application as a severe weather avoidance aid on military aircraft, a research program was developed to evaluate its performance in comparison to LDAR and to airborne weather radar systems.

In 1977 the Air Force Flight Dynamics Laboratory and the 4950th Test Wing conducted a joint test program to evaluate the Ryan Stormscope[4]. The results of this study were inconclusive due to transient noise problems encountered in the Stormscope ADF antenna. It was determined, however, that the results warranted further evaluation of the Stormscope system, and partial funds for further testing were provided by the Federal Aviation Administration. In 1978, the program was again directed by the Flight Dynamics Laboratory while the 4950th Test Wing provided test engineering. The same T-39B aircraft used in the previous program was used as the test bed. The flight test phase of the program took place at Patrick Air Force Base from 5 July to 27 July 1978 and was planned to coincide with the Thunderstorm Research International Program-1978 (TRIP-78). This location was chosen for two principal reasons: 1) high level of isolated thunderstorm activity, and 2) availability of the LDAR system. The ground based LDAR system provided range and azimuth of known accuracy[5] to the electrical activity occurring during the thunderstorm for independent comparison with Stormscope indications.

SECTION III

AIRCRAFT EQUIPMENT INSTALLATION AND DESCRIPTION

1. General

Figure 2 illustrates the equipment installation locations on the aircraft.

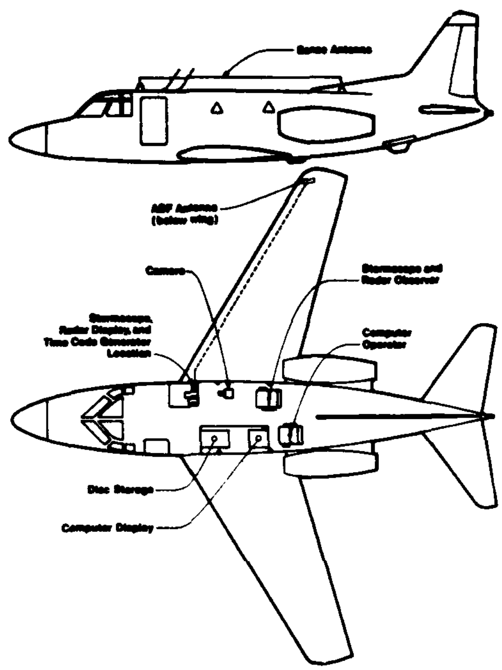

Figure 2. Location of the Test Equipment on T39-B Aircraft

The Stormscope, weather radar, and time code generator were installed in an equipment rack in the cargo/passenger compartment of the aircraft as shown in Figure 3. A timer-controlled 35 mm camera was mounted on the right side of the aircraft to provide a simultaneous photographic record of the Stormscope, weather radar, and time code generator displays (Figure 4).

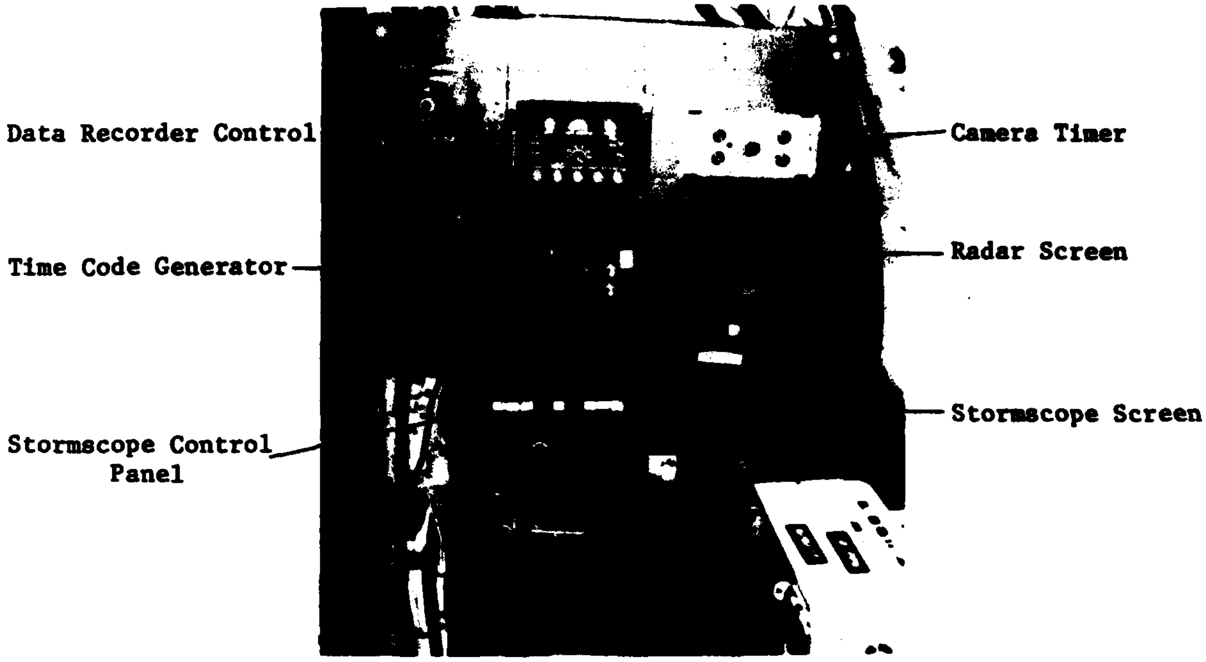

Figure 3. Stormscope, Weather Radar, and Time Code Generator

Figure 4. Camera Installation for Recording Stormscope, Weather Radar, and Time Code Generator Displays

The data acquisition and storage system for storing the raw Stormscope data was installed on the left side of the aircraft as shown in Figure 5.

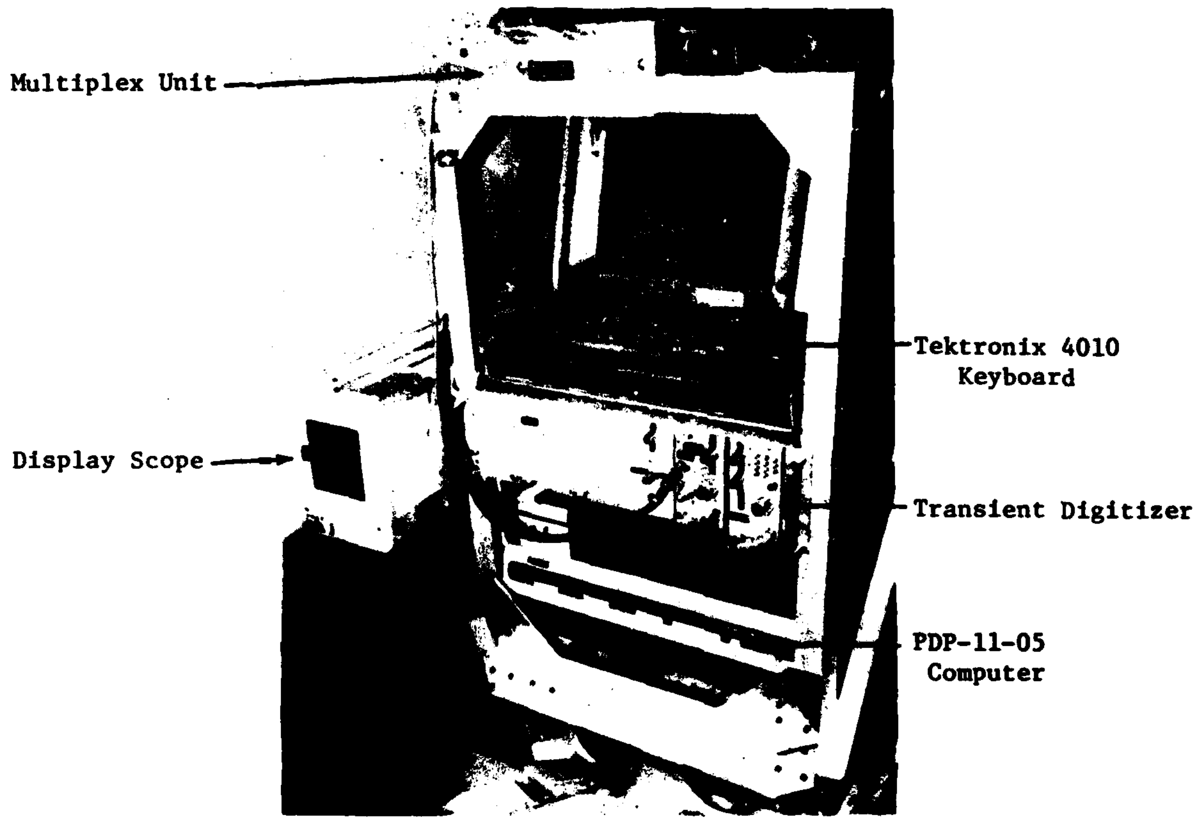

Figure 5. Data Acquisition System Used to Inηut, View and Store Stormscope Data

The crossed loop (ADF) type antenna for the Stormscope was installed on the lower right wing tip (Figure 6). The sense antenna for the Stormscope was a 13 foot wire antenna mounted on top of the fuselage (Figure 7.)

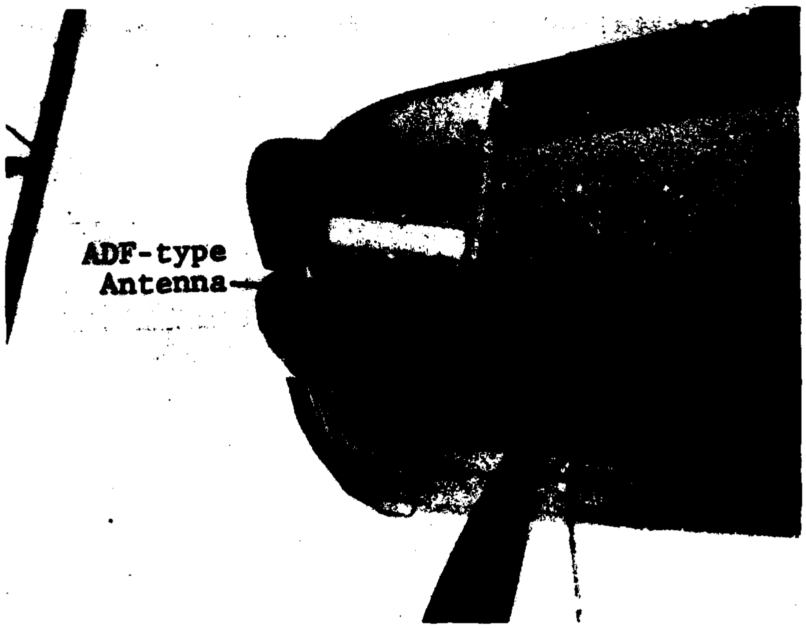

Figure 6. ADF-type Antenna Installation for Stormscope

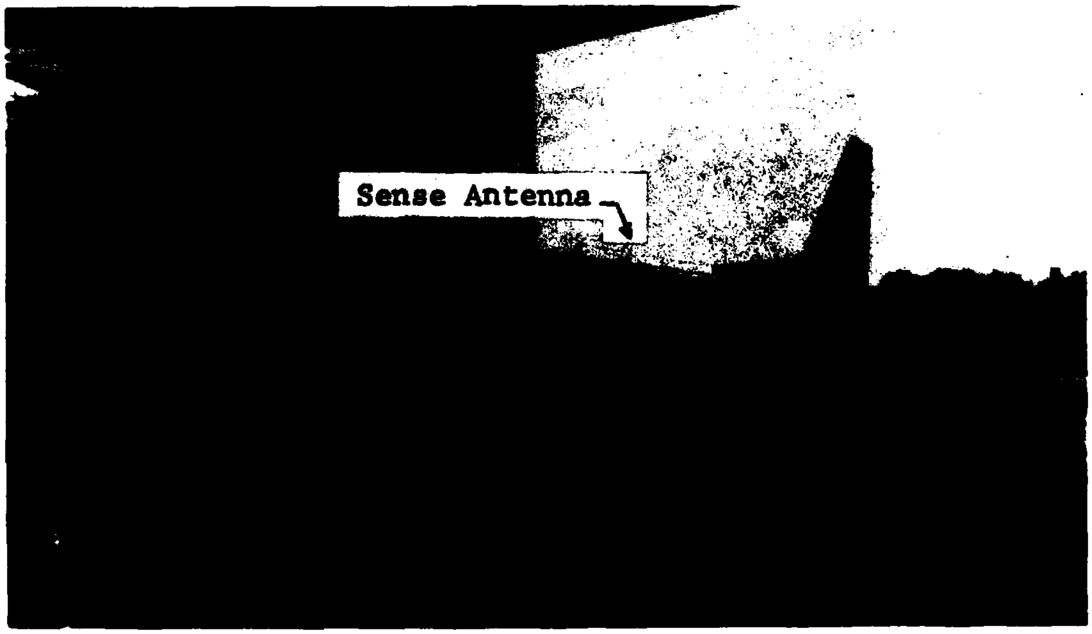

Figure 7. Stormscope Wire Sense Antenna Installation above Fuselage

2. Equipment Description

a. Stormscope System

The Ryan Stormscope (Figure 8) is a three-component, solid-state receiving system designed to detect the bearing and range of electrical disturbances in the 50 KHz frequency region at up to 230 nautical miles from the aircraft over a 360° scan.

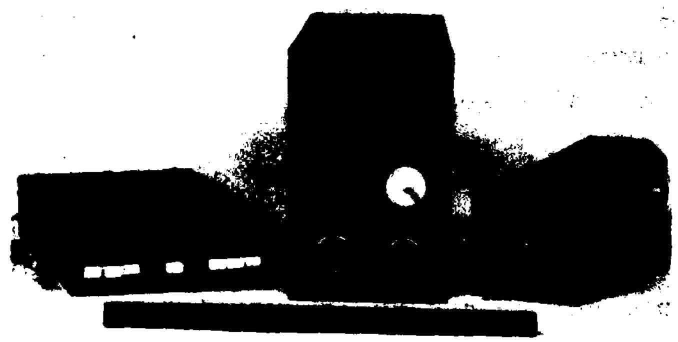

Figure 8. Stormscope Components-Receiver, Central Processing Unit, and Display

The magnetic and electric field components of the electrical discharge radiation are detected by the crossed loop ADF antenna and the wire sense antenna respectively. (Newer versions of the Stormscope system use a single flat pack antenna incorporating both of these functions in a single package.) These signals are routed to the central processing unit for determination of discharge location. Azimuth of the discharge is determined from the ratio of the two crossed loop antenna inputs. Inherent azimuth ambiguity caused by random changes in discharge polarity is resolved by the sense antenna input. Range of the discharge is also derived from the crossed loop antenna based upon the assumption that in the far-field region, (i.e. observation distance much greater than lightning channel length) the magnetic field intensity is

relatively constant from discharge to discharge and is inversely proportional to distance from the discharge. The time domain signature of the magnetic field (i.e. rise time, decay time) is used to modify this basic range computation, thereby reducing error caused by intensity variations from discharge to discharge. To enhance noise rejection capability, the processor unit performs a correlation of the electric and magnetic field waveforms, a high correlation being characteristic of valid far-field discharge radiation.

Each discharge is stored in one of the 128 available memory locations and is subsequently displayed on the CRT monitor. When the 129th discharge event occurs, the oldest event is erased from memory and the newest takes its place.

The CRT has an overlay consisting of a compass rose, two concentric range circles and a small aircraft outline in the center. The range can be varied by pushing a button on the unit so that the circles represent 20 and 40, 50 and 100 or 100 and 200 nautical miles, respectively. The CRT can be erased at any time by pushing the clear button, a process which requires four seconds and begins with the oldest events first. Partial erasure can be obtained by holding the button down for a shorter time. Figure 9 illustrates a typical Stormscope display.

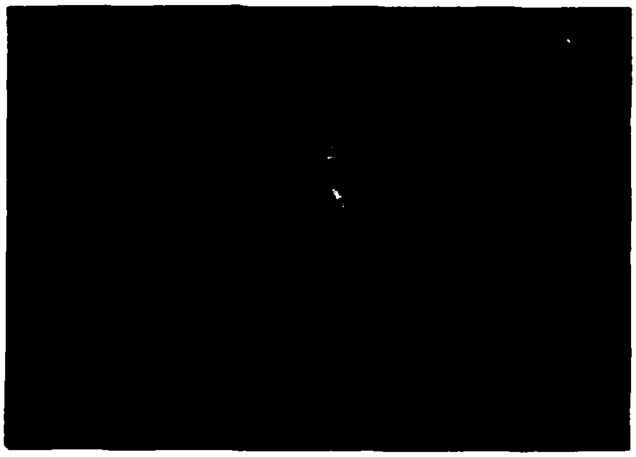

Figure 9. Typical Stormscope Display

Since the location of each electrical discharge is displayed relative to the aircraft as stored in the memory, the CRT will continue to display the information in the same location until the memory is erased or the 129th event occurs. Changes in heading and position of the aircraft will not affect those dots already displayed; consequently, if the electrical activity is low, periodic clearing is necessary to maintain an accurate presentation with respect to the changing position of the aircraft in flight.

b. Onboard Data Acquisition System

The diagram in Figure 10 illustrates the AFFDL system and interface used to input, analyze and store the Stormscope data.

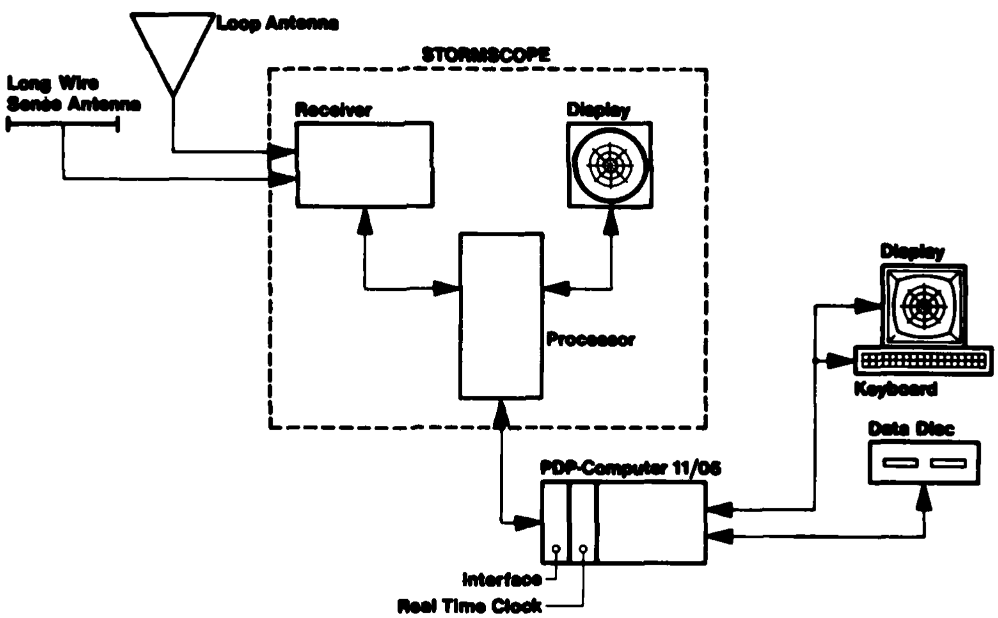

Figure 10. Instrumentation System Used to Input, Analyze, and Store Stormscope Data

The Stormscope used for the flight tests was modified by the manufacturer to output the X and Y coordinates of a given electrical discharge to a buffer for subsequent processing. An interface was constructed to bring the coordinate data from the buffer register into the PDP 11/05 computer system where it was permanently stored together with the signal acquisition time on flexible disc medium. Software was written to generate an updated visual display for inflight analysis.

c. Airborne Weather Radar System

The onboard weather radar system used was a Bendix RDR-1300, 10 kilowatt, X-band unit. The three components of the system are a nose-mounted line-of-sight flat plate antenna, a remote-mounted receiver-transmitter unit and a panel-mounted rectangular screen digital display. Digital techniques are used to display real time information and alphanumeric data on the radar screen. The readout indicates the mode of operation, range and range mark intervals (nautical miles). The system has a contour mode (Weather A) which is used to detect areas of heavy precipitation. The maximum field of view for the system is 120° forward. The system components are illustrated in Figure 11. A typical weather radar display for the weather A mode and 80 nautical mile range is shown in Figure 12.

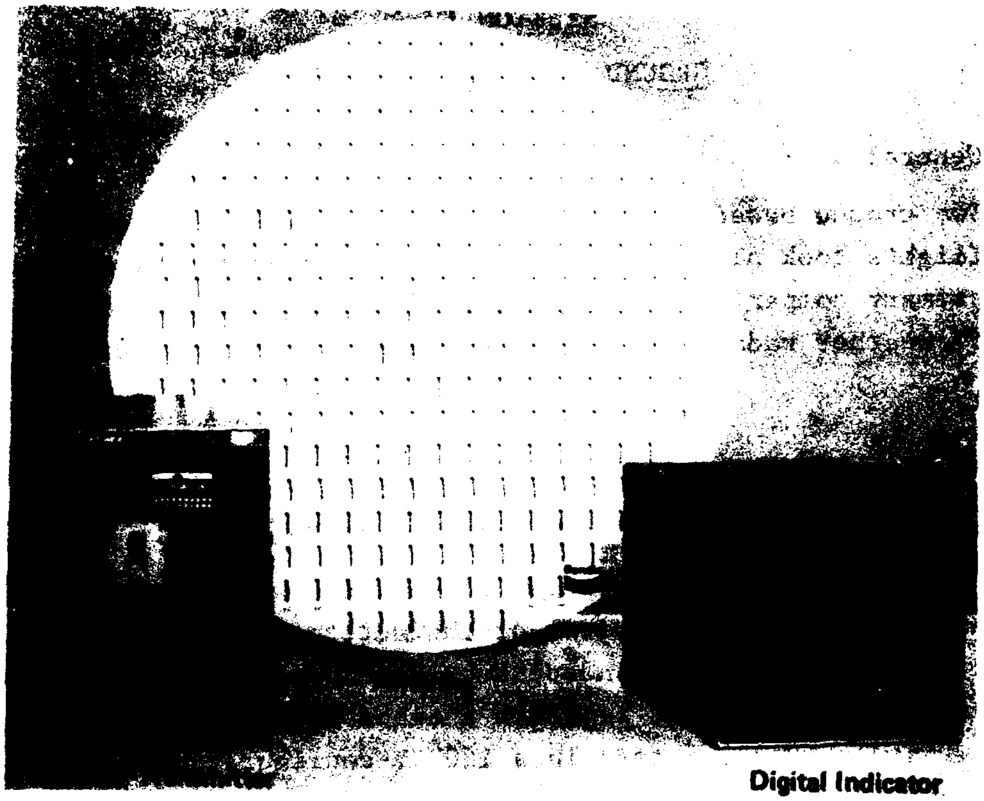

Figure 11. Onboard Weather Radar System Components

Figure 12. Typical Weather Radar Display-Weather A Mode and 80 Nautical Mile Range

SECTION IV

GROUND REFERENCE SYSTEMS

1. General

Two ground based systems that were available in the area where the flights took place were used as Stormscope comparison sources. The primary comparison system was LDAR, while two ground-based WSR-57 weather radars provided alternate sources of useful information.

2. Equipment Description

a. Lightning Detection and Ranging System (LDAR)

The LDAR system computes discharge location by measuring differences in time of arrival of characteristic pulsed RF radiation (60-80 MHz) at two independent receiving networks. Each network consists of four separate antenna sites each separated approximately 10 kilometers in a 120° Y-configuration. The separate networks provide some protection against erroneous data points. In operation, data points are rejected if the network measurements differ by more than 10%. Extensive testing of LDAR[5] indicates a typical accuracy much better than 10%, however. At a 40 NM radius from the central LDAR site, range accuracy is approximately ± 2 NM and azimuth accuracy $\pm \frac{1}{2}^{\circ}$. A typical LDAR display is shown in Figure 13. Additional information on LDAR operation may be found in References 5 and 6.

b. Ground Weather Radar System

Ground weather radar pictures were obtained initially from the weather station at the Daytona Beach Regional Airport, approximately 35 miles northeast of the LDAR site. When a review of these photographs showed that equipment malfunctions had occurred during several times of interest, supplemental pictures were obtained from a weather station near Tampa. The Tampa station is located approximately 105 miles southwest of the LDAR site. A typical ground based weather radar display is shown in Figure 14.

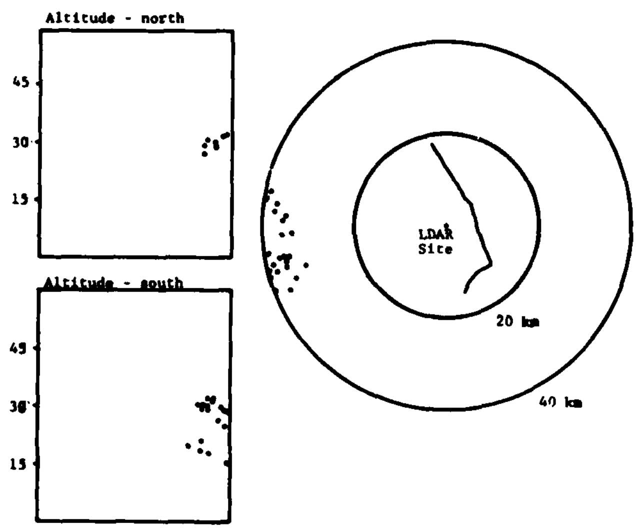

Figure 13. Typical LDAR Display Used for Vectoring Aircraft to Lightning Activity

Figure 14. Typical Ground Weather Radar Photograph

SECTION V

SUMMARY OF EQUIPMENT CHARACTERISTICS

Presumably, an ideal severe weather detection system would: 1) provide highly accurate information at any range and azimuth of interest, 2) use only simple, passive components, and 3) require a minimum of weight, power, space and maintenance. Of course, realistically, the Stormscope, weather radar and LDAR systems each represent, in varying degree, a design compromise between accuracy required and complexity allowed for a given application. Table 2 summarizes some of the major operational differences between the systems.

	STORMSCOPE	WEATHER RADAR	LDAR
OPERATION	PASSIVE 50 KHZ COMPONENT OF DISCHARGE	ACTIVE X-BAND (9375 MHZ) PRECIPITATION ECHOES	PASSIVE 60-80 MHZ COMPONENT OF DISCHARGE
FIELD OF VIEW	360°	120°	360°
MAXIMUM RANGE	230 NM	240 NM	>200 NM
ANTENNAS REQUIRED	1. FLAT PACK (ADF-TYPE) 2. SENSE (WHIP)- SEE NOTE 1	FLAT PLATE PHASED ARRAY WITH MECHANICAL ROTATION	SIX SITES SEPARATED AT LEAST 5 NM
WEIGHT	16 LB	33 LB	N/A
POWER (WATTS)	50	98	N/A
MTBF*	3300	1500 (NOTE 2)	N/A

NOTE 1: LATER MODELS INCORPORATE BOTH ANTENNAS IN A SINGLE FLAT PACK.

NOTE 2: MANUFACTURER'S ESTIMATE-NO FIELD DATA EXISTS. MTBF FOR SPERRY APN 59-B IS 20-25 HOURS.

*Mean Time Between Failures

Table 2. Summary of Equipment Characteristics

SECTION VI

PROCEDURES

AFFDL personnel attended daily weather briefings sponsored by TRIP 78 at the Kennedy Space Center to obtain information on probable thunderstorm activity. When thunderstorms were expected, the LDAR display was activated at the KSC weather station and monitored for electrical activity. If activity was present and equipment operating properly, a mission was flown to collect data.

During the mission, direct communications were maintained by the flight crew, test personnel onboard the aircraft, and the ground weather station to vector the aircraft to areas of weather activity. In general, the aircraft flew straight leg vectors directly toward or away from the activity at distances between 20 and 70 miles from the storm center. Figure 15 illustrates the path of the aircraft during a representative flight. The jagged line in the center of the figure represents the Florida coastline in the vicinity of Kennedy Space Center.

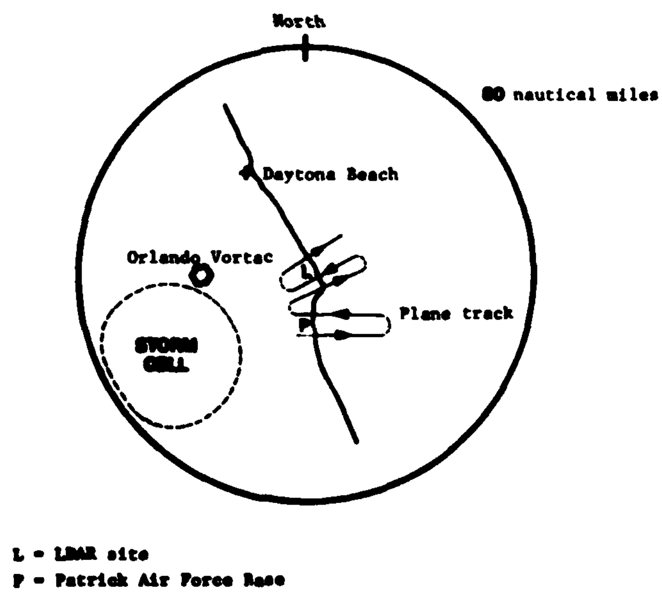

Figure 15. Aircraft Track During Representative Flight

Initially, it was planned to obtain aircraft position information from the aircraft's two TACAN receivers. However, it was found that the TACAN transponder interfered with operation of the test equipment. Therefore, these antennas were disconnected, and aircraft position was determined by recording headings and DME distances from the Orlando Vortac at approximately 30 second intervals during each leg.

At the beginning of each flight, the onboard time code generator was manually synchronized to the LDAR time base. Prior to any data acquisition, the Stormscope was tested, set to the 100 nautical mile range and cleared. During the flight, the display was cleared after each heading change and at approximately two minute intervals. Pictures of the Stormscope, weather radar, and time code generator were taken regularly during each run. As mentioned previously, X and Y coordinates of the Stormscope points in relation to the aircraft were recorded on disc together with the acquisition time.

Data collection efforts were occasionally hampered by weak thunderstorm formations and equipment failure. Of the twelve flight hours available for data collection, approximately three hours of useful comparison data were recorded. These data were recorded on 21, 25, and 26 July during four separate missions. (Two flights occurred on 25 July.)

Flight data consists of approximately two thousand photographic records of Stormscope and on-board weather radar displays. In addition, several thousand Stormscope points were stored on magnetic disc for subsequent processing and analysis.

Ground-based comparison data consists of magnetic tape records of approximately 5600 LDAR points and numerous photographic records of ground radar displays taken at approximately five minute intervals.

During the last flight in the test program it was decided to penetrate a cloud at the freezing level in an attempt to

determine if precipitation static would affect Stormscope's operation. The phenomena encountered during this penetration run had a pronounced and disabling effect, not only on Stormscope but also on several other pieces of digital avionics equipment on the aircraft, including the radar display. Since the flight program was over and the aircraft was not effectively instrumented for precipitation static measurements, no additional evaluation of Stormscope's response to precipitation static was performed. However, because of the increased use of digital avionics in aircraft, it was felt that the results of this incident would be of interest in future investigations and should be reported. Atmospheric conditions and observed equipment effects are summarized in the Addendum to this report. (See page 115).

SECTION VII

DATA ANALYSIS

1. General

Analysis of the inflight and ground based data consisted of both quantitative and qualitative comparisons made between: 1) Stormscope and LDAR, 2) Stormscope and airborne weather radar, and 3) Stormscope, LDAR, and ground weather radar.

Before interpreting the results of the quantitative comparisons made between LDAR and Stormscope, it is important to keep in mind two significant differences between the systems:

a. Operating Frequency: LDAR detects RF radiation in the 60-80 MHz range. Energy in this frequency band is generated in a wide variety of processes associated with lightning generation including preliminary breakdown, initial stepped leader, interstroke processes, return strokes and others[7]. In short, LDAR does not discriminate between lightning processes; it simply displays general regions of high electrical activity. Stormscope on the other hand, operates in the VLF range of approximately 50 KHz. This low frequency is generated primarily by K processes in cloud discharges and by cloud to ground return strokes[7]. Thus Stormscope rejects or does not detect many of the data points acquired by the LDAR system.

b. Data acquisition rate: LDAR requires three dedicated computers to achieve its high throughput rate for storage and display of the discharge activity. Stormscope relies on a single processor to perform ranging and azimuth computations, waveform correlation, and display updating. The requirement for a compact, airborne installation for the Stormscope thus limits the data acquisition rate (and display clarity) compared to LDAR.

From the above discussion of system differences, it is perhaps apparent that the only valid LDAR/Stormscope comparison to be made must involve regions of electrical activity rather than attempting a point by point comparison of individual discharges.

2. Quantitative Comparisons

a. Methodology

In order to make a quantitative evaluation of the range and azimuth accuracy of Stormscope as compared to LDAR, it was first necessary to develop software to rotate and translate the Stormscope points from the aircraft coordinate system to a common coordinate system based at the central LDAR site. This transformation was accomplished on a point by point basis using the following equations:

$$R_X = S_x \cos \Theta - S_y \sin \Theta + P_X$$

$$R_Y = S_y \cos \Theta + S_x \sin \Theta + P_Y$$

where: S_x = Stormscope x coordinate relative to aircraft

S_y = Stormscope y coordinate relative to aircraft

P_X = Aircraft x coordinate relative to LDAR site

P_Y = Aircraft y coordinate relative to LDAR site

Θ = 360° - aircraft heading

R_X = Translated x coordinate relative to LDAR

R_Y = Translated y coordinate relative to LDAR

Software was also required to re-format the LDAR data originally provided on 7-track magnetic tape to a flexible disc medium suitable for use on the PDP 11/05 computer system. The software was written to eliminate LDAR data points which differed more than 1°

azimuth and 2 nautical miles in range between the two groups of independent receiving networks.

Following translation and re-formatting, activity region boundaries were defined for each system using the concept of a density factor (d_p), to eliminate those points which did not exhibit a specific degree of clustering in the region of interest. The test for inclusion of a point in a given group is described as follows:

Assume a group starting point P_o with coordinates X_o, Y_o and define the following sets:

$S_1 = (P_o: P_n)$ all points under consideration

$S_2 = (P'_o:P'_m)$ points defining the group

Now the arbitrary point $P_i \in S_1$, is tested for inclusion in S_2:

$$P_i \in S_2 \text{ if } d_i \leq d_p$$

where:

$$d_i = \min (r_j) \Big| \; j = o,n \quad j \neq i \tag{3}$$

$$r_j = \{(x_i - x_j)^2 + (y_i - y_j)^2\}^{\frac{1}{2}} \tag{4}$$

That is, every point whose distance from at least one other point is less than or equal the chosen value of d_p is included in the set S_2. With the group thus defined, the centroid coordinates are given by:

$$\bar{r} = \frac{\sum_{i=1}^{m} r_i}{m} \qquad \bar{\Theta} = \frac{\sum_{i=1}^{m} \Theta_i}{m} \tag{5}$$

where: r_i, Θ_i represent the polar coordinates of the point pair x_i, y_i.

As a measure of the relative group dispersion, the standard deviations in range (σ_R) and azimuth (σ_Θ) for each group were computed from [8]:

$$\sigma_R = \sqrt{\frac{\sum_{i=1}^{m} (\bar{r} - r_i)^2}{m - 1}} \tag{6}$$

$$\sigma_\Theta = \sqrt{\frac{\sum_{i=1}^{m} (\bar{\Theta} - \Theta_i)^2}{m - 1}} \tag{7}$$

Complete program listings of the software used for data reduction are contained in Appendix A to this report. Examples of typical results obtained from the above analysis are shown in Figures 16 and 17. The data points depicted in Figures 16a and 17a represent the unprocessed discharge locations for the Stormscope and LDAR systems respectively. These data were acquired during a five minute interval on 25 July. The coordinate axes shown are referenced to the central LDAR site. Figures 16b and 17b show the corresponding processed data with individual group centroids depicted by the small crosses. Standard deviation in range (DR) and azimuth (DA) for each group is listed in the upper right corner of each figure. The results of eight comparisons made from data collected during flights on 25 and 26 July are shown in Appendix B and summarized in Table 3.

From the cases studied and presented in Table 3, Stormscope tends to depict activity centroids farther away than does LDAR, with the average range difference being approximately 15 NM. Table 3 also indicates an average azimuth difference of approximately 11° between the two systems with no consistent angular bias evident in one direction or another. Random measurement error ($\pm$ 3.5 NM, $\pm$ 6° worst case) may be present in the Stormscope data due to combined heading error and tolerances in the VOR/DME positioning system (see Section VI, Procedures). The range standard deviations (σ_{RL}, σ_{RS}) listed in Table 3 indicate

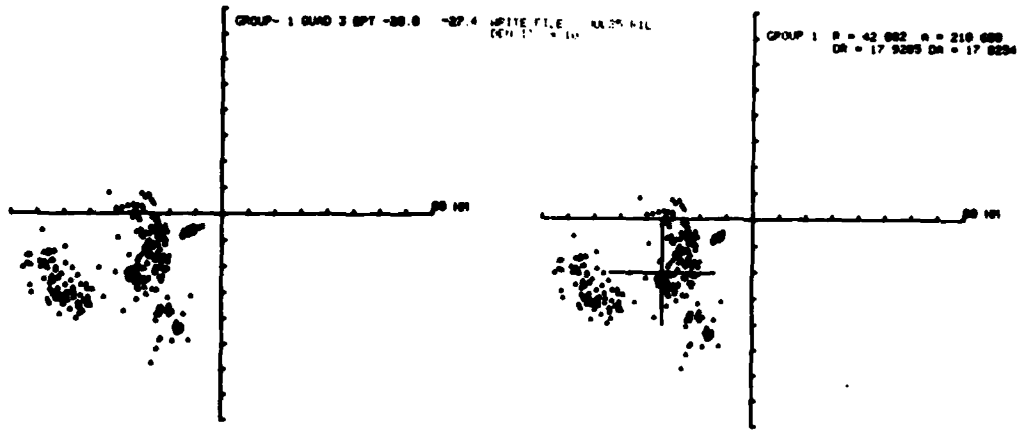

a. LDAR Electrical Activity

b. Centroid(s) of LDAR Electrical Activity

Figure 16. Raw LDAR Data and Sample Centroid Calculation

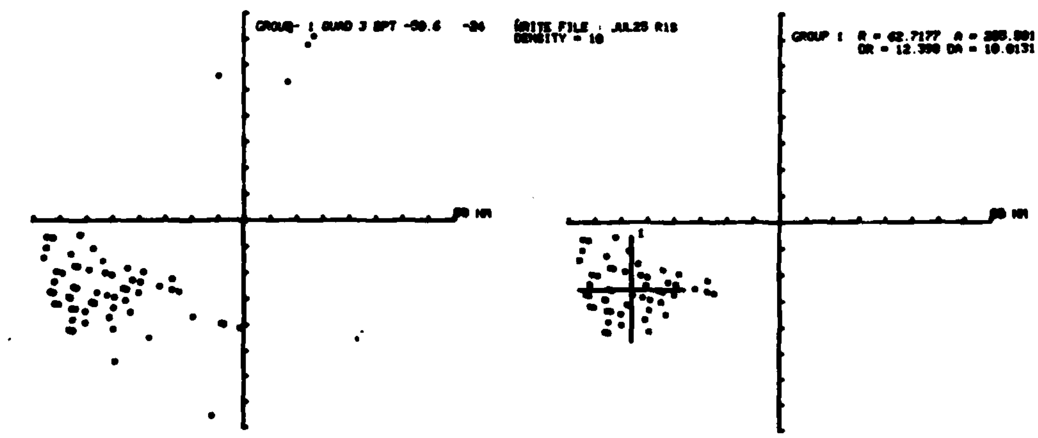

a. Stormscope Electrical Activity

b. Centroid(s) of Stormscope Electrical Activity

Figure 17. Raw Stormscope Data and Sample Centroid Calculation

	Range (Nautical Miles)				Azimuth (Degrees)			
File Name	r_L*	r_S	σ_{rL}	σ_{rS}	θ_L	θ_S	$\sigma_{\theta L}$	$\sigma_{\theta S}$
Jul 25 R1	42.1	62.7	17.9	12.4	210.7	205.6	17.8	10.0
Jul 25 R2	45.4	60.4	18.4	12.8	217.5	202.5	19.6	14.0
Jul 25 R3	65.4 47.5	56.9	5.7 6.5	11.8	208.9 244.6	219.5	6.4 7.6	13.2
Jul 25 R4	68.3 47.9	61.5 74.4	5.4 5.5	13.0 3.4	211.8 241.8	195.9 258.8	6.7 6.1	13.7 8.0
Jul 26 R1	69.2	71.4	8.8	18.6	142.1	126.3	6.7	15.8
Jul 26 R2	70.0	78.8	8.2	16.6	142.9	133.5	7.9	14.4
Jul 26 R3	71.4	89.0	10.1	19.9	143.0	147.1	8.6	18.4
Jul 26 R4	70.3	96.9	9.1	18.1	144.7	152.3	8.5	7.1

*Subscripts 'L' and 'S' denote LDAR and Stormscope data, respectively.

Table 3. Summary of Differences in Centroid Coordinates and Group Standard Deviations for Stormscope and LDAR Data

that, except in two cases, Stormscope activity groups are more range dispersed (74% on average) than corresponding LDAR groups. Conversely, differences in azimuth standard deviations ($\sigma_{\theta L}$, $\sigma_{\theta S}$) listed in Table 3 vary widely, with no consistent indication of more or less azimuthal dispersion.

In addition to centroid range and azimuth comparisons, total area and 'overlap' area were calculated for corresponding activity groups. These measurements provide an indication of the effectiveness of Stormscope in defining a conservative avoidance area; i.e. a Stormscope overlap area which at least encompasses the majority of the LDAR activity area. (See Figure 18.)

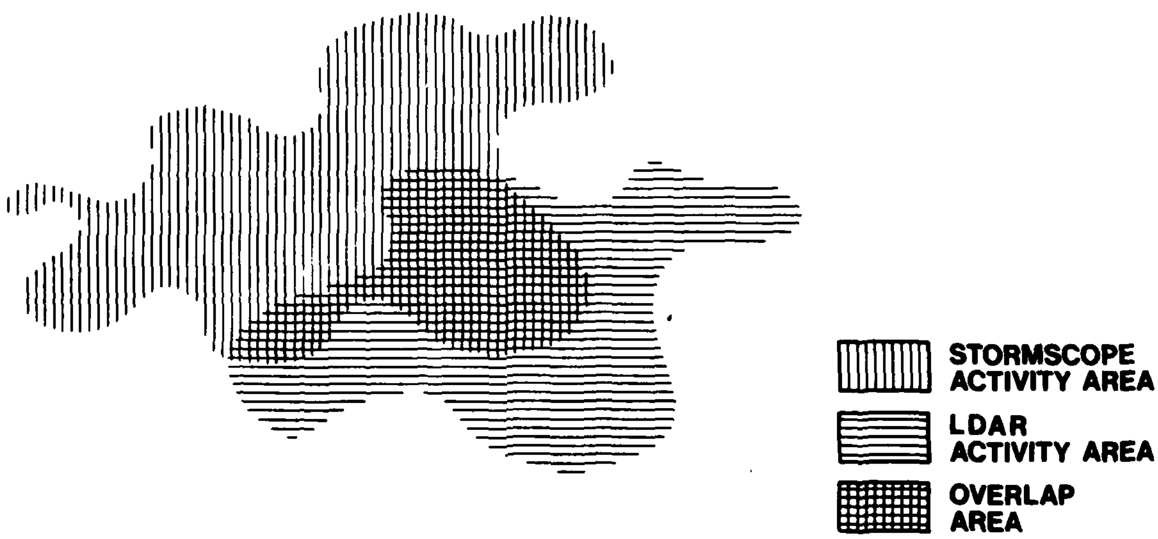

Figure 18. Illustration of Group Overlap Areas

The area enclosed by an arbitrary figure whose boundaries are defined by n x,y coordinate pairs is given by:[8]

$$A = -1/2 \sum_{i=1}^{n} x_i(y_{i+1}-y_{i-1}) \qquad (8)$$

where: $y_0=y_n$, $y_{n+1}=y_1$ (as required for closure)

Utilizing equation 8, software was written (see Appendix A) to compute and display the overlap areas for each pair of groups listed in Table 3. Results of these calculations are summarized in Table 4 and presented in graphic form in Appendix C.

File Name	LDAR Area*	Stormscope Area	Area of Overlap	% Overlap
Jul 25 R1	1828.1	986.0	805.5	44.1
Jul 25 R2	1216.0	1234.2	532.4	43.8
Jul 25 R3	774.7	1095.3	367.4	47.4
Jul 25 R4	599.9	1425.0	395.1	65.9
Jul 26 R1	2488.7	2646.8	1011.7	40.7
Jul 26 R2	1576.1	2354.2	989.3	62.8
Jul 26 R3	2538.9	3218.8	2196.6	86.5
Jul 26 R4	2116.7	3590.0	1578.7	74.5
			Average 58.2%	
			Average weighted by overlap area 65.2%	

* All areas in NM^2

Table 4. Overlap Comparison Between Stormscope and LDAR Activity Regions

Table 4 indicates a large variance in the overlap area, although the average overlap is acceptable. Again, some variance in overlap area must be expected due to differences in the atmospheric phenomena detected by each system.

3. Qualitative Comparisons

a. Stormscope vs Airborne Weather Radar

The comparison between Stormscope and airborne weather radar was accomplished through visual analysis of the photographic records of the two displays. Seven representative photographs from four different flights have been selected for discussion purposes. To facilitate analysis of the photographs, an interpretive graphic presentation is included to the side of each. This presentation illustrates heavy precipitation contour areas on the radar display, areas of high electrical activity on the Stormscope display, and the probable flight path which would be chosen by an observer relying on only the radar or the Stormscope presentation to avoid severe weather. The reader is cautioned against additional interpretation of these photographs since some multi-level precipitation contours have been eliminated by the various reproduction and printing processes. Additionally, the time variations in both displays observed during the actual mission are important to the interpretation and are excluded here.

The photograph in Figure 19 was taken at 14:48:42 EDT on 21 July. Weather radar, set on the 80 nautical mile range, is showing precipitation patterns at 330-340^{o}, 40-60 NM and a pattern with second level contours at 360-030^{o}, 60-70 NM. Stormscope, on the 100 NM range, shows activity at 330-360^{o}, 70-100 NM and at 360-030^{o}, 30-100 NM. Both displays suggest deviation left or right of course as shown to avoid the severe weather patterns, although the Stormscope left deviation would penetrate two radar contours.

The photograph in Figure 20 was taken approximately 10 minutes later at 15:07:41 EDT. The storm has now intensified, as evidenced by both the increased localized electrical activity displayed on Stormscope and by the increased area of heavy precipitation returns displayed on radar.

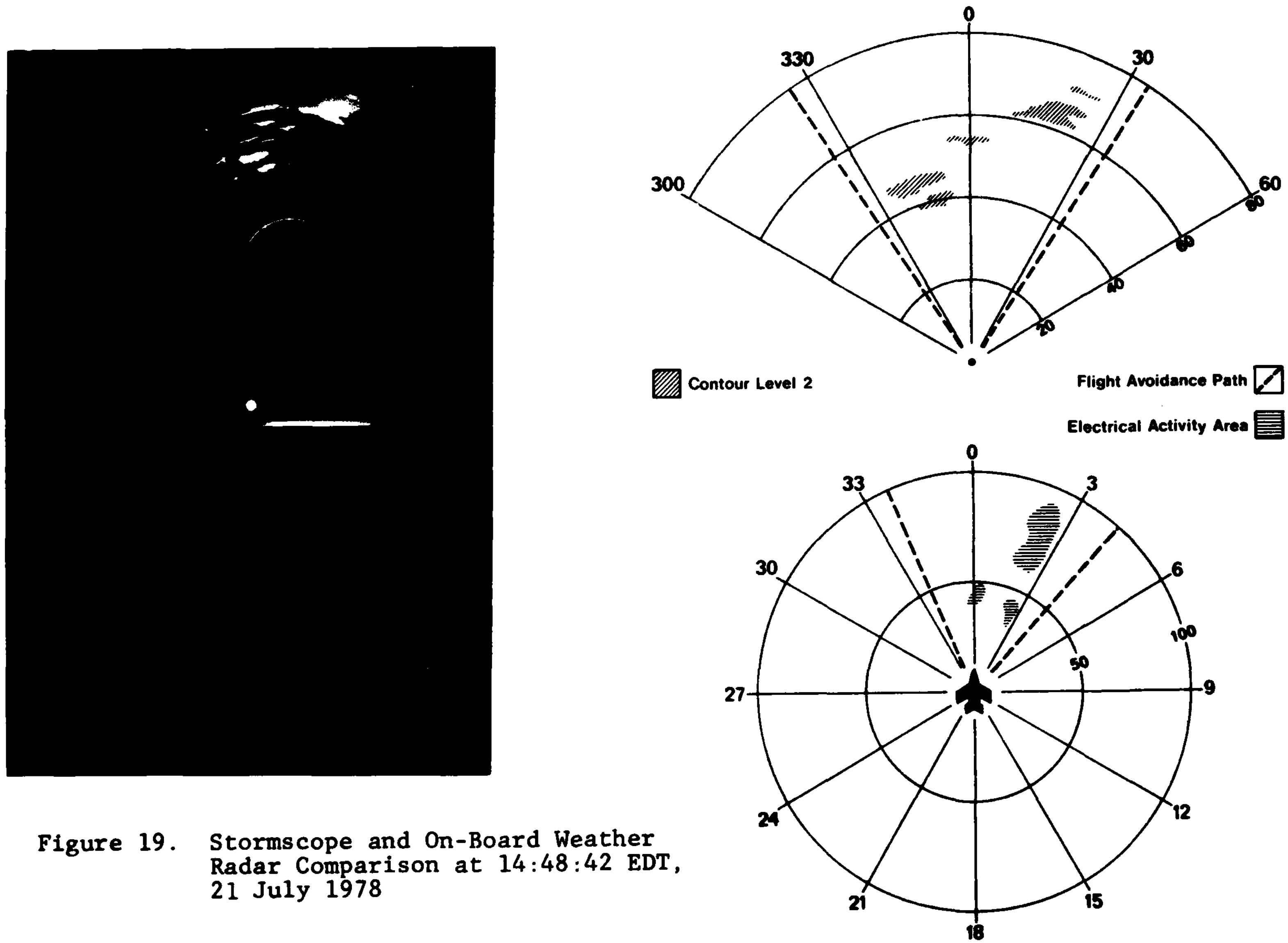

Figure 19. Stormscope and On-Board Weather Radar Comparison at 14:48:42 EDT, 21 July 1978

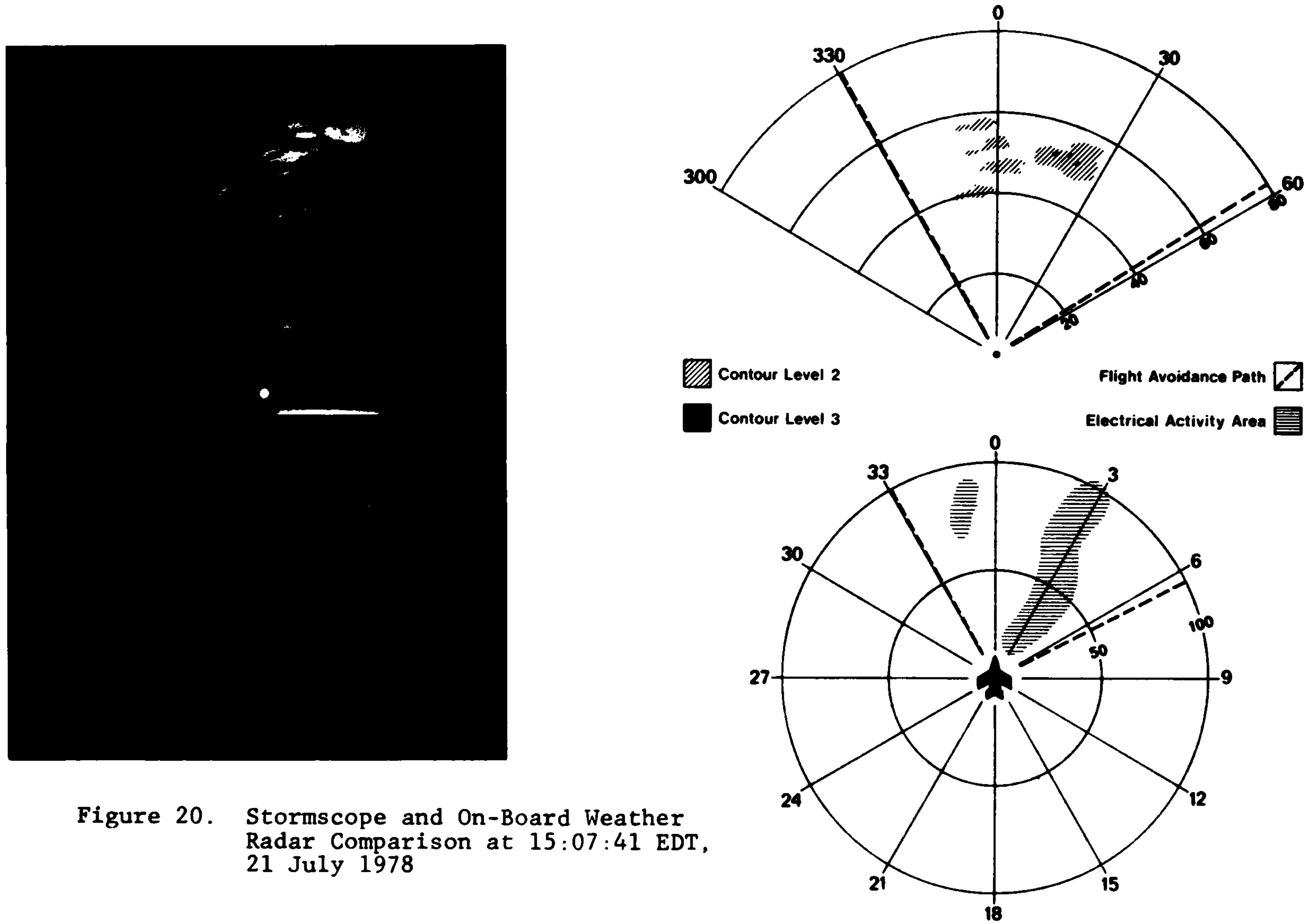

Figure 20. Stormscope and On-Board Weather Radar Comparison at 15:07:41 EDT, 21 July 1978

Some radial spreading or dispersion is apparent on the Stormscope display (notice the 'spoke' of activity on the 25-30^{o} radials). This effect is much less noticeable when the 40 NM range is selected on Stormscope. In an operational situation, Stormscope would typically be placed on an outer range (100-200 NM) to provide early warning of electrical activity. If substantial activity were then detected, the display would be cleared, and the range set to 40 NM to obtain improved storm definition before making a final decision for course correction. In most cases, however, Stormscope display accuracy is sufficient even at the 100-200 NM ranges to provide coarse weather avoidance information. In this specific figure, for example, both Stormscope and weather radar indicate feasible course corrections on either the 60^{o} or 330^{o} radials.

Figure 21 was taken at 15:27:19 EDT on 25 July. Radar shows a third level contour at 330^{o}, 45 NM and several second level contours from 300-360^{o}, 35-60 NM. Notice that Stormscope again exhibits the radial spreading characteristic of the outer range displays but that there is good azimuthal correlation with the third level radar contour at 330^{o}. Notice also in this photograph that the Stormscope indicates considerable activity present on the 270-300^{o} radials, which is out of the radar field of view. Although in this case both radar and Stormscope indicate similar course corrections on the 20^{o}-30^{o} radials, it is possible that in certain weather formations, the 360^{o} Stormscope display could provide avoidance information that is not available with radar.

Figures 22 and 23 were taken at 17:15:33 and 17:31:12, respectively, during a second flight on 25 July. In Figure 22 two activity clusters appear on Stormscope, one at 340-350^{o}, 20-50 NM and one at 330-360^{o}, 60-100 NM. Weather radar shows a third level contour at 310-350^{o}, 35 NM and a second level contour at 350^{o}, 60-75 NM.

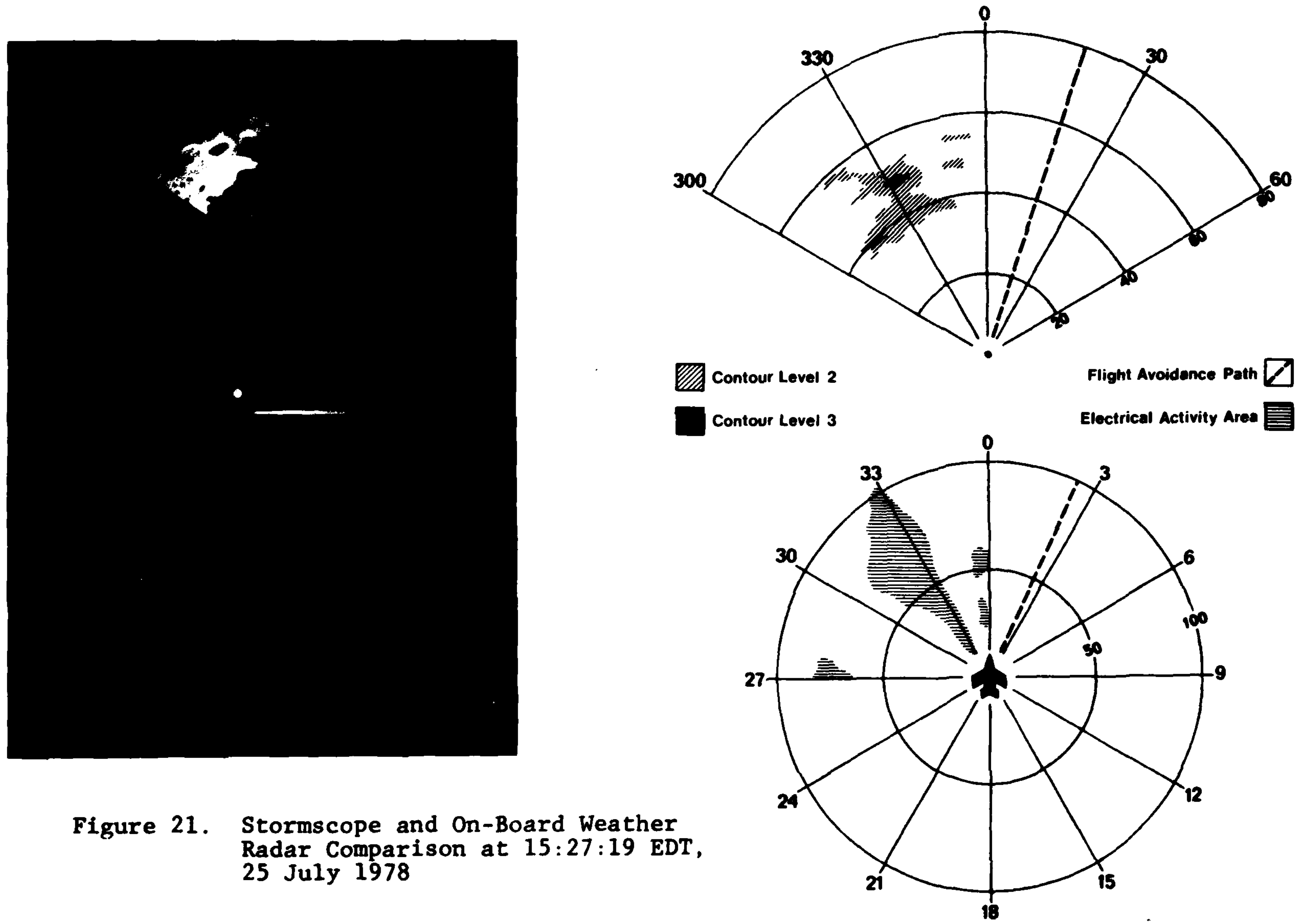

Figure 21. Stormscope and On-Board Weather Radar Comparison at 15:27:19 EDT, 25 July 1978

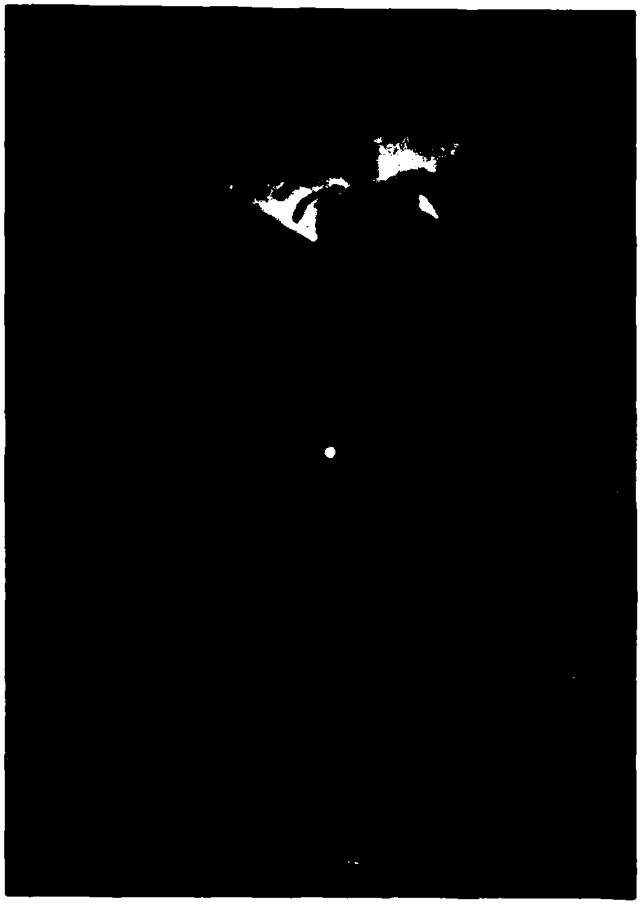

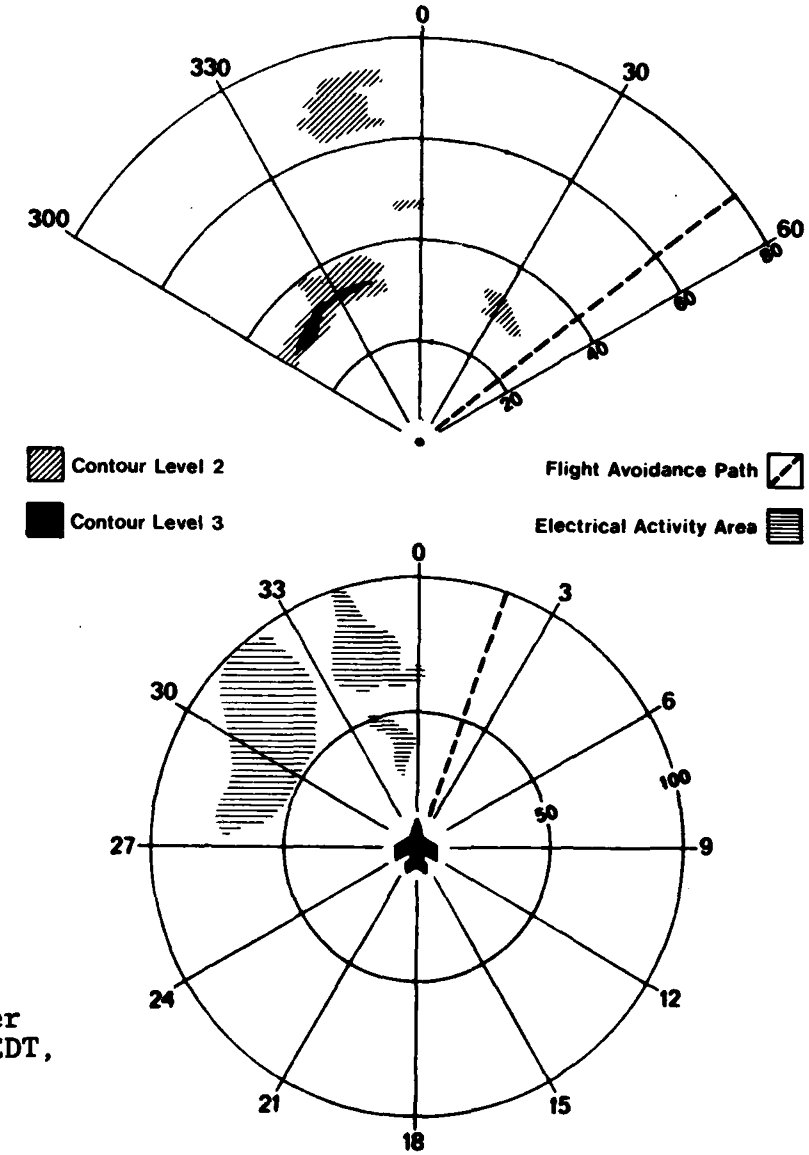

Figure 22. Stormscope and On-Board Weather Radar Comparison at 17:15:33 EDT, 25 July 1978

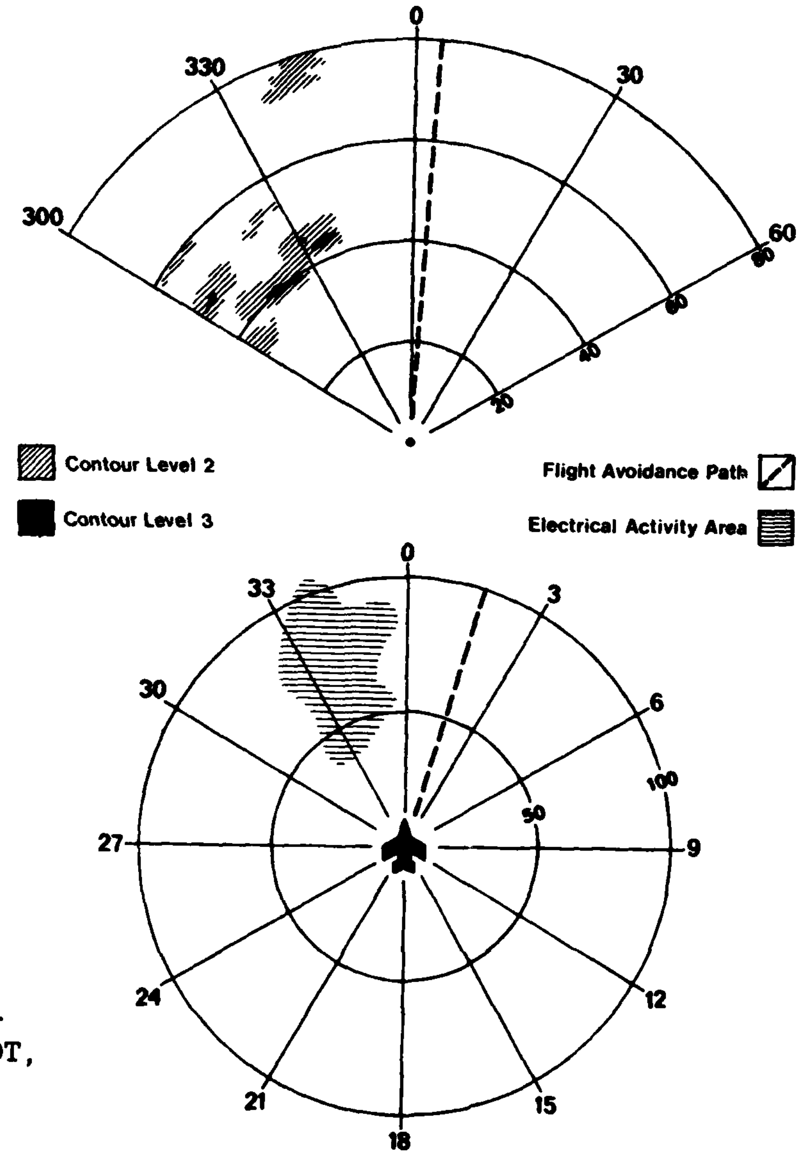

Figure 23. Stormscope and On-Board Weather Radar Comparison at 17:31:12 EDT, 25 July 1978

An analysis of several photographs prior to the one illustrated in Figure 22 reveals that the formation shown as a second and third level contour region at 330-360°, 30-50 NM on radar, has gradually merged with the semi-circular formation at 340-030°, 40-80 NM. Stormscope indicates strong activity at the 'pocket' formed by the juncture of these two formations. Radar also shows an area of precipitation at 360-030°, 30-60 NM, an area where Stormscope has very little electrical activity depicted. One small, second level contour exists at 030°, 30 NM. Review of the LDAR data collected during this time indicates electrical activity was occurring in this area but, without actual storm penetration, it is not possible to conclude that an aircraft flying through this area would encounter more than heavy rain. In this type of situation, direct penetration into the activity area in question would have provided an excellent comparison of the systems. Unfortunately, this was not possible in the aircraft used for these tests.

Figure 23 is a photograph of the same formations taken approximately 15 minutes later with radar indicating storm dissipation has taken place. Stormscope, however, still displays heavy and comparatively localized activity in the pocket region. The contour area at 030°, 30 NM has disappeared and the cloud formations are breaking up. Both Stormscope and radar displays now agree that a course of 010-020° would be suitable for avoiding severe weather.

The final two examples, Figures 24 and 25, were taken at 15:56:25 and 16:12:29, respectively, on 26 July. Radar indicates a third level contour at 0°, 70 NM surrounded by a small second level contour and a broad region of first level contours. There is also a broad second level contour at 300-345°, 30-50 NM. Stormscope indicates some localized, low-level activity at approximately 0°, 60-80 NM. As in several previous

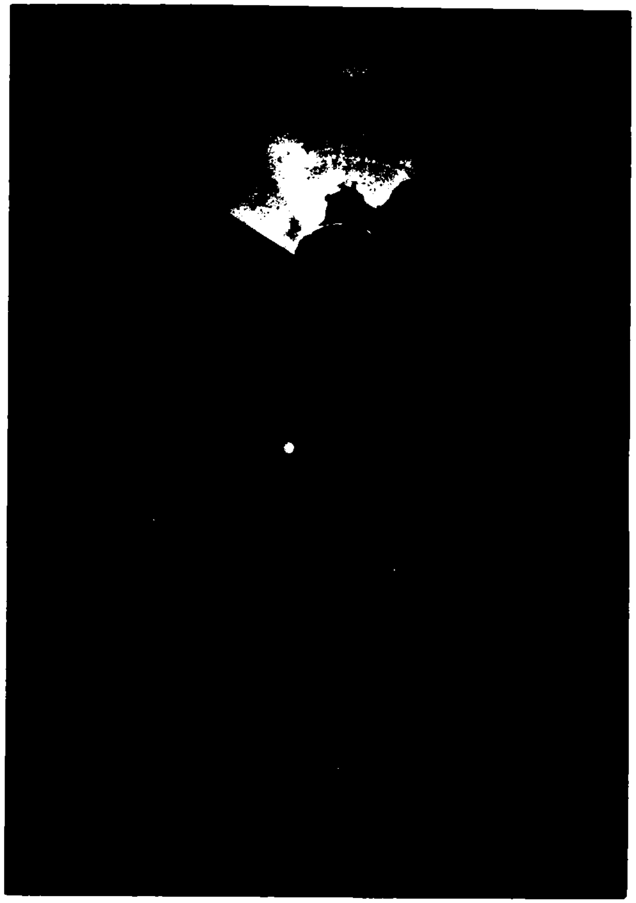

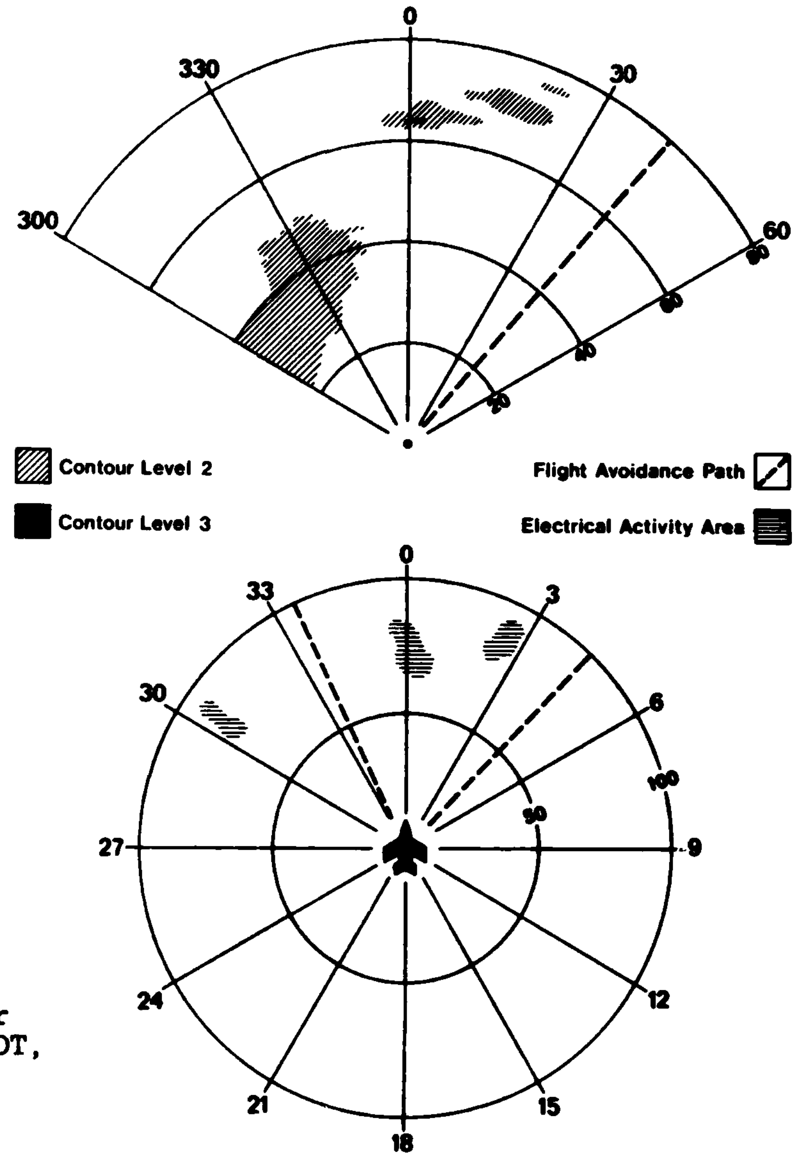

Figure 24. Stormscope and On-Board Weather Radar Comparison at 15:56:25 EDT, 26 July 1978

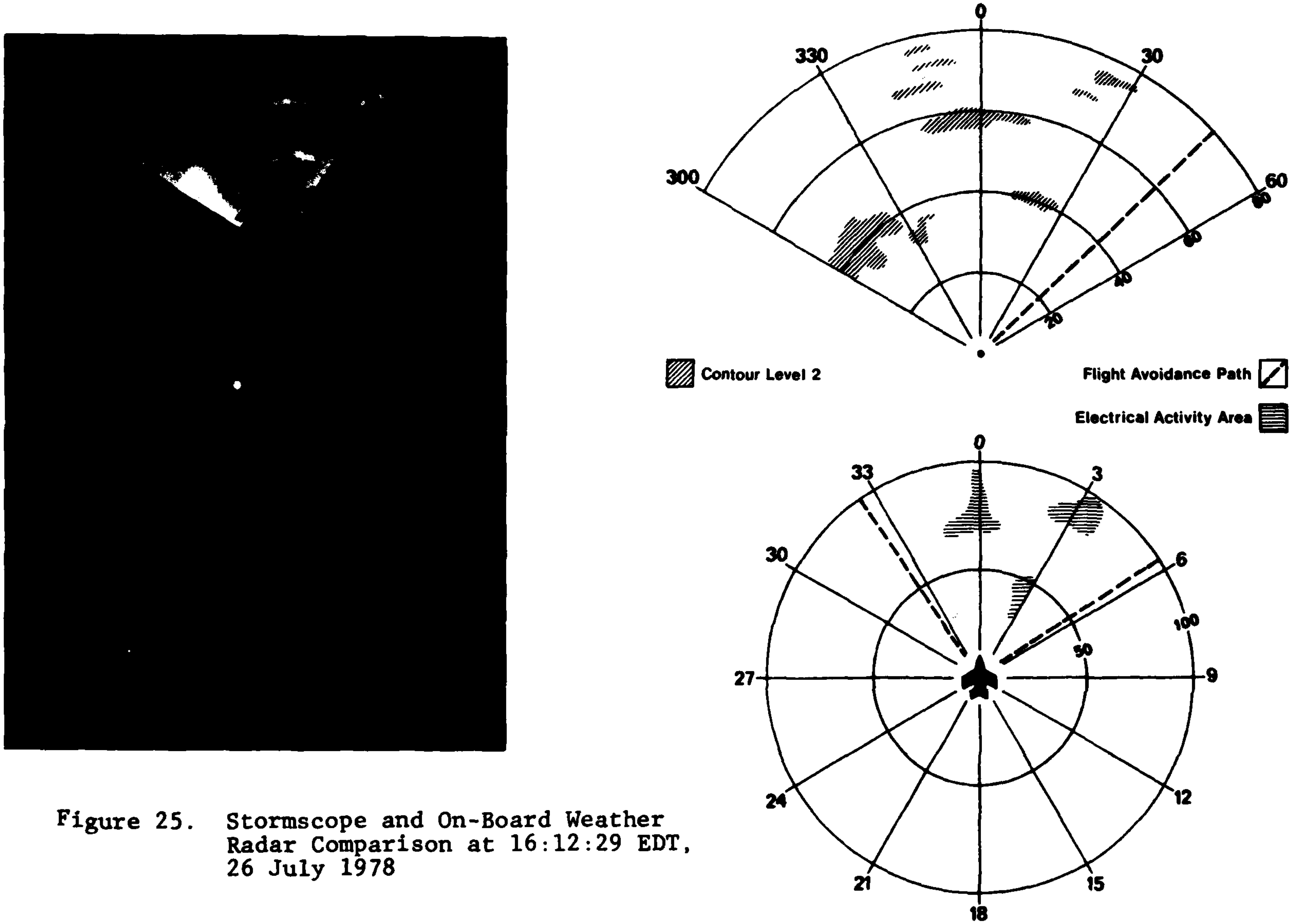

Figure 25. Stormscope and On-Board Weather Radar Comparison at 16:12:29 EDT, 26 July 1978

examples, the clustered Stormscope activity seems to occur in regions where weather radar displays a high precipitation 'gradient' (i.e. abruptly changing from first to third level contour). Based on the Stormscope display, a course deviation on the 330^o or 045^o radials would be feasible. LDAR, in agreement with Stormscope, does not indicate activity in the area covered by the radar contour along the 330^o path; an aircraft following this course probably would only encounter heavy rain. Stormscope also displays low level activity outside the radar field of view but it is non-localized and provides no additional avoidance information.

The same weather formation, shown in Figure 25 approximately 15 minutes later, has dissipated considerably, with radar indicating only scattered first and second level contour areas. Stormscope continues to display activity at 030^o, 70-80 NM and 0^o, 70-80 NM, corresponding in each case to the approximate location of small first to second level contour interface areas displayed on radar.

Analysis of these photographs has permitted several conclusions to be drawn regarding correlation between Stormscope and weather radar:

1. Stormscope gives reliable indications of third level contours, although significant variations in range and more minor variations in azimuth were noted.

2. Stormscope activity correlates primarily with the radar precipitation gradient, not with precipitation intensity itself.

3. Stormscope is capable of displaying activity outside radar's field of view which may be useful in weather avoidance.

4. Direct weather penetration by the test aircraft is the only way of resolving some discrepancies noted between Stormscope and weather radar.

b. Stormscope vs LDAR and Ground Weather Radar

A visual comparison of Stormscope, LDAR and ground weather radar was performed by preparing plots of data acquired from the Stormscope and LDAR systems over several short intervals (approximately 5 minutes) and superimposing these plots on corresponding WSR-57 ground weather radar displays obtained from one of two weather stations, either in Tampa or Daytona Beach. For this comparison, the Stormscope data points were translated to the Central LDAR reference site as described in Section VII. Since ground weather radar pictures were usually available only at five minute intervals, some difficulty was experienced in obtaining photographs which corresponded exactly to the time windows during which the LDAR and Stormscope data were collected. In all cases presented, however, this time difference is never greater than 3 minutes.

The key in the upper right corner of each composite lists the beginning and ending times for data acquisition and the aircraft heading during the run. The aircraft ground track over this time interval is shown as a dotted line. The jagged line running diagonally across the display represents the southeast Florida coastline. The cross mark in the display center indicates the central LDAR site, and the 'P' symbol represents Patrick AFB. The Orlando Vortac symbol is also shown on the 270^{o} radial of each display for reference.

The reader should exercise caution in interpreting these figures. As explained earlier, time variations in the various system displays play an important role in determining valid severe weather patterns. For example, some isolated Stormscope points appearing in these figures may result from the arbitrary five minute acquisition interval chosen for display purposes. Under actual operational conditions, high electrical activity can completely update the Stormscope display in less than one minute causing isolated points to be rapidly 'dropped' from the

display. Thus, the observer interested in severe weather avoidance naturally tends to disregard isolated, low-rate activity, concentrating instead on areas showing consistent heavy clustering.

Figures 26 and 27, from the first flight on 25 July, show rather poor Stormscope correlation with both LDAR and ground radar. Figure 26 in particular shows considerable Stormscope activity at 350-005^{o}, 40-80 NM which is not displayed on either of the other systems. Notice in Figure 26, however, that Stormscope does display an activity group on the 320^{o} radial and other less clustered activity on the 260-320^{o} radials which is supported by LDAR activity on the same approximate azimuths. In both Figures 26 and 27, Stormscope displays the principal activity areas but also indicates other widely dispersed activity throughout the quadrant.

Figure 28 from the second flight on 25 July illustrates an apparent discrepancy between Stormscope and the LDAR system. Notice that while Stormscope displays tightly clustered activity in the southwest quadrant (which corresponds well with radar and LDAR indications), it shows no indication of the electrical activity displayed by LDAR in the region of precipitation shown on the ground weather radar at 220-280^{o}, 10-30 NM. As shown in Figure 22, on-board weather radar at this time shows a broad first level contour in this area and a small, second level contour at 030^{o}, 30 NM. For this particular flight, the aircraft was inbound on a heading of 284^{o}, 20 NM south of LDAR, placing the undetected activity directly ahead of the aircraft. Of the many plots and photographs reviewed for this report, this is the only instance in which Stormscope did not provide adequate weather avoidance information; that is, where Stormscope was inconsistent with both LDAR and radar information. The only practical way to determine whether this area contained turbulence and/or significant electrical activity would have been to perform an actual penetration. However, LDAR data acquired only two minutes later (Figure 29) indicate

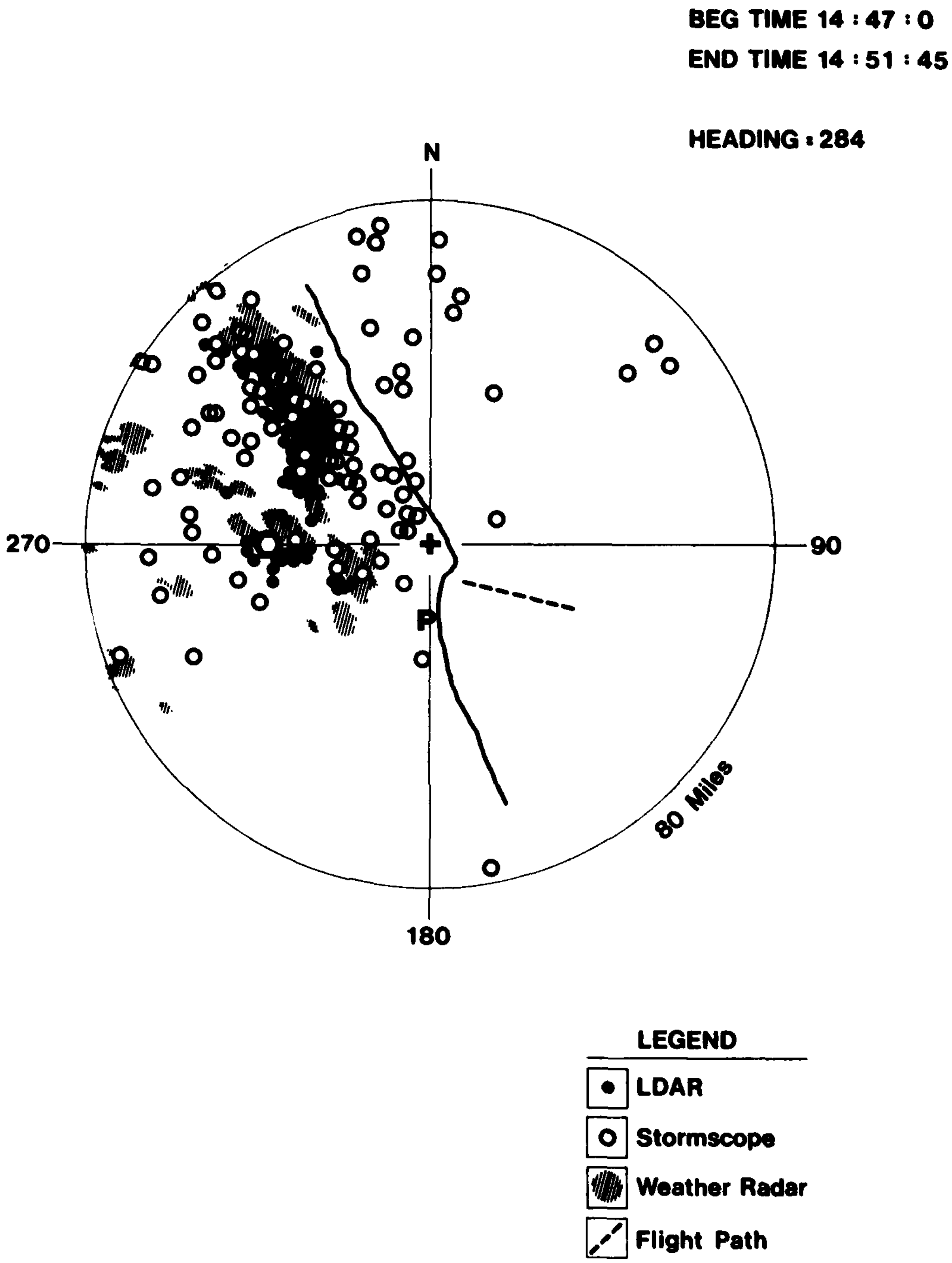

Figure 26. Composite of Stormscope, LDAR and Ground Weather Radar Displays - Run 1, Flight 1, 25 July

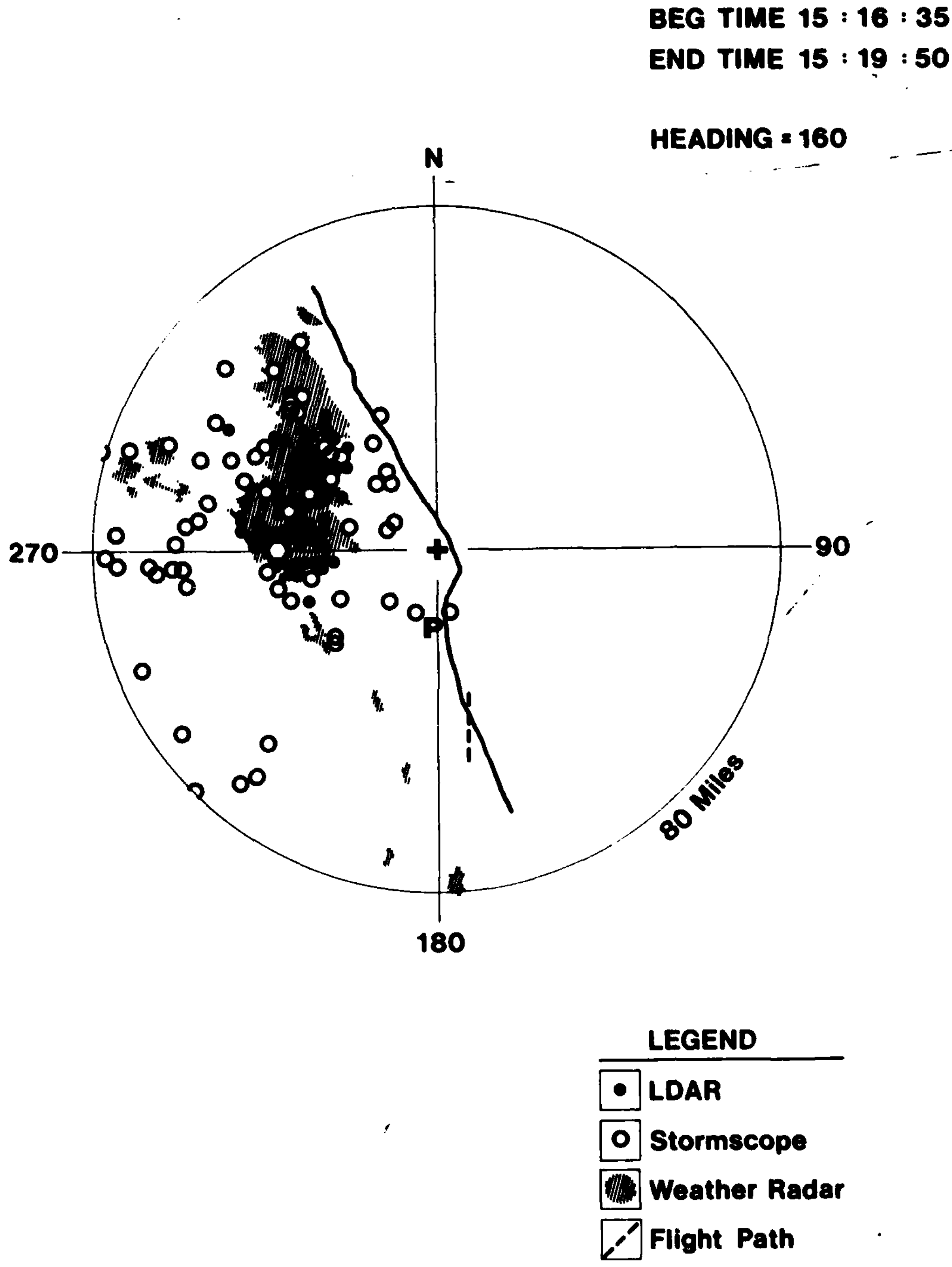

Figure 27. Composite of Stormscope, LDAR and Ground Weather Radar Displays - Run 4, Flight 1, 25 July

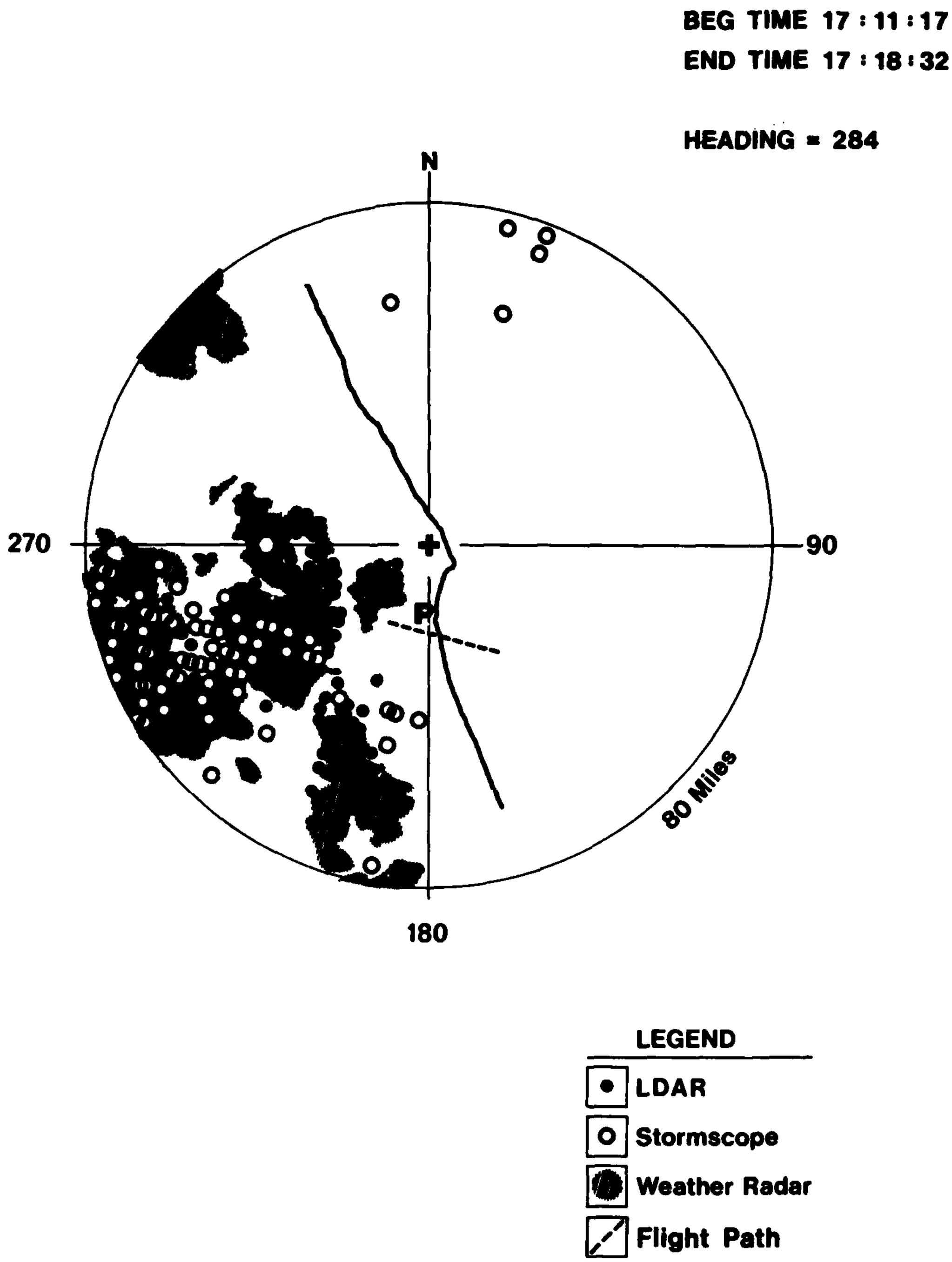

Figure 28. Composite of Stormscope, LDAR and Ground Weather Radar Displays - Run 1, Flight 2, 25 July

very little activity in the area. Comparison of weather radar photographs taken during and shortly after the time in question (Figures 22 and 23 respectively) also indicates a rapidly dissipating storm region. The temporary discrepancy between Stormscope and LDAR therefore, is most likely a result of the type of electrical activity predominant in a decaying storm cell, and it is unlikely (though unproven) that this area presented a significant threat to flight safety.

Figures 29, 30, 31, again from the second flight on 25 July, show good to excellent Stormscope correlation with LDAR and radar. These figures generally show tightly clustered Stormscope activity regions with very little extraneous activity. Furthermore, there are no major discrepancies between systems nor undetected activity regions such as the one shown in Figure 28.

Figures 32, 33, and 34 are from the flight on 26 July. In contrast to the figures from 25 July, which showed activity within 80 NM of LDAR, these figures display activity to 120 NM for comparison purposes. Due to radar malfunctions at Daytona Beach on 26 July, radar photographs from the Tampa weather station were utilized. The limit of the Tampa radar range is denoted by the curved line appearing near the top of each figure. To eliminate misinterpretation, data outside this range have not been shown in these figures.

In Figure 32, Stormscope shows good agreement with the activity region depicted by radar and LDAR at 290-330^{o}, 40-100 NM, although the Stormscope activity rate is relatively low compared to LDAR and some range dispersion is evident. The small region of LDAR activity shown at 190^{o}, 50-70 NM is not apparent on Stormscope, although some widespread Stormscope activity appears on the same approximate azimuth.

In Figure 33, the systems again show largely acceptable agreement, with Stormscope now displaying a more clustered though still lowrate activity group at 190^{o}, 50-90 NM. The small,

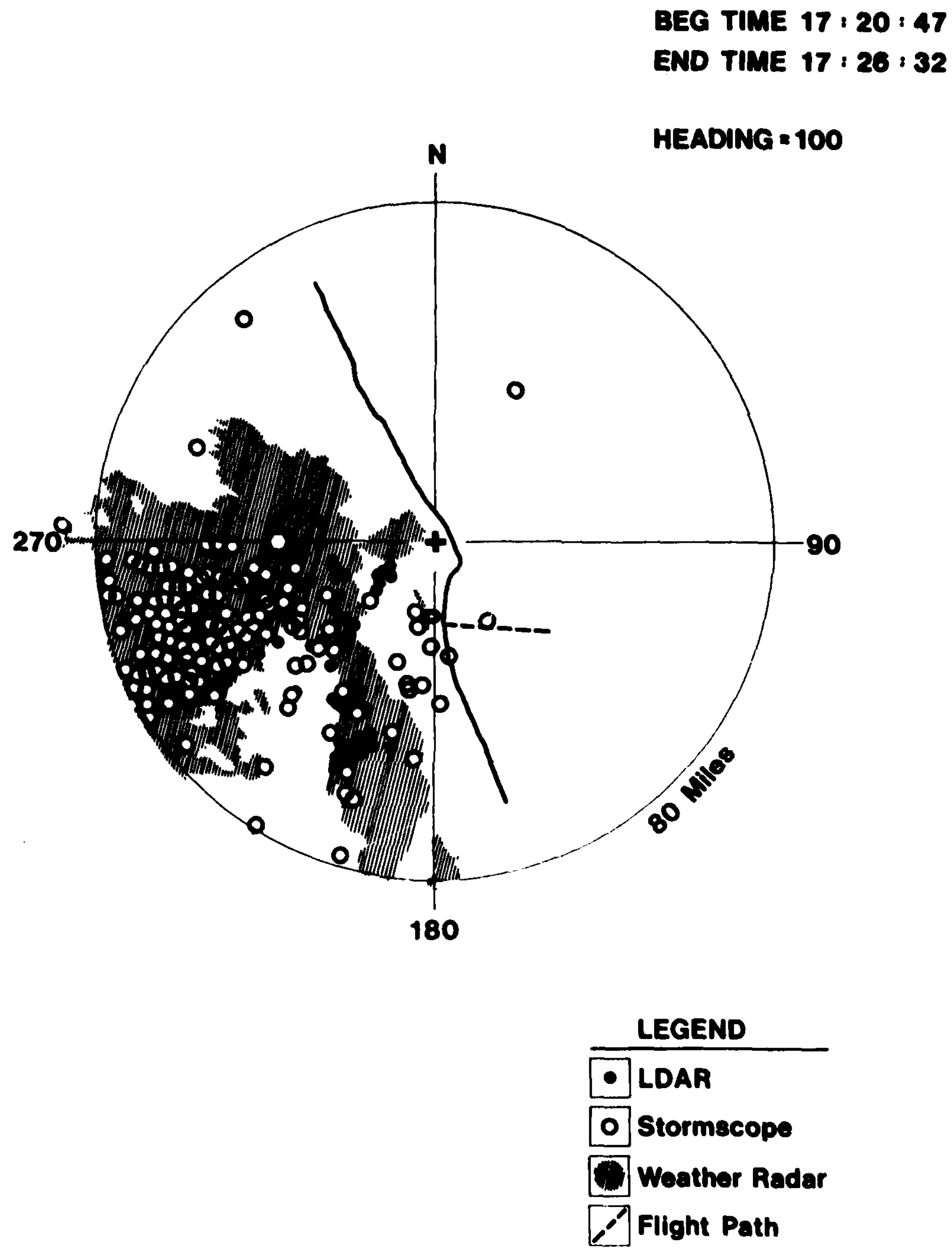

Figure 29. Composite of Stormscope, LDAR and Ground Weather Radar Displays - Run 2, Flight 2, 25 July

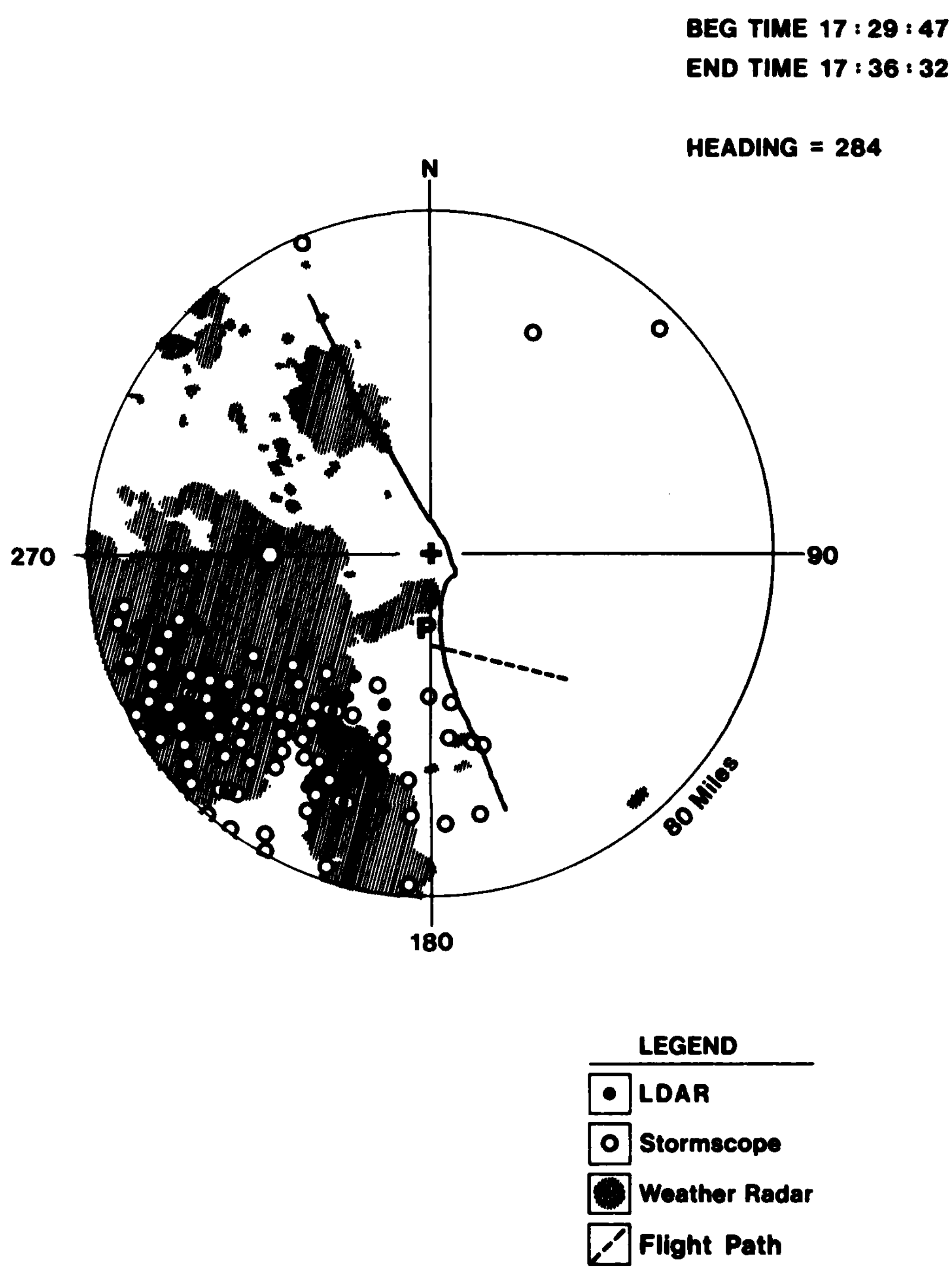

Figure 30. Composite of Stormscope, LDAR and Ground Weather Radar Displays - Run 3, Flight 2, 25 July

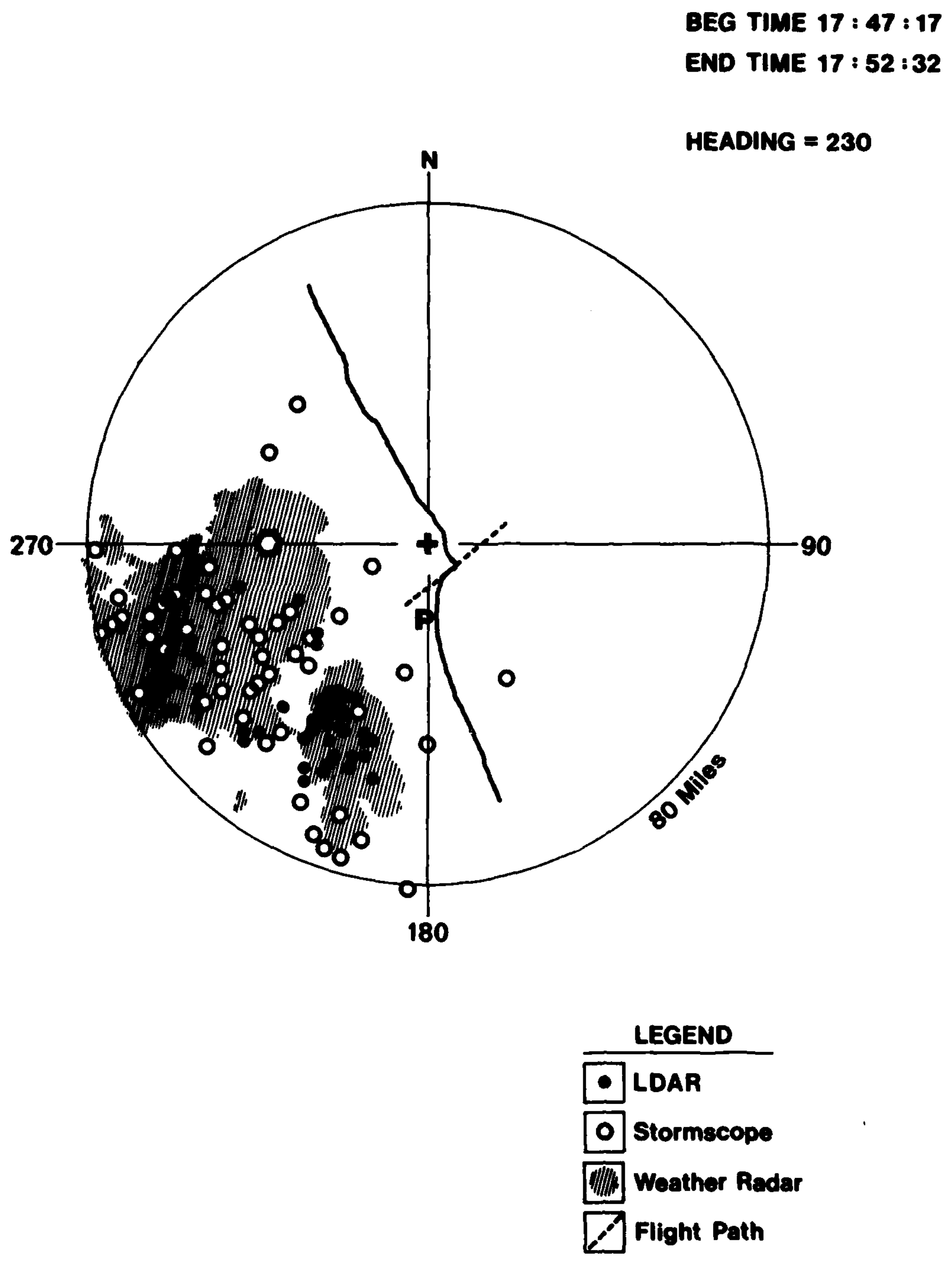

Figure 31. Composite of Stormscope and LDAR Displays
Run 5, Flight 2, 25 July

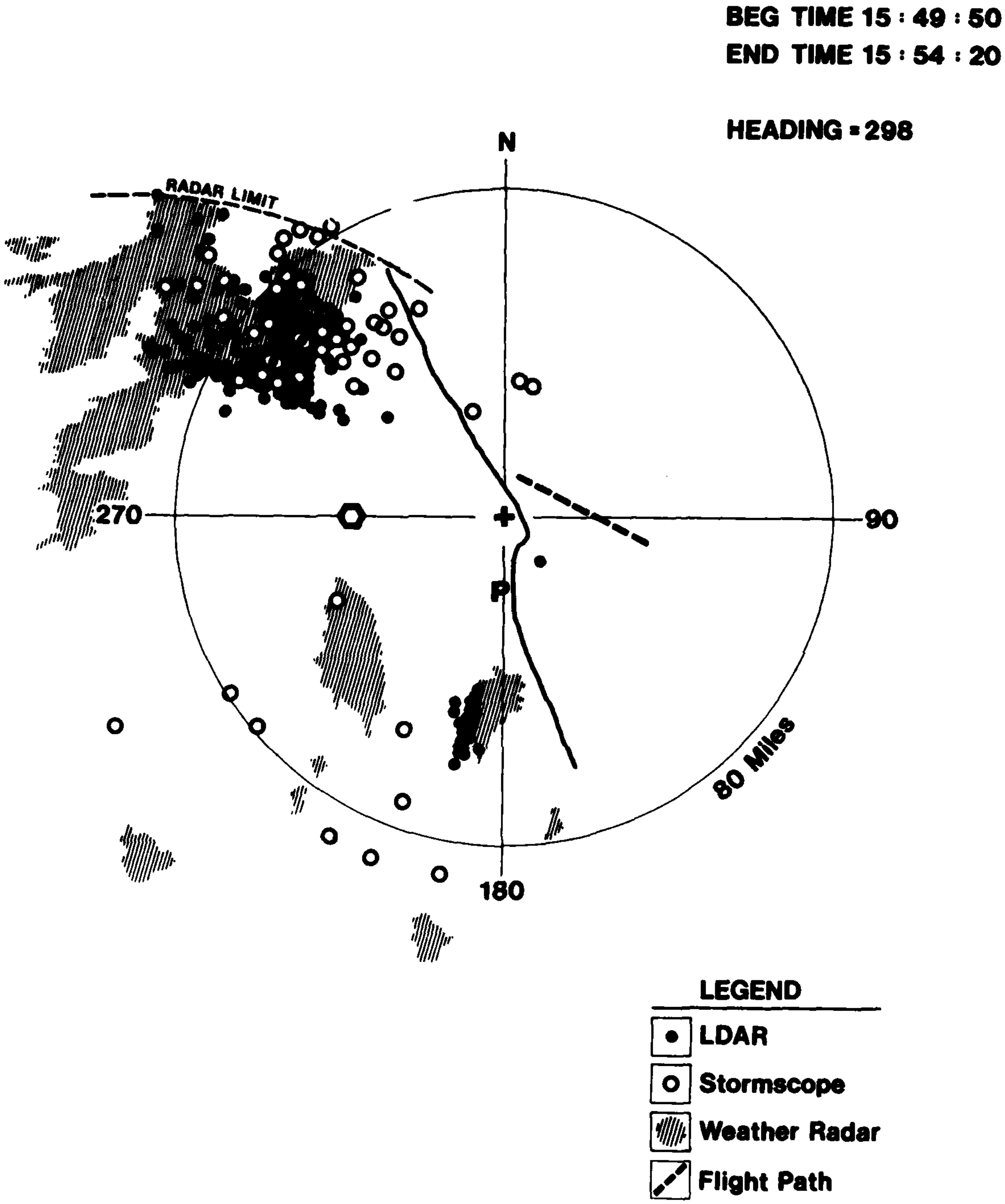

Figure 32. Composite of Stormscope, LDAR and Ground Weather Radar Displays - Run 1, 26 July 1978

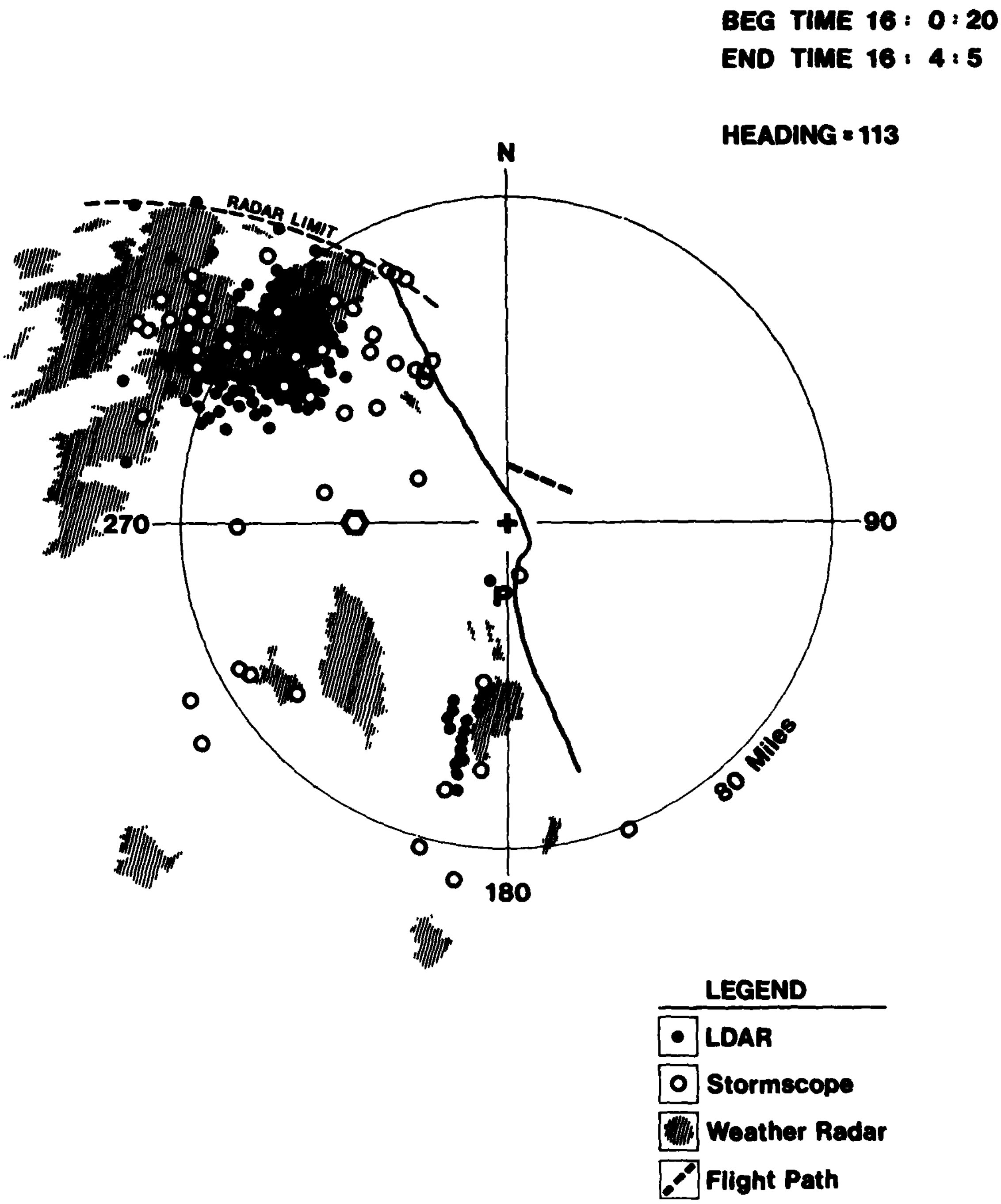

Figure 33. Composite of Stormscope, LDAR and Ground Weather Radar - Run 2, 26 July 1978

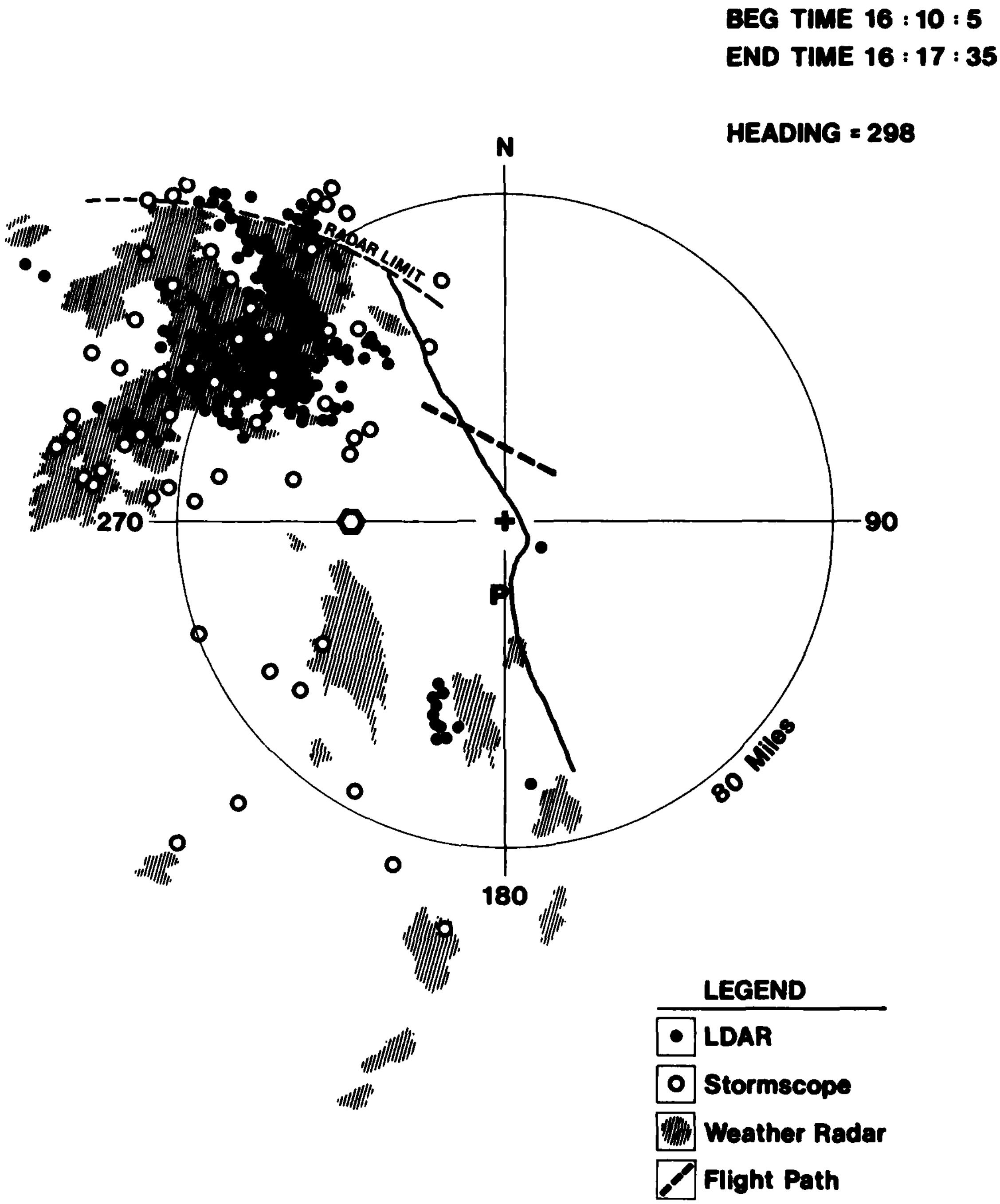

Figure 34. Composite of Stormscope, LDAR and Ground Weather Radar - Run 3, 26 July 1978

isolated characteristics of this particular group indicate a diminishing storm with decreasing electrical activity present. Indeed, in the 13 minute time span shown between Figures 33 and 34, the LDAR acquisition rate in this area has decreased approximately 30%.

With the exception noted in Figure 28, and possibly an exception at the 190^{o} radial in Figures 32 and 34, all of the composite figures discussed in this section indicate Stormscope provides coarse yet adequate weather avoidance capability. Particularly good correlation was found between the systems for data recorded on 25 July during the second flight. Due to the many system differences noted earlier, the correlation obtained is very likely a function of the characteristics of the storm itself (i.e. building, decaying, widespread, isolated, etc.)

SECTION VIII

SUMMARY OF RESULTS

1. Statistical comparisons between LDAR and Stormscope indicate several differences in portrayal of centroids and boundaries of electrical activity regions.

Specifically:

- Difference in centroid range averaged 15 NM with Stormscope tending to depict activity to be more distant than did LDAR.

- Difference in centroid azimuth averaged 11^{o} with no consistent angular bias evident in one direction or another. Some random measurement error ($\pm$ 3.5 NM, $\pm$ 6^{o} worst case) may be present in the Stormscope data due to combined heading error and tolerances in the VOR/DME positioning system (see Section VI, Procedures).

- Activity area overlap averaged approximately 60%, with the majority of Stormscope activity areas being somewhat larger (150% on average) than corresponding LDAR areas.

2. Visual comparisons between Stormscope and onboard weather radar indicate the following:

- Stormscope activity typically occurs in regions which are depicted as isolated second and third level precipitation contours on radar. Reliable indications of these contours are provided, although significant variations in range and more minor variations in azimuth were observed.

- Stormscope activity rate correlates primarily with radar precipitation gradient (i.e. abrupt first-third level interface areas) rather than with precipitation intensity itself.

- Weather avoidance paths based on the location of second and third level precipitation contour areas show good

agreement with avoidance paths based on areas of high electrical activity displayed by Stormscope. Two discrepancies in avoidance paths noted in the report were not resolved due to the restricted penetration capabilities of the test aircraft.

- Several cases were noted in which the 360° field of view available from Stormscope provided potentially useful avoidance information not shown on radar.

3. Additional visual comparisons between Stormscope, LDAR and ground weather radar indicate the following:

- Stormscope activity groups were highly variable in nature, at times being wide spread with instances of apparently extraneous activity, and at other times being tightly clustered showing good correlation with LDAR and radar indications.

- With the few exceptions noted in the report, Stormscope activity regions provided conservative (i.e. larger) avoidance boundaries compared to LDAR.

SECTION IX

CONCLUSIONS

1. Stormscope provides coarse definition of electrical activity areas, which was shown in most cases to be adequate for the purpose of severe weather avoidance. "Severe weather" here is taken to mean regions displaying both LDAR electrical activity and level 2 radar return.

2. Significant variations were found in range and azimuth location of Stormscope activity areas vs weather radar indications of precipitation contours. Recent data (Reference 2) tend to support correlation of turbulence with the occurrence of electrical activity rather than heavy precipitation. In any case, course corrections for severe weather avoidance were largely the same for both systems in spite of the variations noted.

3. Stormscope offers numerous installation and operation advantages compared to radar: 1) Stormscope is passive and completely electronic whereas radar requires an active, high frequency transmitter/receiver with electromechanical antenna rotation. Stormscope should exhibit a high MTBF compared to radar. 2) Recent models of Stormscope require only the installation of a single flat-pack antenna whereas radar requires a radome, dish antenna and associated extensive support structure. 3) Stormscope offers a 360^{o} field of view with the option of ground based preview whereas radar offers a more limited field of view (typically 120^{o}) and no ground usage.

4. Several disadvantages in Stormscope installation and operation are also apparent: 1) Stormscope is very sensitive to electrical currents induced by the various generators, motors, strobe lights, etc., onboard the aircraft. Location of the flat-pack antenna must therefore be closely coordinated with the manufacturer. 2) The Stormscope processor is limited both in rate and accuracy of data acquisition and no provision is made for active display update except through the CLEAR operation or acquisition of new data. As concluded earlier, however, these

limitations in display resolution do not seriously affect the severe weather avoidance capability provided by Stormscope.

SECTION X

RECOMMENDATIONS

1. An effort should be made to obtain additional data on Stormscope operation by performing direct penetration flights into thunderstorm formations. The test aircraft should be protected from the effects of hail, turbulence and direct lightning attachment and instrumented with Stormscope, radar, turbulence measuring devices and photographic recording equipment. Particular attention should be paid to radar contour areas of heavy precipitation in which Stormscope indicates low electrical activity.

2. An operational evaluation of Stormscope should be conducted by installing the unit on selected Air Force aircraft to obtain pilot and navigator reports on accuracy, reliability and ease of operation. Participating aircraft should be chosen from the major operational categories (e.g. cargo, trainer, fighter, etc.) and should be both radar and non-radar equipped to provide a broad cross section of flight profiles and operating conditions.

3. Consideration should be given to developing a display which would combine Stormscope and weather radar indications. This unit should be designed so that the two systems are not interdependent, thereby providing a backup if one system should fail.

APPENDIX A

SOFTWARE DEVELOPED FOR IN-FLIGHT EVALUATION OF STORMSCOPE

SOFTWARE TO CALCULATE POSITION
OF AIRCRAFT WITH TIME

```
1000 CLOSE #1
1010 REM ** INPUT START,STOP TIMES,FLIGHT LENGTH,HEADING,RANGE
1020 PRINT "START TIME";\INPUT BT
1030 PRINT "STOP TIME";\INPUT ST
1040 PRINT "NAUTICAL MILES";\INPUT NM
1050 PRINT "THETA";\INPUT TH
1060 PRINT "RANGE";\INPUT RG
1070 REM ** COMPUTE SCALE FACTOR FOR GRAPHIC DISPLAY
1080 SF=390/RG
1090 REM ** COMPUTE NUMBER OF 15 SECOND INCREMENTS FOR FLIGHT
1100 NI=((ST-BT)/15)
1110 REM ** COMPUTE THETA
1120 TH=450-TH
1130 PI=3.1416\TH=TH*(PI/180)
1140 MC=NM/NI
1150 REM ** DELETE VARIABLES
1160 DELETE PX,PY,TX
1170 REM ** DIMENSION PLANE X,Y COORDINATES, TIMES
1180 DIM PX(NI),PY(NI),TX(NI)\TX(0)=BT
1190 REM ** INPUT STARTING POINT FOR FLIGHT, FILE NAME
1200 PRINT "STARTING POINTS";\INPUT PX(0),PY(0)
1210 PRINT "FILE NAME";\INPUT FL$
1220 REM ** CALCULATE PLANE POSITION WITH TIME
1230 FOR I=1 TO NI
1240 PX(I)=MC*I*COS(TH)+PX(0)
1250 PY(I)=MC*I*SIN(TH)+PY(0)
1260 TX(I)=TX(I-1)+15
1270 NEXT I
1280 OPEN #1 AS DX1:FL$ FOR WRITE
1290 FOR I=0 TO NI
1300 WRITE #1,PX(I),PY(I),TX(I)\NEXT I
```

```
1310 PAGE\MOVE PX(0)*SF+512,PY(0)*SF+390
1320 REM ** PLOT PLANE TRACK TO VERIFY
1330 FOR I=1 TO NI
1340 DRAW PX(I)*SF+512,PY(I)*SF+390
1350 NEXT I
1360 REM ** PRINT NUMBER OF INCREMENTS CALCULATED
1370 PRINT NI
1380 CLOSE #1\STOP

READY
*
```

SOFTWARE TO PLOT STORMSCOPE DATA
FOR COMPARISON WITH LDAR

```
1000 CLOSE #1\CLOSE #2
1010 REM ** INPUT INCREMENTS,RANGE,HEADING
1020 PRINT "STORMSCOPE POINTS";\INPUT ST
1030 PRINT "NI";\INPUT NI
1040 PRINT "RANGE";\INPUT RG
1050 PRINT "HEADING";\INPUT HD
1060 REM ** CALCULATE THETA
1070 PI=3.1416\TH=360-HD\TH=TH*PI/180
1080 REM ** INPUT FILENAMES FOR PLANE TRACK, STSC POINTS
1090 PRINT "FILENAME 1";\INPUT FL$
1100 PRINT "FILENAME 2";\INPUT GL$
1110 REM ** DELETE ARRAYS
1120 DELETE SX,SY,T3,T2,T1,PX,PY,TY,TT,RX,RY
1130 REM ** DIMENSION ARRAYS FOR TIMES, PLANE STORMSCOPE POINTS
1140 DIM SX(ST),SY(ST),T3(ST),T2(ST),T1(ST),PY(NI),PX(NI)
1150 DIM TY(NI),TT(ST),RX(ST),RY(ST)
1160 REM ** READ STORMSCOPE POINTS AND TIMES
1170 OPEN #1 AS DX1:FL$ FOR READ
1180 FOR I=0 TO ST
1190 READ #1,SX(I),SY(I),T3(I),T2(I),T1(I)\EOF #1 GOTO 1200\NEXT I
1200 CLOSE #1\F1=0\F2=0
1210 REM ** CONVERT STORMSCOPE TIMES TO SECONDS
1220 TT=T3*3600+T2*60+T1
1230 REM ** READ PLANE TRACK POINTS
1240 OPEN #2 AS DX1:GL$ FOR READ
1250 FOR I=0 TO NI
1260 READ #2,PX(I),PY(I),TY(I)\EOF #2 GOTO 1270\NEXT I
1270 CLOSE #2
1280 REM ** CALCULATE SCALE FACTOR
1290 SF=390/RG
1300 REM ** DRAW COASTLINE, ETC
```

```
1310 PAGE\GOSUB 1610
1320 REM ** PRINT START TIME
1330 T4=ITP(TY(0)/3600)\T5=ITP((TY(0)-T4*3600)/60)
1340 T6=ITP(TY(0)-T4*3600-T5*60)
1350 XC=750\YC=770\MOVE XC,YC
1360 PRINT "BEG TIME";T4;":";T5;":";T6
1370 REM ** COMPARE TIMES FOR STSC AND PLANE TRACK POINTS
1380 IF TT(F2)>TY(F1) THEN GOTO 1400
1390 GOTO 1470
1400 F1=F1+1
1410 WAIT 500
1420 REM ** DRAW PLANE TRACK
1430 MOVE PX(F1-1)*SF+512,PY(F1-1)*SF+390
1440 DRAW PX(F1)*SF+512,PY(F1)*SF+390
1450 GOTO 1380
1460 REM ** CALCULATE ROTATION COORDINATES FOR STSC POINTS
1470 RX(F2)=SX(F2)*COS(TH)-SY(F2)*SIN(TH)+PX(F1)
1480 RY(F2)=SY(F2)*COS(TH)+SX(F2)*SIN(TH)+PY(F1)
1490 REM ** CHECK FOR OUT OF RANGE POINTS
1500 EX=SQR(RX(F2)*RX(F2)+RY(F2)*RY(F2))\IF EX>RG THEN 1540
1510 REM ** DRAW STORMSCOPE POINT
1520 SMOVE RX(F2)*SF+512,RY(F2)*SF+390
1530 RSDRAW 1,1,-1,0,0,-1,1,0,0,1
1540 F2=F2+1\IF F2=ST THEN GOTO 1550\GOTO 1380
1550 REM ** PRINT FINISH TIME
1560 T4=ITP(TY(NI)/3600)\T5=ITP((TY(NI)-T4*3600)/60)
1570 T6=ITP(TY(NI)-T4*3600-T5*60)
1580 MOVE XC,YC-30
1590 PRINT "END TIME";T4;":";T5;":";T6
1600 WAIT\STOP
1610 INITG
1620 REM ** OPEN FILE, READ COASTLINE POINTS
1630 OPEN #1 AS DX:"COAST1" FOR READ
1640 DIM FX(18),FY(18)
1650 READ #1,FX,FY\CLOSE #1
```

```
1660 REM ** INPUT RANGE, CALCULATE SCALE FACTOR
1670 SF=390/RG
1680 REM ** DRAW COASTLINE
1690 FX=FX*SF+512\FY=FY*SF+390
1700 SMOVE FX(0),FY(0)
1710 FOR I=1 TO 18
1720 DRAW FX(I),FY(I)
1730 NEXT I
1740 REM ** MARK LOAR SITE
1750 MOVE 510,396\DRAW 510,386,516,386
1760 REM ** LABEL GROUND RADAR SITE
1770 X=-20\Y=36\SMOVE X*SF+512,Y*SF+390
1780 RSMOVE 0,5\RSDRAW 0,-10\RSMOVE -5,5\RSDRAW 10,0
1790 REM ** DRAW VORTAC SYMBOL
1800 X=-36.9*SF+512\Y=0*SF+390\GOSUB 2010
1810 REM ** LABEL PATRICK AFB
1820 X=46*SF+512\Y=-17.5*SF+390\SMOVE X-6,Y-1
1830 SDRAW X,Y-1,X,Y+4,X-6,Y+4,X-6,Y-8
1840 REM ** DRAW CIRCLE
1850 NC=45\RD=260
1860 DIM CX(NC),CY(NC)
1870 OPEN #1 AS DX:"CIRCLE" FOR READ
1880 READ #1,CX,CY\CLOSE #1
1890 SMOVE 512+RD,390
1900 FOR I=0 TO 45
1910 DRAW CX(I)+512,CY(I)+390\NEXT I
1920 FOR I=45 TO 0 STEP -1\DRAW 512-CX(I),CY(I)+390\NEXT I
1930 FOR I=0 TO 45\DRAW 512-CX(I),390-CY(I)\NEXT I
1940 FOR I=45 TO 0 STEP -1\DRAW CX(I)+512,390-CY(I)\NEXT I
1950 MOVE 700,590\LB=260/SF\PRINT ITP(LB)
1960 MOVE 511,RD+400\RSDRAW 0,-20
1970 MOVE 750,YC-60\PRINT FL$
1980 MOVE 750,YC-90\PRINT "HEADING =":HD
1990 RETURN
2000 REM ** SUBROUTINE FOR DRAWING VORTAC SYMBOLS
```

SOFTWARE DEVELOPED TO REFORMAT LDAR DATA FROM 7-TRACK MAGNETIC TAPE TO FLEXIBLE DISC MEDIUM

```
      PROGRAM LDAR(INPUT,OUTPUT,TAPE5=INPUT,TAPE6=OUTPUT,
     *TAPE10,TAPE11)
C**
C** DEFINITION OF VARIABLES
C** AAV =  AVERAGE AZIMUTH OF LDAR STRIKE
C** AER =  AZIMUTH TOLERANCE ERROR
C** ER  =  ERROR TOLERANCE(NM) OF LDAR POINTS
C** KBT =  BEGIN TIME (HOUR/MIN OF PLOT START)
C** KET =  END TIME (HOUR/MIN OF PLOT STOP)
C** RAV =  AVERAGE RANGE OF LDAR STRIKE
C** RER =  RANGE TOLERANCE ERROR
C** RG  =  RANGE OF LDAR POINTS
C** TD  =  TIME (JULIAN DAY) OF LDAR STRIKE
C** THM =  TIME(HOUR/MIN)OF LDAR STRIKE
C** TS  =  TIME(SEC/MILSEC) OF LDAR STRIKE
C** X1  =  X STRIKE COORD. FROM LDAR STA. 1
C** X2  =  X STRIKE COORD. FROM LDAR STA. 2
C** Y1  =  Y STRIKE COORD. FROM LDAR STA. 1
C** Y2  =  Y STRIKE COORD. FROM LDAR STA. 2
C**
C** INIT. FILE & READ ERROR TOL., RANGE
      REWIND 10
      REWIND 11
      LCNT=0
      KCNT=0
      PRINT *,'FILE ? '
      READ(5,220)FILNM
      PRINT *,'RANGE ? '
      READ(5,*)RG
      PRINT *,'RANGE ERROR, ANGULAR ERROR ? '
      READ 5,*,RER,AER
      AER=AER/57.29578
      RG=1.5*RG
C** INIT. TERMINAL & SET PLOT SIZE
      CALL TERM(2,4096)
      CALL INITT(120)
      CALL CHRSIZ(4)
      IU=1.66*KCM(16.5)
      MINX=(4096-IU)/2
      MAXX=MINX+IU
      MINY=(3121-IU)/2
      MAXY=MINY+IU
      CALL TWINDO(MINX,MAXX,MINY,MAXY)
      CALL DWINDO(-RG,RG,-RG,RG)
  100 CALL ANMODE
C** INPUT TIME INTERVAL FOR PLOT
      PRINT *,'BEG. TIME, END TIME ? '
      READ(5,*)KBT,KET
      CALL NEWPAG
C** READ TIME, XSY COORD.
  140 READ(10,190)X1,Y1,Z1,X2,Y2,Z2,TD,THM,TS
      IF(EOF(10))160,150
  150 LCNT=LCNT+1
      X1=X1/1853.2
      Y1=Y1/1853.2
      X2=X2/1853.2
      Y2=Y2/1853.2
C** TEST ACQUIS. TIME
      IF(THM.LT.KBT)GO TO 140
      IF(THM.GT.KET)GO TO 160
C** TEST FOR POINT OUT OF TOLERANCE
      R1=SQRT(X1*X1+Y1*Y1)
      R2=SQRT(X2*X2+Y2*Y2)
      IF(ABS(R1-R2).GT.RER)GO TO 140
      A1=ATAN(Y1/X1)
      IF(X1.LT.0.0)A1=A1+3.14159
      A2=ATAN(Y2/X2)
      IF(X2.LT.0.0)A2=A2+3.14159
      IF(ABS(A1-A2).GT.AER)GO TO 140
C** CALC. AVERAGE & SAVE
      RAV=(R1+R2)/2.
      AAV=(A1+A2)/2.
      WRITE(11,200)RAV,AAV,TD,THM,TS
C** PLOT POINT
      CALL MOVEA(RAV*COS(AAV),RAV*SIN(AAV))
      CALL SYMBL
      KCNT=KCNT+1
      GO TO 140
C** PLOT RANGE MARKERS & PRINT FILE INFORMATION
  160 CALL MOVEA(0,0)
      CALL CROSS
      CALL MOVEA(0,RG/1.5)
      CALL CROSS
      CALL CHRSIZ(4)
      CALL MOVABS(3500,3000)
      CALL ANMODE
      AER=AER*57.29578
      WRITE(6,240)FILNM,KBT,KET,RER,AER,KCNT,LCNT
      CALL HDCOPY
      STOP
  190 FORMAT(9(E15.8))
  200 FORMAT(5(E15.8))
  220 FORMAT(A10)
  240 FORMAT(1HX,A10/1HX,I4,'-',I4/1HX,'RER=',F4.1,
     *2X,'AER=',F4.1/1HX,I4,'/',I4)
      END
C**
C**
      SUBROUTINE SYMBL
      CALL MOVREL(-10,-5)
      CALL DRWREL(10,10)
      CALL DRWREL(10,-10)
      CALL DRWREL(-20,0)
      RETURN
      END
C**
C**
      SUBROUTINE CROSS
      CALL MOVREL(-20,0)
      CALL DRWREL(40,0)
      CALL MOVREL(-20,20)
      CALL DRWREL(0,-40)
      RETURN
      END
```

THIS PAGE IS BEST QUALITY PRACTICABLE
FROM COPY FURNISHED TO DDC

SOFTWARE DEVELOPED TO PLOT LDAR POINTS

```
1000 CLOSE #1
1010 PRINT "RANGE";\INPUT RG\SF=390/RG
1020 PRINT "FILENAME";\INPUT GL$
1030 PRINT "LDAR POINTS";\INPUT LD
1040 PAGE\PRINT "START TIME";\INPUT BT
1050 PRINT "STOP TIME";\INPUT ST
1060 DELETE RR,A,AA,D,HM,TL,LX,LY
1070 DIM TL(LD),LX(LD),LY(LD)
1080 OPEN #1 AS DX1 GL$ FOR READ
1090 FOR I=0 TO LD
1100 READ #1,RR,AA,D,HM,TL(I)
1110 IF RR>120 THEN 1160
1120 LX(I)=RR*COS(AA)\LY(I)=RR*SIN(AA)
1130 M=HM/100-ITP(HM/100)\M=M*6000
1140 H=(ITP(HM/100)-4)*3600
1150 TL(I)=TL(I)+M+H
1160 EOF #1 GOTO 1170\NEXT I
1170 CLOSE #1
1180 X=0\Y=0\SMOVE X*SF+512,Y*SF+390
1190 RSMOVE 0,5\RSDRAW 0,-10\RSMOVE -5,5\RSDRAW 10,0
1200 MOVE 512,80*SF+390\DRAW 512,82*SF+390
1210 MOVE 520,80*SF+390\PRINT (2*RG)/3;" NM"
1220 FOR I=0 TO LD
1230 IF TL(I)>BT THEN 1240\GOTO 1270
1240 IF TL(I)>ST THEN 1280
1250 SMOVE LX(I)*SF+512,LY(I)*SF+390
1260 RSDRAW 1,1,-1,0,0,-1,1,0,0,1
1270 NEXT I
1280 WAIT\GOTO 1040

READY
```

```
2010 SMOVE X-5,Y+8
2020 SDRAW X+5,Y+8,X+10,Y,X+5,Y-8,X-5,Y-8,X-10,Y,X-5,Y+8
2030 RETURN

READY
*
```

SOFTWARE DEVELOPED FOR QUANTITATIVE
ANALYSIS OF DATA POINTS

```
1010 REM ***** INPUT FILE NAMES, POINT DENSITY
1020 PAGE\PRINT "READ FILE ";\INPUT RF$
1030 PRINT "WRITE FILE ";\INPUT WF$
1040 CLOSE #1\CLOSE #2
1050 OPEN #1 AS DX1:RF$ FOR READ
1070 PRINT "POINT DENSITY ";\INPUT DN\DN=DN*DN
1080 PRINT "NO. POINTS ";\INPUT TP\TP=TP-1\SP=TP
1090 REM ***** READ UNPROCESSED ARRAYS
1100 NL=0\RA=120\RS=RA*RA\GOSUB 1940
1110 REM ***** SETUP PLOT AXES & PLOT POINTS
1120 VIEWPORT 100,900,0,800
1130 WINDOW -RA,RA,-RA,RA
1160 GOSUB 8000\GOSUB 2040
1170 REM ***** DIMEN. GROUP ARRAYS
1180 SMOVE 0,680\PRINT "NO. GROUPS ";\INPUT NG\NG=NG-1
1190 DELETE BX,BY,SX,SY,QN$,QX,QY
1200 DIM BX(NG),BY(NG),SX(NG),SY(NG),QN$(NG),QX(NG),QY(NG)
1210 REM ***** ESTABLISH QUAD. & BEGIN PT. FOR EACH GP.
1220 FOR I=0 TO NG
1230 K=775-I*30
1240 SMOVE 525,K\PRINT "GROUP-";I+1;" QUAD "\GIN QN$(I),QX(I),QY(I)
1250 SMOVE 525,K\PRINT TAB(14);QN$(I)
1260 SMOVE 525,K\PRINT TAB(16);"BPT"\GIN AN$,BX(I),BY(I)
1270 SMOVE 525,K\PRINT TAB(20);BX(I),BY(I)
1280 GOTO ASC(QN$(I))-48 OF 1290,1300,1310,1320
1290 SX(I)=1\SY(I)=1\GOTO 1330
1300 SX(I)=-1\SY(I)=1\GOTO 1330
1310 SX(I)=-1\SY(I)=-1\GOTO 1330
1320 SX(I)=1\SY(I)=-1
1330 NEXT I
1340 PRINT "^E^W"\GOSUB 8000
1370 SMOVE 0,775\PRINT "WRITE FILE : ";WF$
1375 PRINT "DENSITY =";SQR(DN)
1380 REM *****
```

```
1390 REM ***** PROCESS EACH GROUP
1400 REM *****
1410 FOR I=0 TO NG
1420 REM ***** ELIM. PTS. BY QUADRANT
1430 FOR J=0 TO TP
1440 IF SGN(PX(J)-QX(I))=SX(I) THEN 1450\GOTO 1460
1450 IF SGN(PY(J)-QY(I))=SY(I) THEN 1510
1460 IF J<TP THEN 1470\TP=TP-1\GOTO 1520
1470 PX(J:TP-1)=PX(J+1:TP)
1480 PY(J:TP-1)=PY(J+1:TP)
1490 J=J-1
1500 TP=TP-1
1510 NEXT J
1520 PRINT "^G"
1530 REM ***** ELIM. PTS. BY DENSITY
1540 DELETE GX,GY\DIM GX(TP+1),GY(TP+1)
1550 GX(0)=BX(I)\GY(0)=BY(I)
1560 K=0\L=0
1570 FOR J=0 TO TP
1580 TX=GX(K)-PX(J)\TX=TX*TX
1590 TY=GY(K)-PY(J)\TY=TY*TY
1600 IF TX+TY>DN THEN 1670
1610 IF J<TP THEN 1620\GOTO 1680
1620 L=L+1\GX(L)=PX(J)\GY(L)=PY(J)
1630 PX(J:TP-1)=PX(J+1:TP)
1640 PY(J:TP-1)=PY(J+1:TP)
1650 J=J-1
1660 TP=TP-1
1670 NEXT J
1680 IF K=L THEN 1700\K=K+1\GOTO 1570
1690 REM ***** GROUP ESTABLISHED - COMP. CENTROID
1700 PX(0:K)=GX(0:K)\PY(0:K)=GY(0:K)
1710 CX=MEA(PX(0:K))\CY=MEA(PY(0:K))
1740 REM ***** PLOT GROUP
1750 TP=K\GOSUB 2040
```

```
1760 MOVE CX-20,CY\DRAW CX+20,CY
1770 MOVE CX,CY-20\DRAW CX,CY+20
1772 PRINT I+1
1780 REM ***** CONV. TO POLAR & COMP. STD. DEV.
1790 POLAR PX(0:K),PY(0:K)
1792 GY(0:K)=PY(0:K)/6.2832
1794 PY(0:K)=PY(0:K)-ITP(GY(0:K))
1796 FOR J=0 TO K
1798 IF PY(J)<0 THEN PY(J)=PY(J)+6.2832
1799 NEXT J
1800 MR=MEA(PX(0:K))\MT=MEA(PY(0:K))
1810 DR=0\DT=0
1820 FOR J=0 TO TP
1830 K=PX(J)-MR\K=K*K
1840 L=PY(J)-MT\L=L*L
1850 DR=DR+K\DT=DT+L
1860 NEXT J
1870 DR=SQR(DR/TP)\DT=SQR(DT/TP)
1890 SMOVE 525,750-NL*25\PRINT "GROUP";I+1;
1892 PRINT "  R =";MR;"  A =";MT*57.296
1900 SMOVE 525,750-(NL+1)*25\PRINT TAB(8);
1902 PRINT " DR =";DR;" DA =";DT*57.296
1910 TP=SP\NL=NL+2\GOSUB 1940
1920 NEXT I
1930 PRINT "^E^W"\STOP
1940 REM ***** ROUTINE TO READ UNPROCESSED ARRAYS
1950 CLOSE #1\OPEN #1 AS DX1:RF$ FOR READ
1955 EOF #1 GOTO 2020
1960 DELETE PX,PY\DIM PX(TP),PY(TP)
1970 FOR J=0 TO TP
1980 READ #1,DA,HM,SS,PX(J),PY(J)
1990 IF PX(J)*PX(J)+PY(J)*PY(J)<RS THEN 2010
2000 J=J-1\TP=TP-1
2010 NEXT J
2020 RETURN
```

SOFTWARE FOR QUANTITATIVE COMPARISON OF
AREA COVERAGE FOR STORMSCOPE AND LDAR

```
1000 NE=500\DELETE XP,YP,T
1010 DIM XP(NE),YP(NE+1),T(4)
1020 PAGE\SMOVE 0,750
1030 PRINT "1 = INPUT POINTS"\PRINT "2 = CALIBRATE PAD"
1040 INPUT AN\IF AN>2 THEN 1020\IF AN<1 THEN 1020
1050 GOTO AN OF 1070,1410
1060 REM *****
1070 REM INPUT POINTS
1080 REM *****
1090 REM SETUP COORD. AXES
1100 GOSUB 1700
1110 FOR J=1 TO NG
1120 NP=0
1130 GOSUB 1530
1132 SMOVE 500,500
1140 REM CONVERT TO USER UNITS
1150 REM *****
1170 REM INCR. PTR. & CHK FOR FULL ARRAYS
1180 NP=NP+1\IF NP<NE THEN 1192
1190 PRINT "^GARRAY FULL"\GOTO 1030
1192 XP(NP)=SX*(X-XI)\YP(NP)=SY*(Y-YI)
1204 XP(NP)=(XP(NP)-511)*RX/1023
1206 YP(NP)=(YP(NP)-390)*RY/780
1210 REM CHK FOR INPUT END
1220 GETLOC "177570",CS\IF CS=0 THEN 1130
1230 PRINT "^G"\GOSUB 1260
1240 NEXT J
1241 WAIT
1242 GOTO 1020
1250 REM *****
1260 REM DISPLAY POINTS
1270 REM *****
1280 MOVE XP(1),YP(1)
1290 FOR I=1 TO NP
```

```
1300 DRAW XP(I),YP(I)
1310 NEXT I
1320 REM COMP ENCLOSED AREA
1330 A=0\YP(0)=YP(NP)\YP(NP+1)=YP(1)
1340 FOR I=2 TO NP
1350 A=A+XP(I)*(YP(I+1)-YP(I-1))
1360 NEXT I
1370 A=ABS(A/2)
1380 MOVE XP(1),YP(1)\PRINT "AREA = ";A
1390 RETURN
1400 REM *****
1410 REM CALIBRATE PAD
1420 REM *****
1430 PRINT "PUT PEN IN LOWER LEFT CORNER"
1440 GOSUB 1520\XI=X\YI=Y
1450 PRINT "MOVE PEN TO UPPER RIGHT CORNER"
1460 GOSUB 1520\SX=1023/(X-XI)\SY=780/(Y-YI)
1470 PRINT "X RANGE (USER UNITS) ";\INPUT RX
1480 PRINT "Y RANGE (USER UNITS) ";\INPUT RY
1490 WINDOW -RX/2,RX/2,-RY/2,RY/2
1500 VIEWPORT 100,900,0,800
1510 GOTO 1030
1520 REM *****
1530 REM ROUTINE TO READ POINTS
1540 REM *****
1550 PUTLOC "167740",1
1560 FOR I=0 TO 4
1570 GETLOC "167740",C,15,15
1580 IF C=0 THEN 1570
1590 GETLOC "167744",C\PUTLOC "167742",C
1600 IF I<>0 THEN 1630
1610 GETLOC "167742",C,15,15
1620 IF C=1 THEN 1630\GOTO 1570
1630 GETLOC "167742",T(I),0,5
1640 NEXT I
```

```
1650 PUTLOC "167740",0
1660 X=T(1)+(T(2)*64)\Y=T(3)+(T(4)*64)
1670 PRINT "^G"
1680 RETURN
1690 REM *****
1700 REM ROUTINE TO PLOT COORD. AXES
1710 REM *****
1720 PRINT "FILE NAME ";\INPUT FL$
1730 PRINT "NO. GROUPS ";\INPUT NG
1740 PAGE\MOVE 0,780\PRINT "FILE : ";FL$
1745 MOVE -RX/2,0
1750 SI=10\K=RX/SI
1760 FOR I=1 TO K\RSDRAW 0,7\RSMOVE 0,-7\RDRAW SI,0\NEXT I
1770 RSDRAW 0,7\PRINT RX/2\MOVE 0,-RY/2
1780 K=RY/10
1790 FOR I=1 TO K\RSDRAW 7,0\RSMOVE -7,0\RDRAW 0,SI\NEXT I
1800 RSDRAW 7,0\PRINT RY/2
1810 RETURN
1820 REM *****

READY
*
```

APPENDIX B

COMPARISON OF ELECTRICAL ACTIVITY CENTROIDS CALCULATED FROM LDAR AND STORMSCOPE DATA

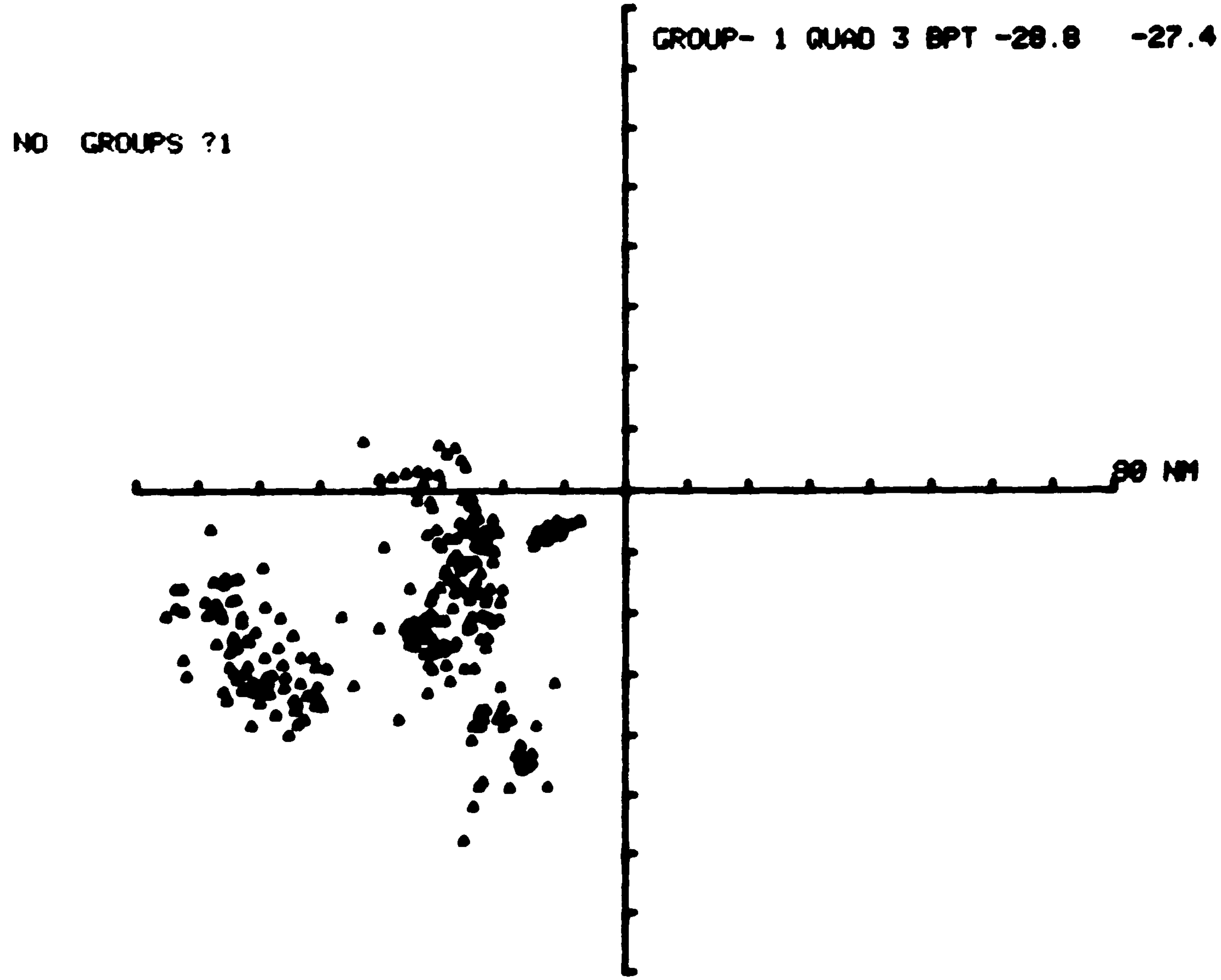

a. LDAR Electrical Activity

Figure B-1. Comparison of LDAR and Stormscope Electrical Activity, Run 1, 25 July 1978.

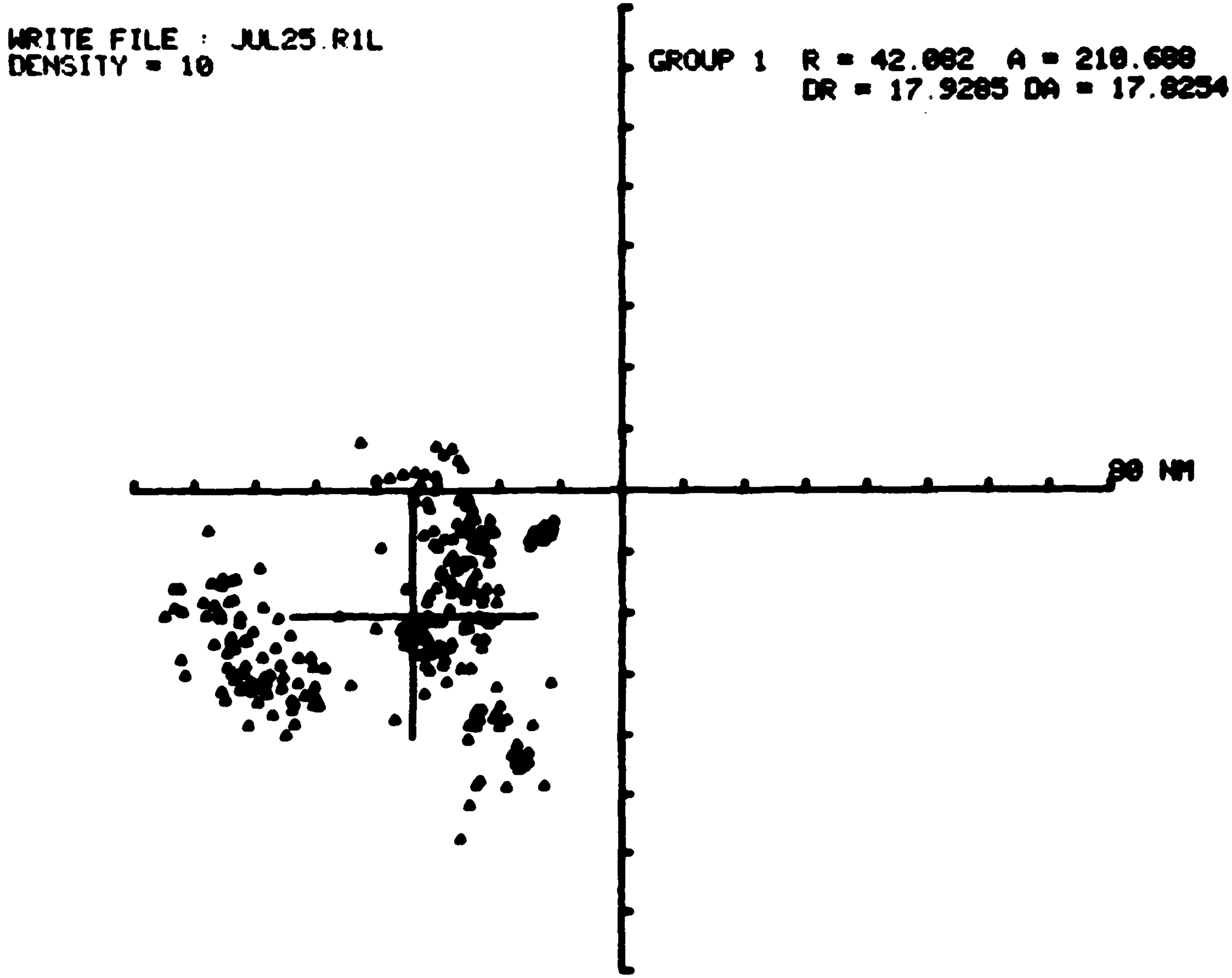

b. Centroids of LDAR Electrical Activity

Figure B-1. Comparison of LDAR and Stormscope Electrical Activity, Run 1, 25 July 1978.

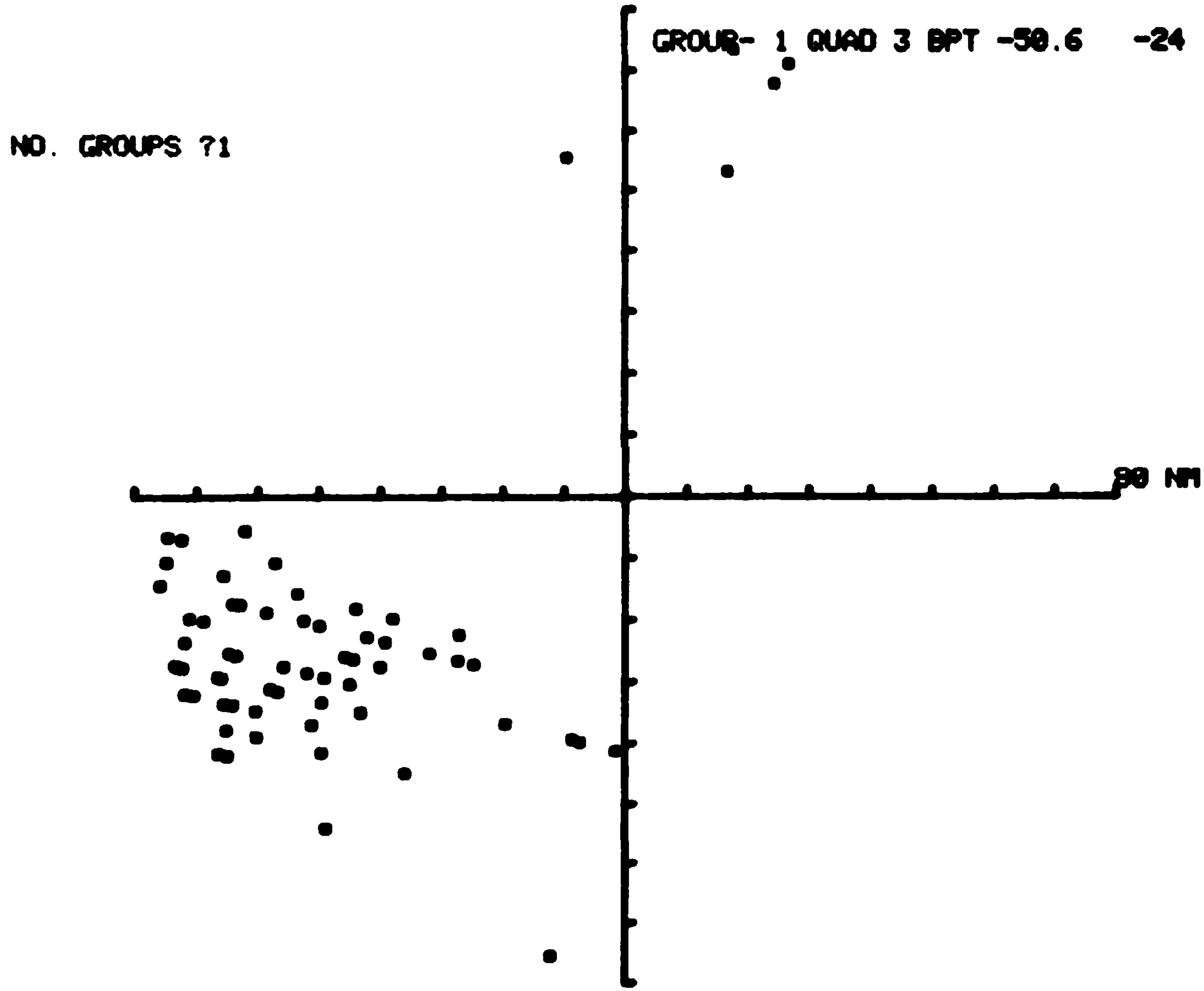

c. Stormscope Electrical Activity

Figure B-1. Comparison of LDAR and Stormscope Electrical Activity, Run 1, 25 July 1978.

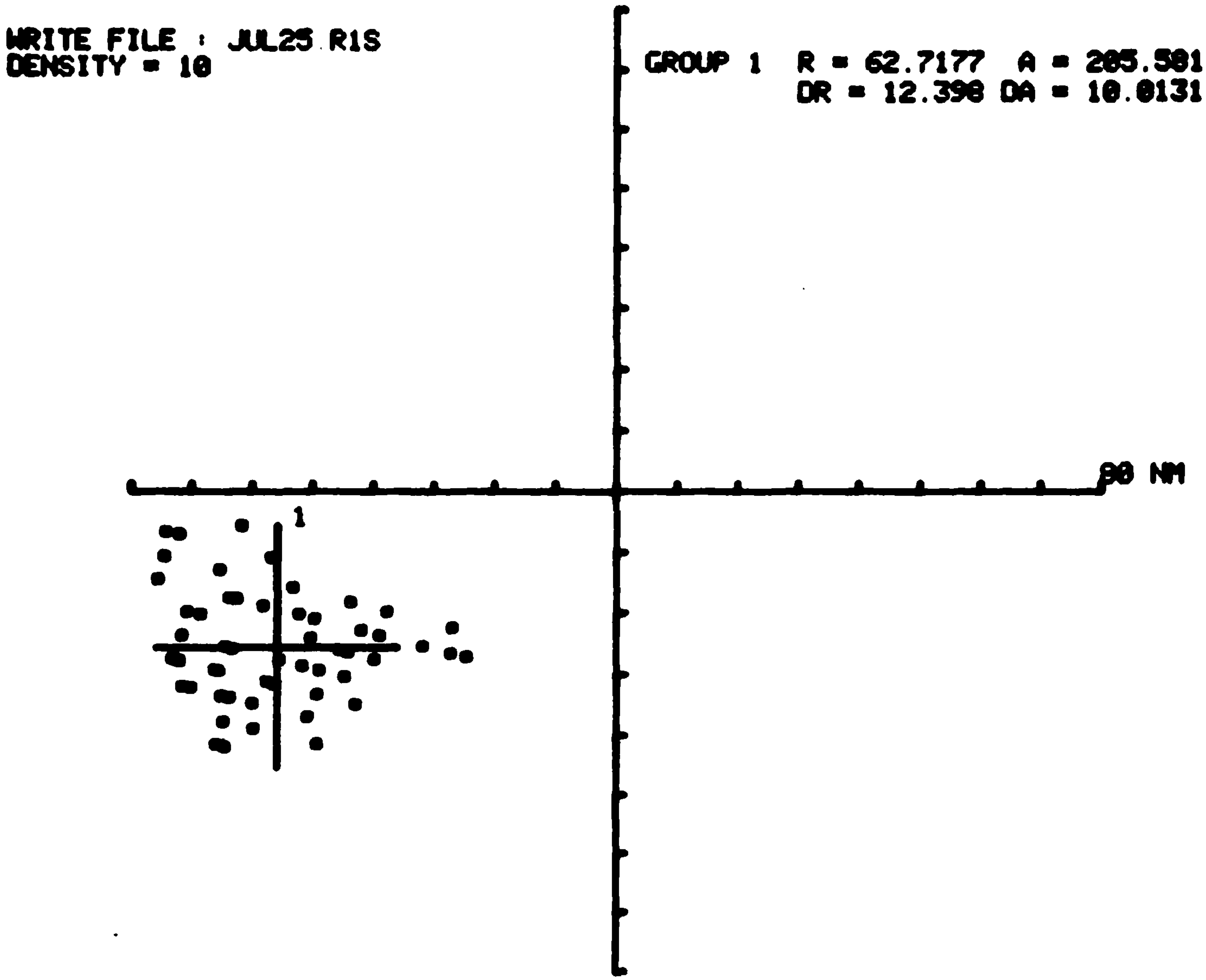

d. Centroids of Stormscope Electrical Activity

Figure B-1. Comparison of LDAR and Stormscope Electrical Activity, Run 1, 25 July 1978.

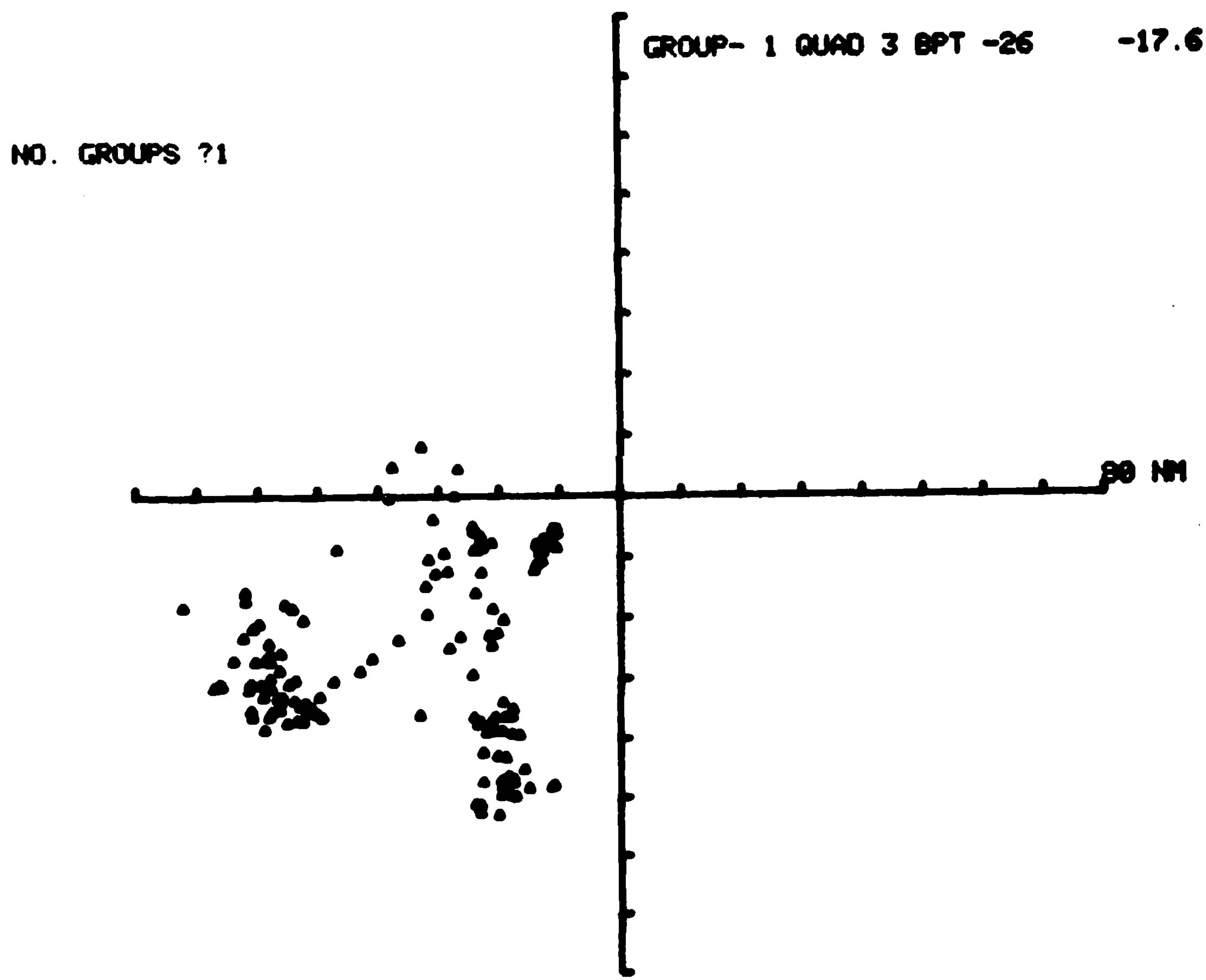

a. LDAR Electrical Activity

Figure B-2. Comparison of LDAR and Stormscope Electrical Activity, Run 2, 25 July 1978.

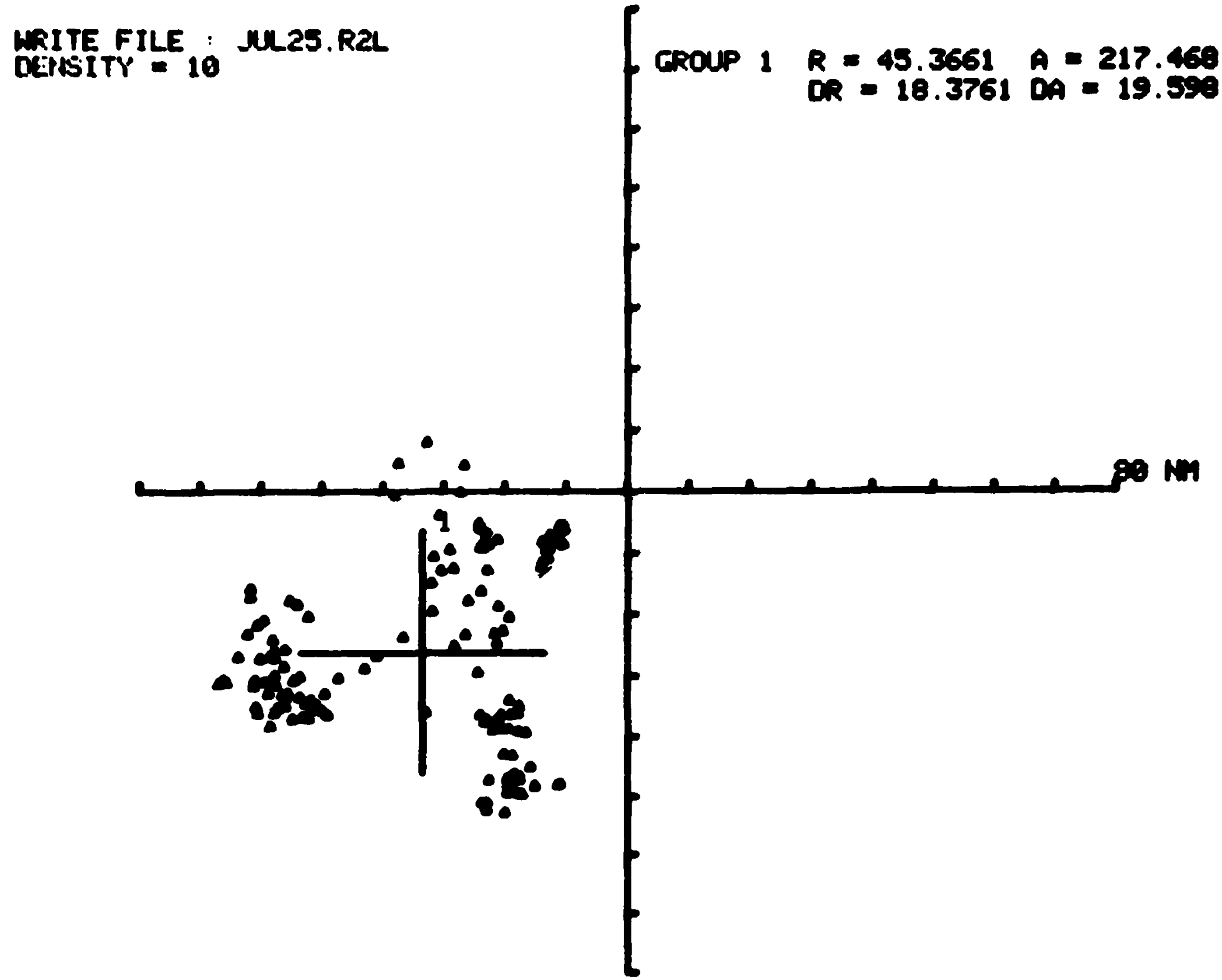

b. Centroids of LDAR Electrical Activity

Figure B-2. Comparison of LDAR and Stormscope Electrical Activity, Run 2, 25 July 197..

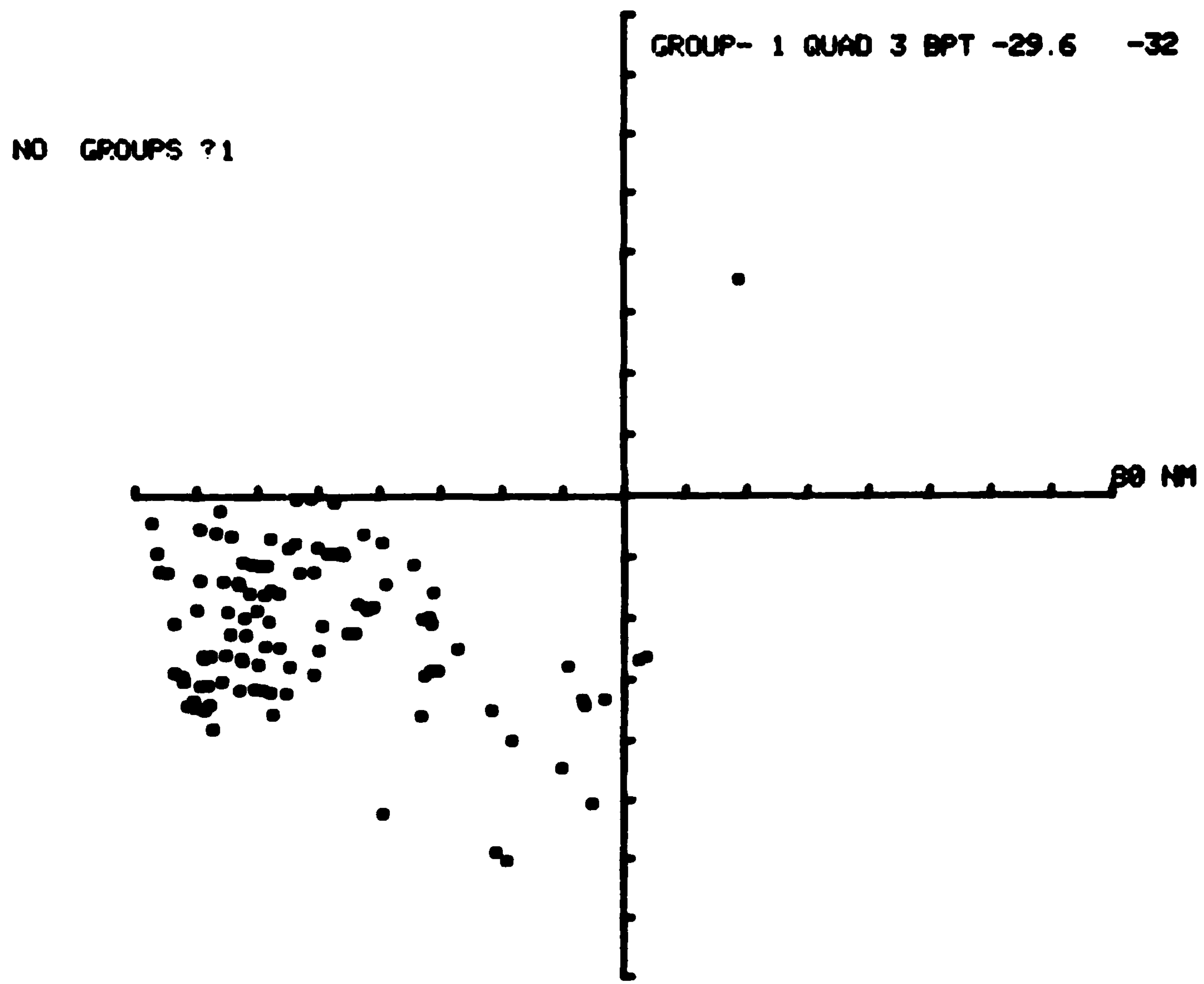

c. Stormscope Electrical Activity

Figure B-2. Comparison of LDAR and Stormscope Electrical Activity, Run 2, 25 July 1978.

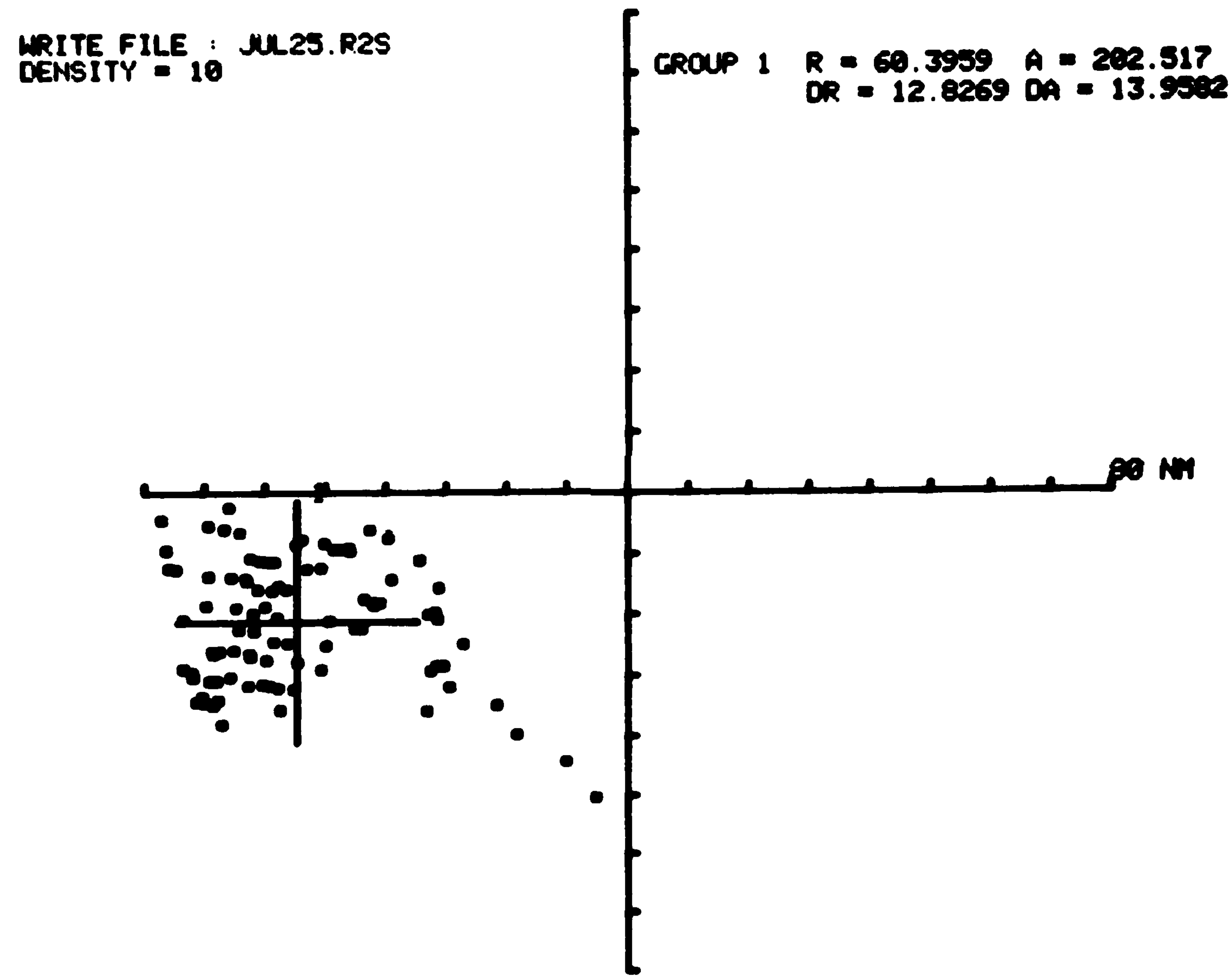

d. Centroids of Stormscope Electrical Activity

Figure B-2. Comparison of LDAR and Stormscope Electrical Activity, Run 2, 25 July 1978.

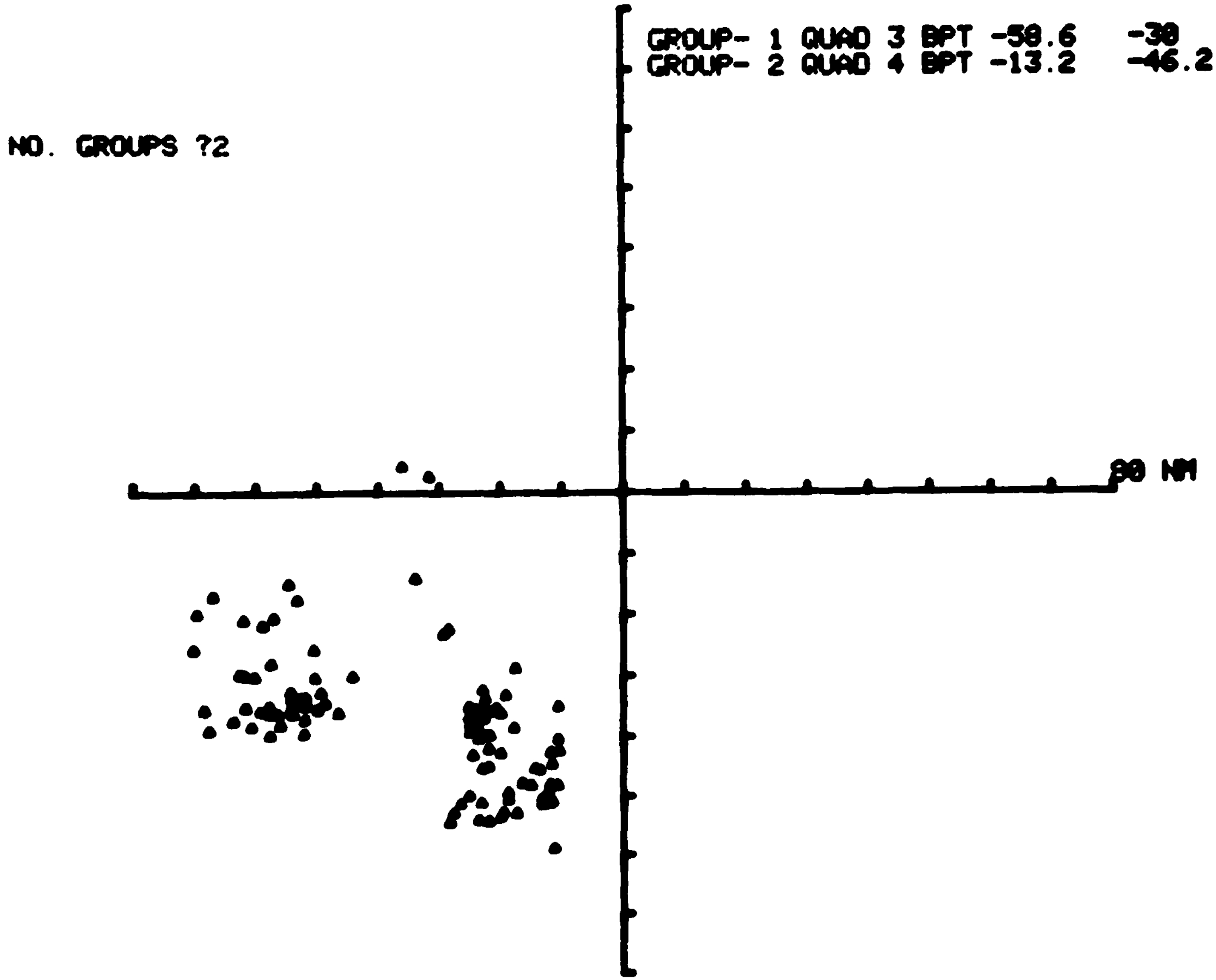

a. LDAR Electrical Activity

Figure B-3. Comparison of LDAR and Stormscope Electrical Activity, Run 3, 25 July 1978.

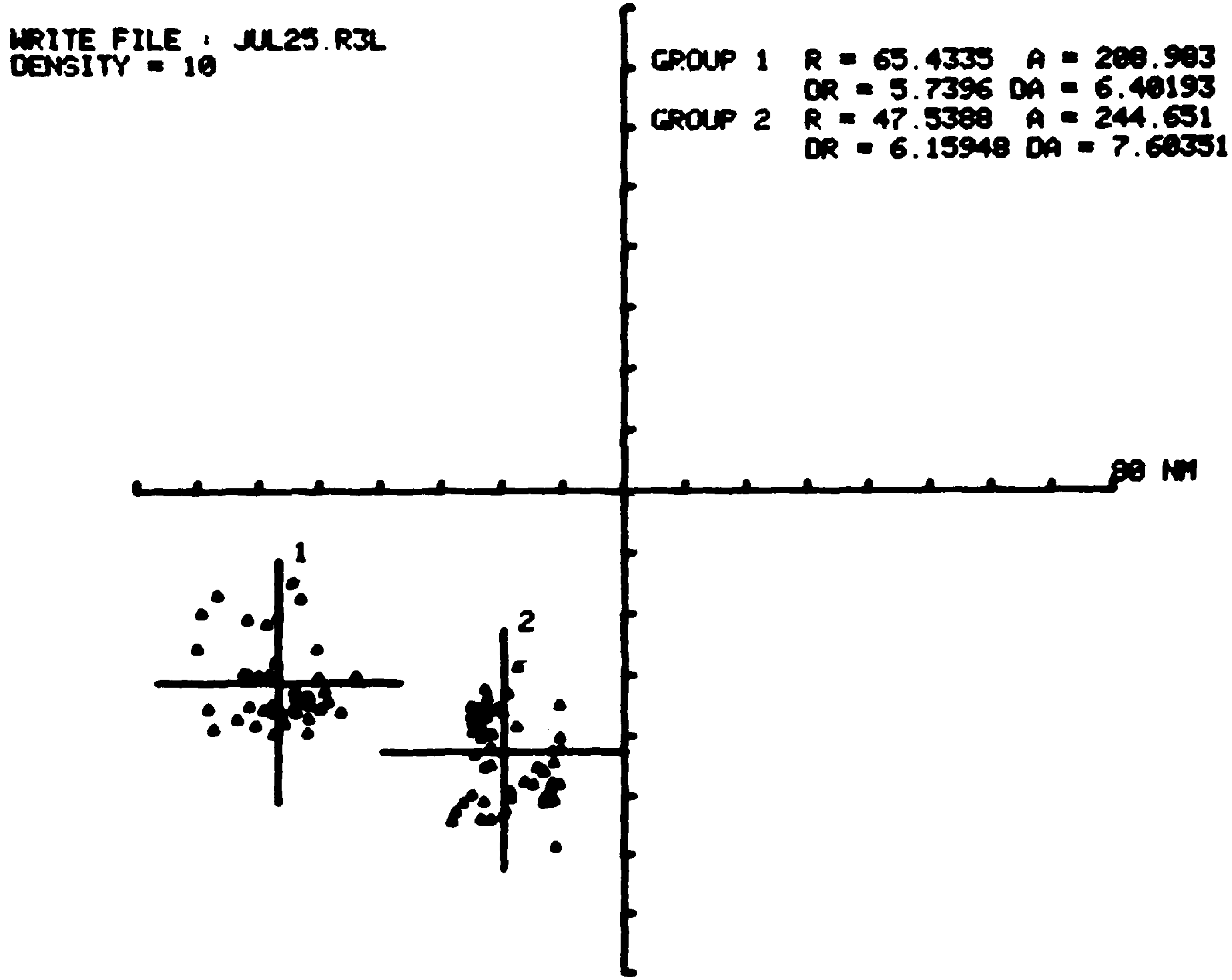

b. Centroids of LDAR Electrical Activity

Figure B-3. Comparison of LDAR and Stormscope Electrical Activity, Run 3, 25 July 1978.

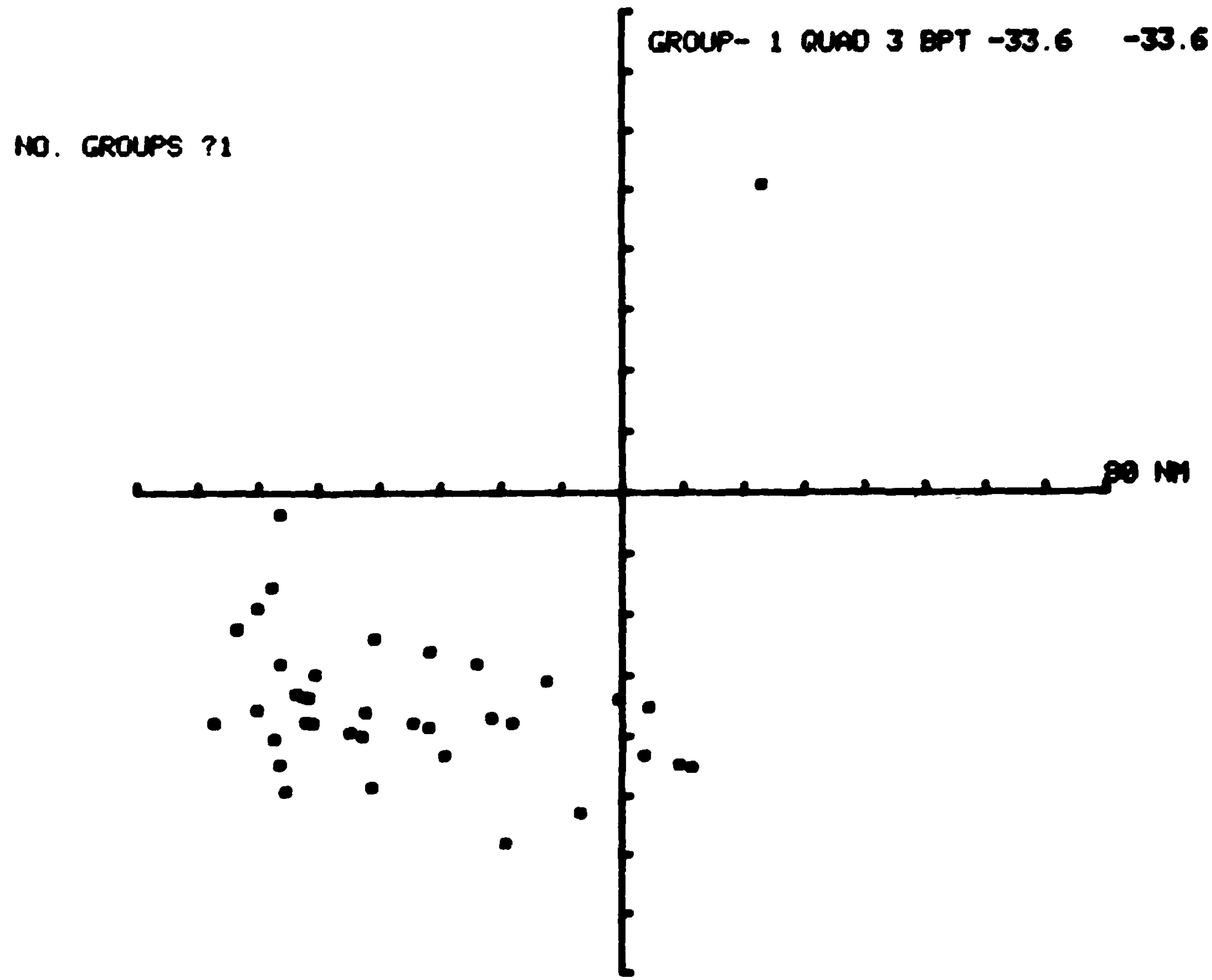

c. Stormscope Electrical Activity

Figure B-3. Comparison of LDAR and Stormscope Electrical Activity, Run 3, 25 July 1978.

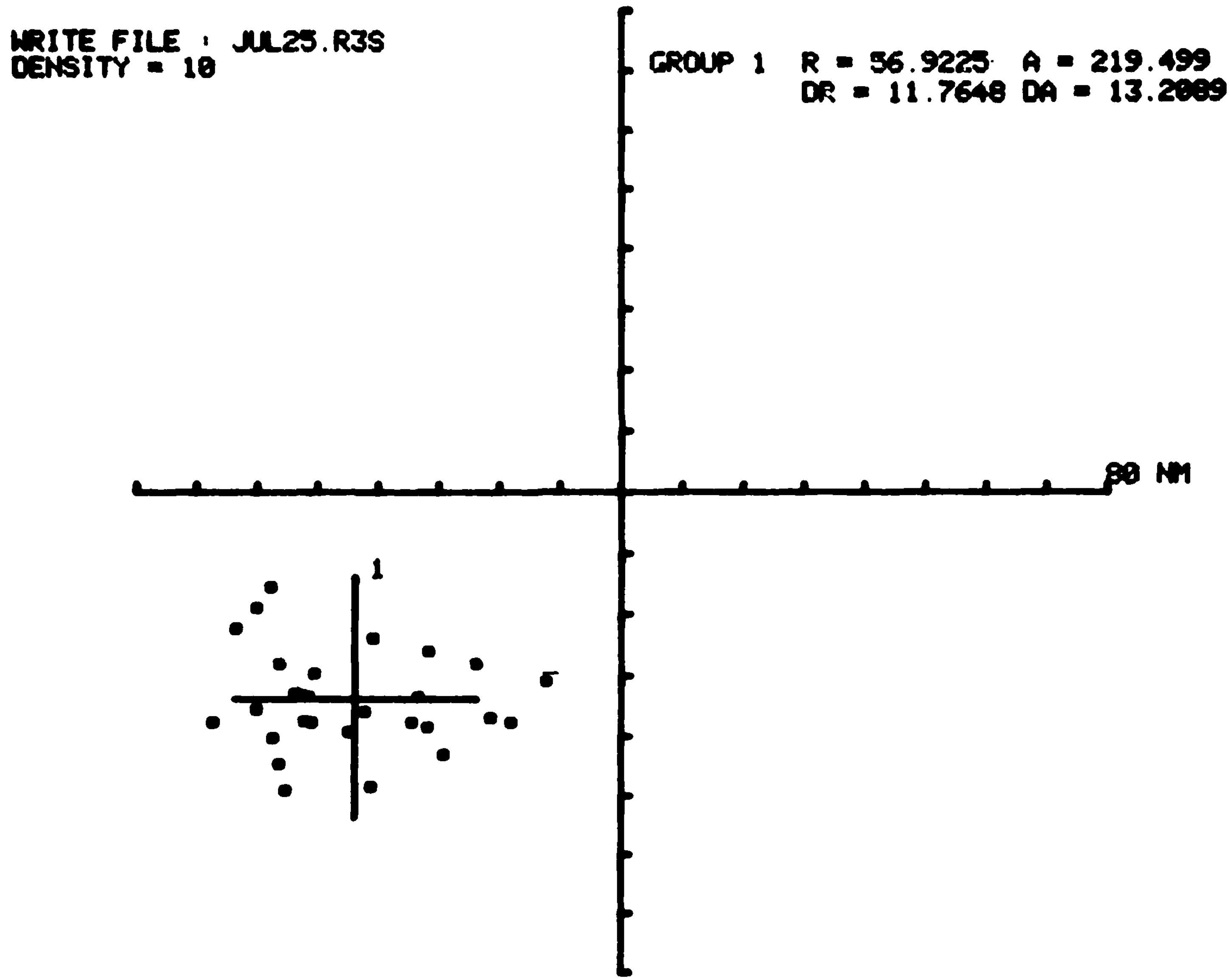

d. Centroids of Stormscope Electrical Activity

Figure B-3. Comparison of LDAR and Stormscope Electrical Activity, Run 3, 25 July 1978.

AD-A087 426   AIR FORCE WRIGHT AERONAUTICAL LABS WRIGHT-PATTERSON AFB OH   F/G 1/2
IN-FLIGHT EVALUATION OF A SEVERE WEATHER AVOIDANCE SYSTEM FOR A--ETC(U)
MAY 80   R K BAUM, T J SEYMOUR   FAA/ARD-740
UNCLASSIFIED   AFWAL-TR-80-3022   NL

2 . 2

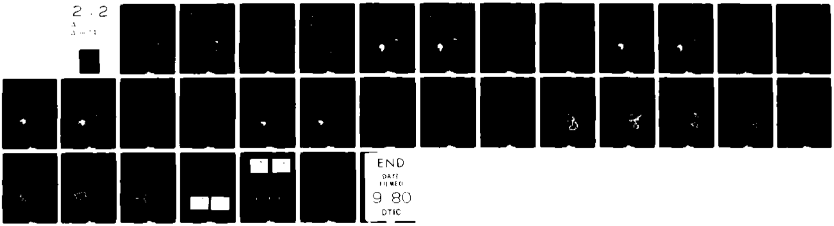

END
DATE
FILMED
9 80
DTIC

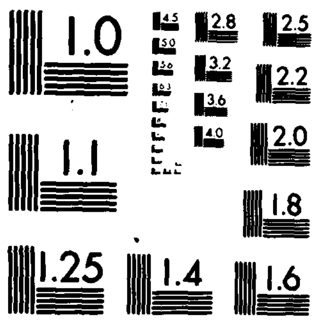

MICROCOPY RESOLUTION TEST CHART
NATIONAL BUREAU OF STANDARDS 1963-A

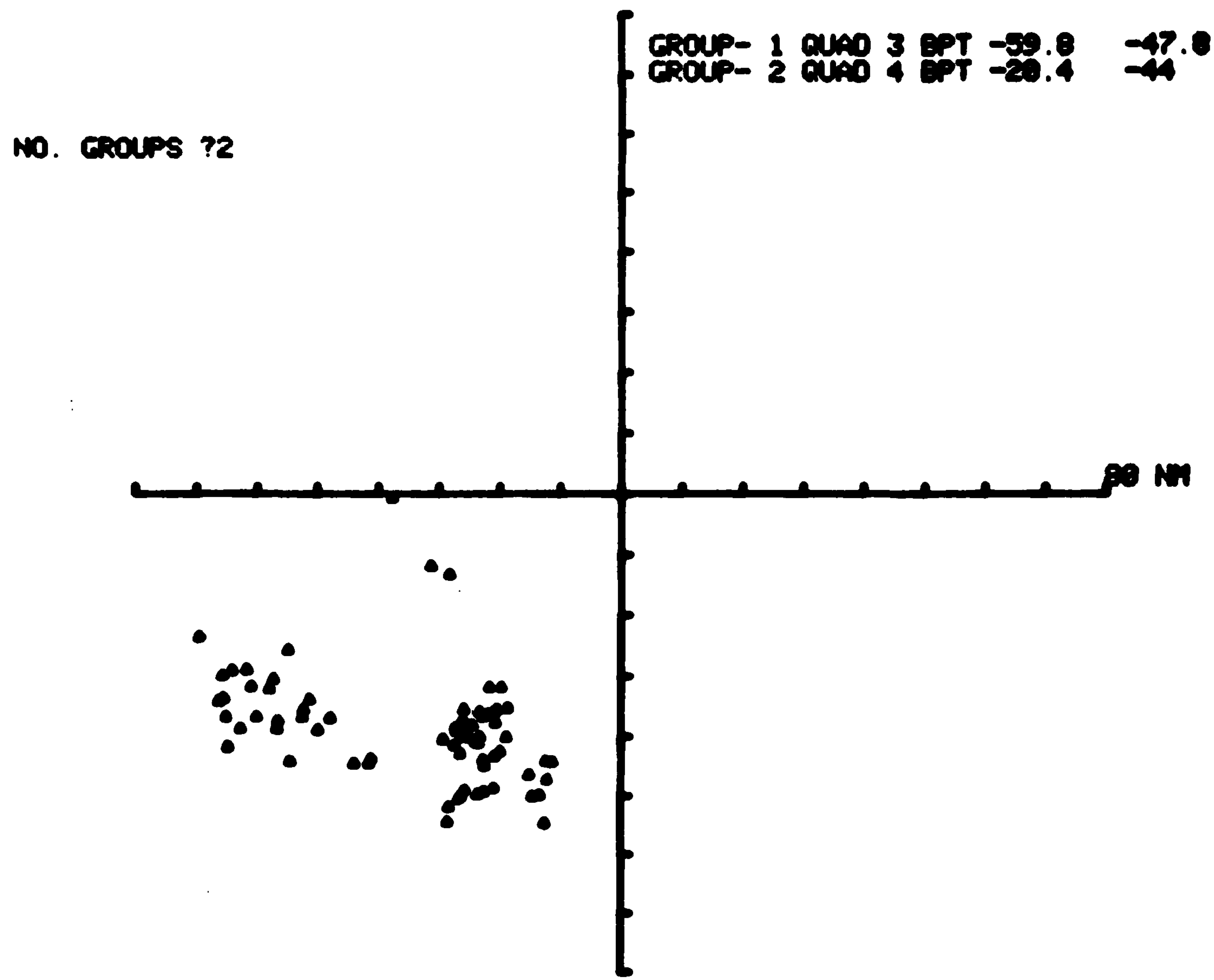

a. LDAR Electrical Activity

Figure B-4. Comparison of LDAR and Stormscope Electrical Activity, Run 4, 25 July 1978.

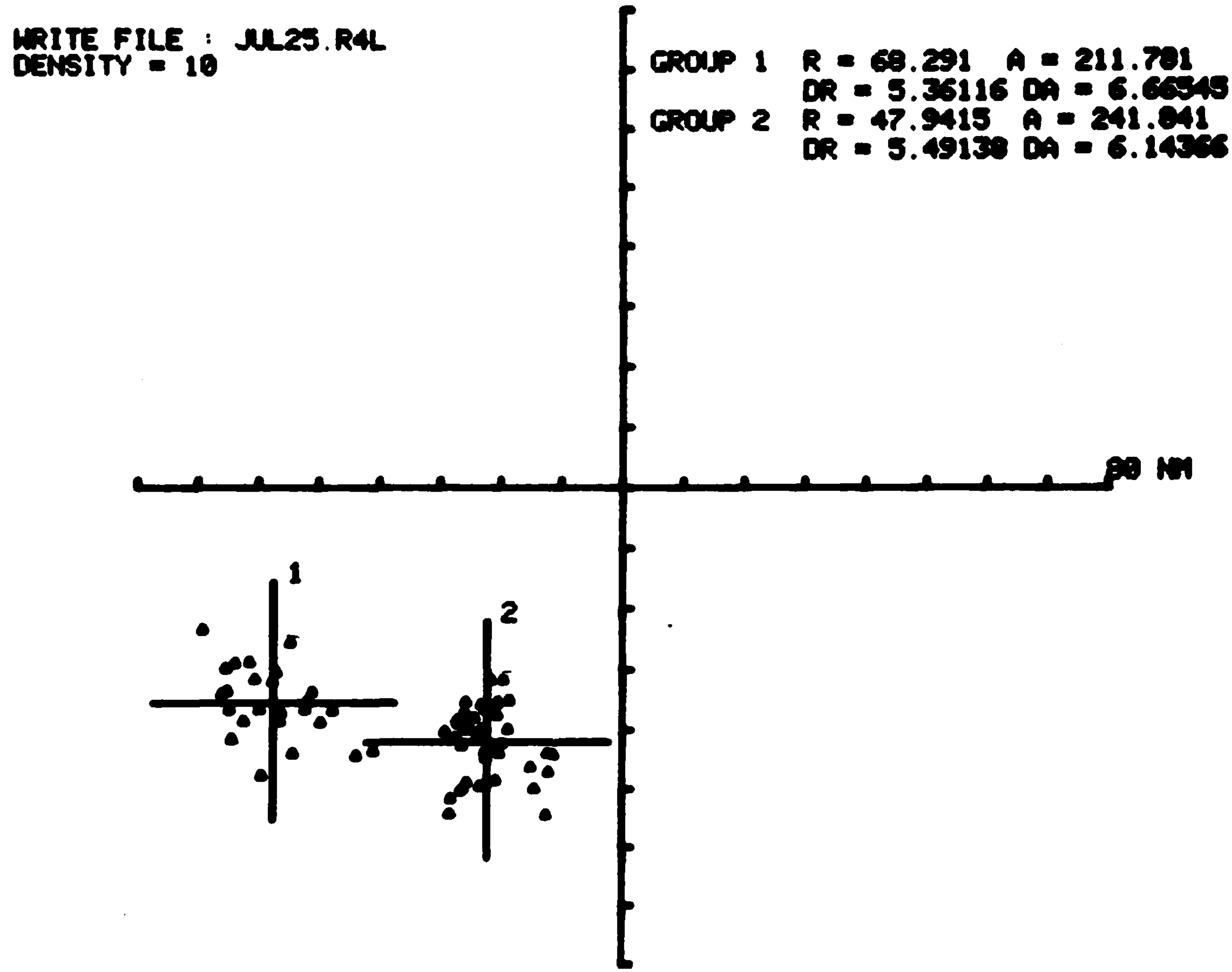

b. Centroids of LDAR Electrical Activity

Figure B-4. Comparison of LDAR and Stormscope Electrical Activity, Run 4, 25 July 1978.

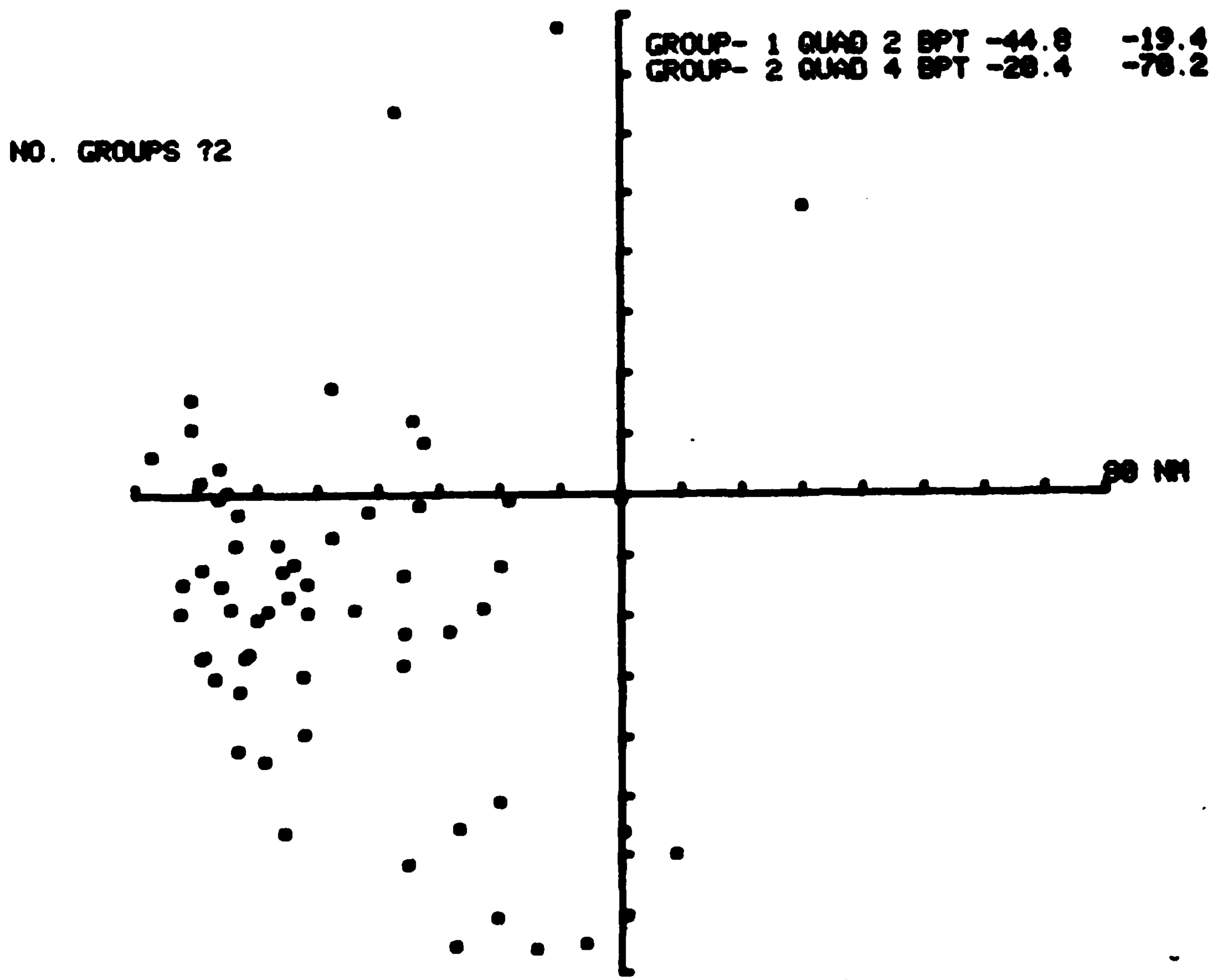

c. Stormscope Electrical Activity

Figure B-4. Comparison of LDAR and Stormscope Electrical Activity, Run 4, 25 July 1978.

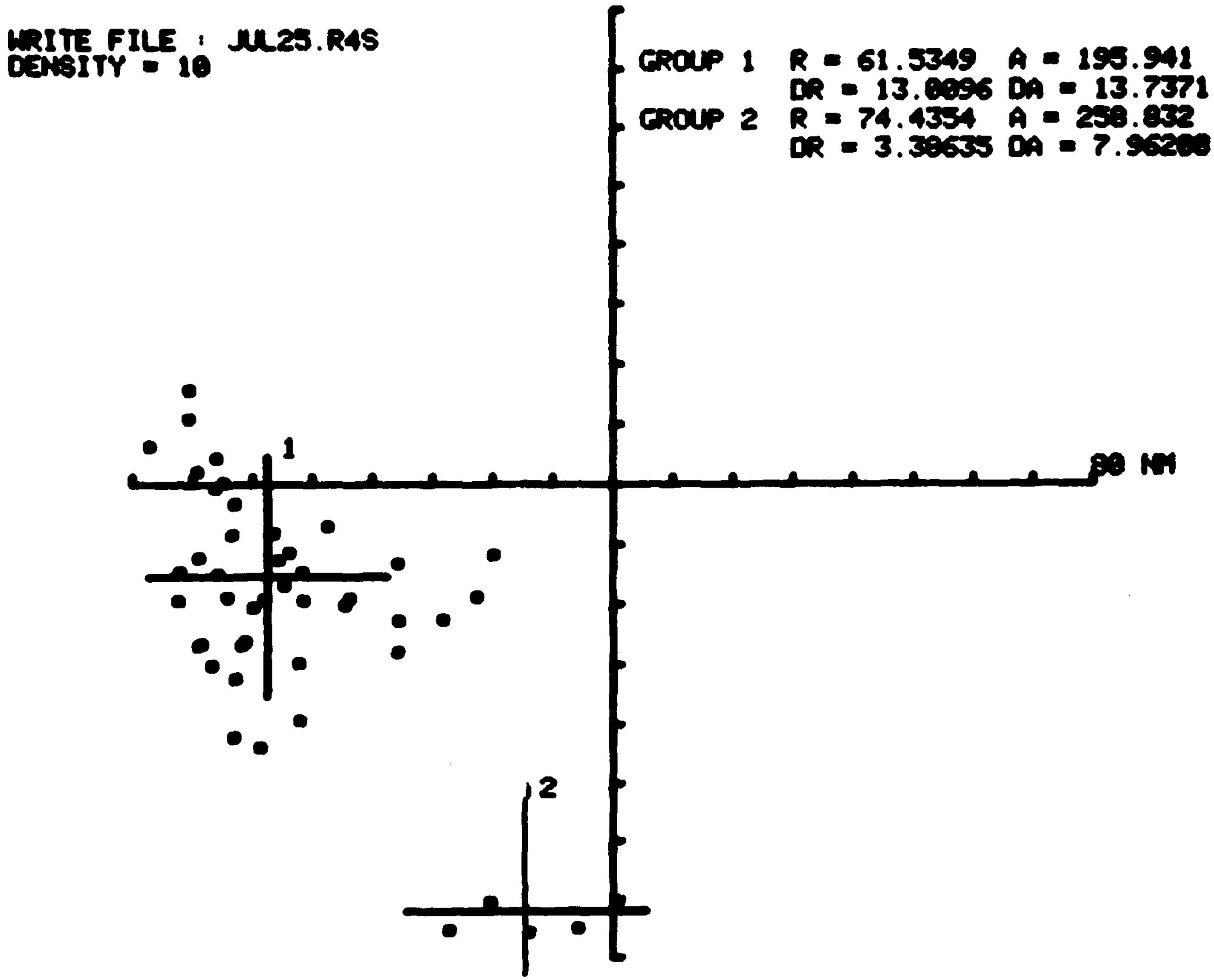

d. Centroids of Stormscope Electrical Activity

Figure B-4. Comparison of LDAR and Stormscope Electrical Activity, Run 4, 25 July 1978.

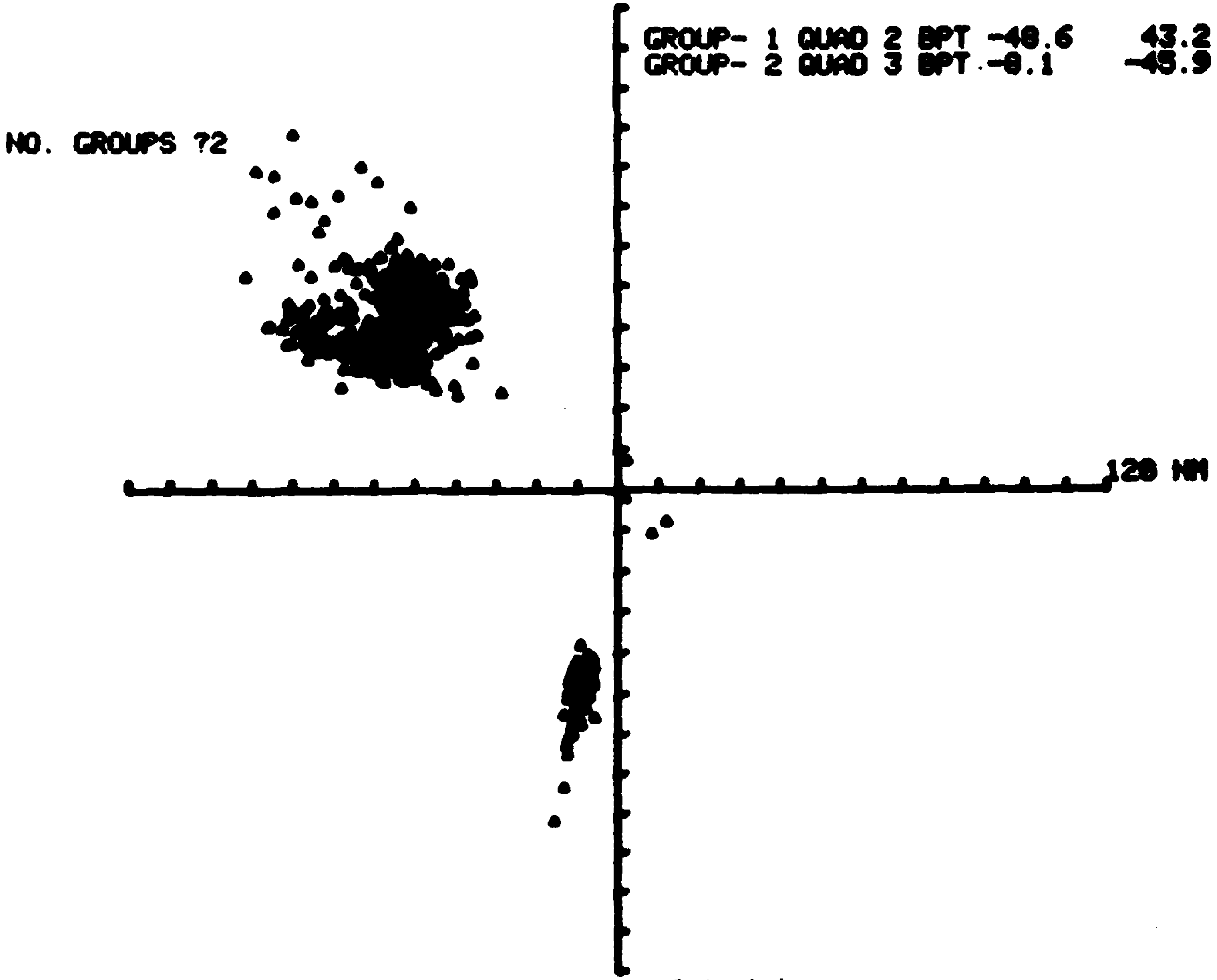

a. LDAR Electrical Activity

Figure B-5. Comparison of LDAR and Stormscope Electrical Activity, Run 1, 26 July 1978.

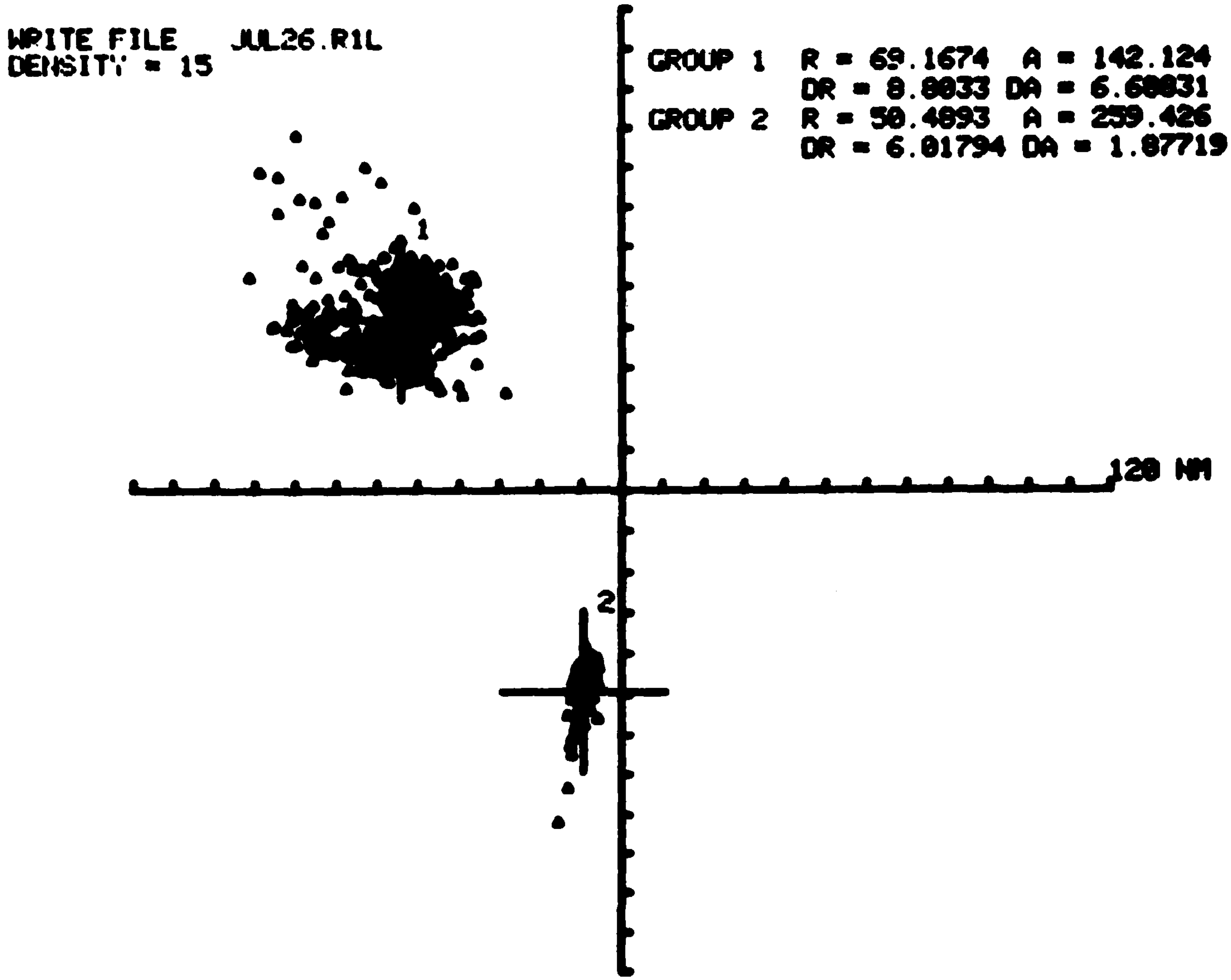

b. Centroids of LDAR Electrical Activity

Figure B-5. Comparison of LDAR and Stormscope Electrical Activity, Run 1, 26 July 1978.

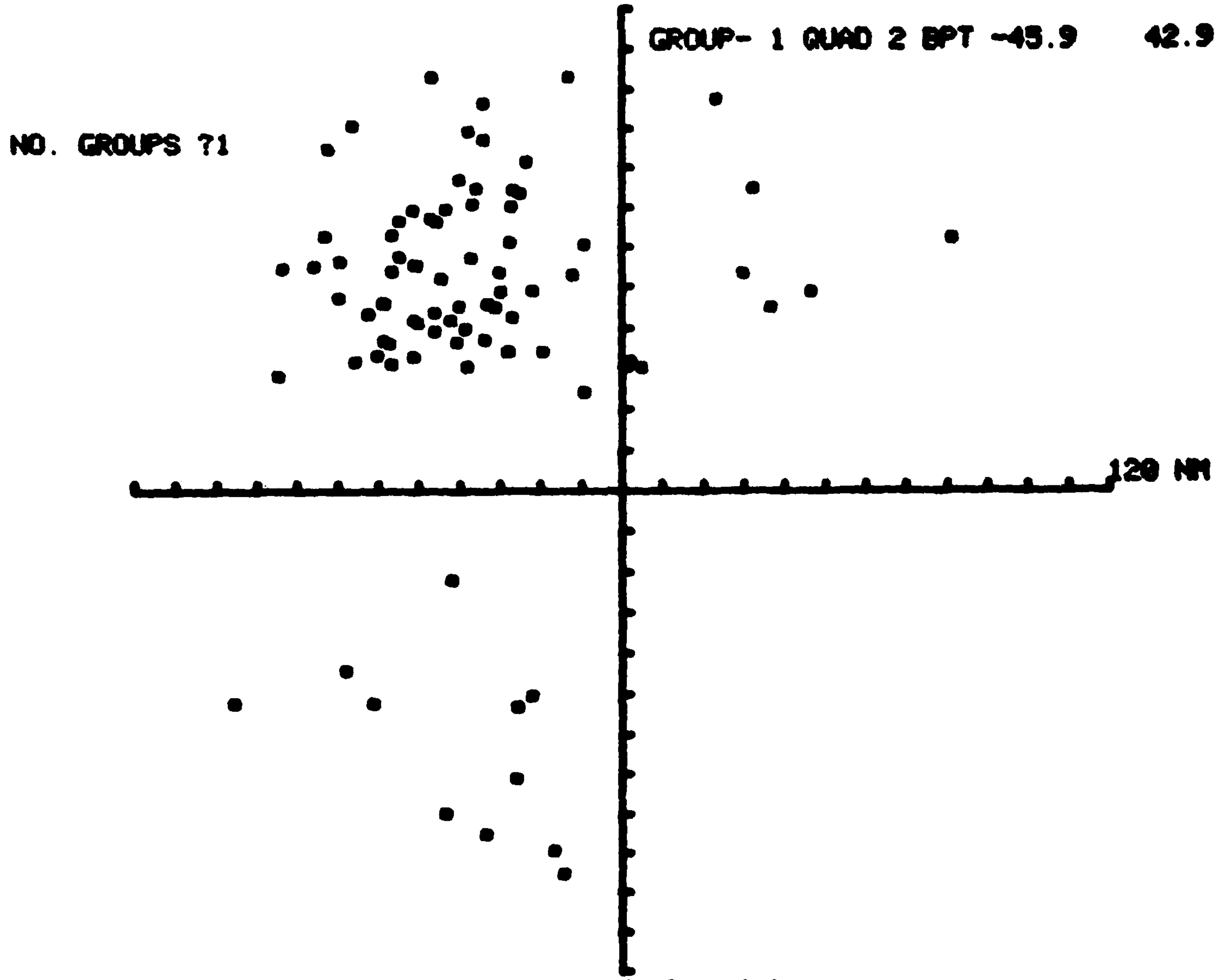

c. Stormscope Electrical Activity

Figure B-5. Comparison of LDAR and Stormscope Electrical Activity, Run 1, 26 July 1978.

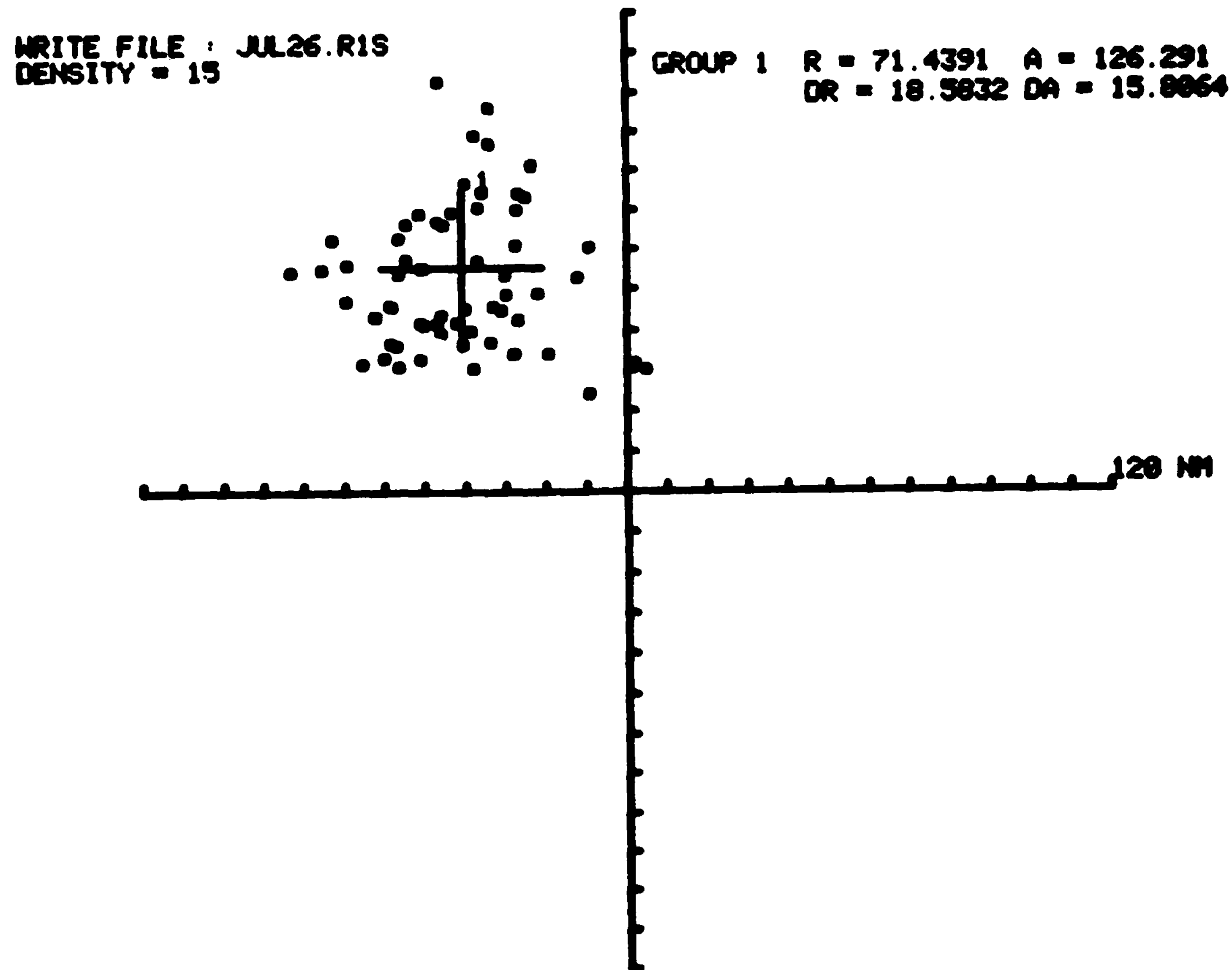

d. Centroids of Stormscope Electrical Activity

Figure B-5. Comparison of LDAR and Stormscope Electrical Activity, Run 1, 26 July 1978.

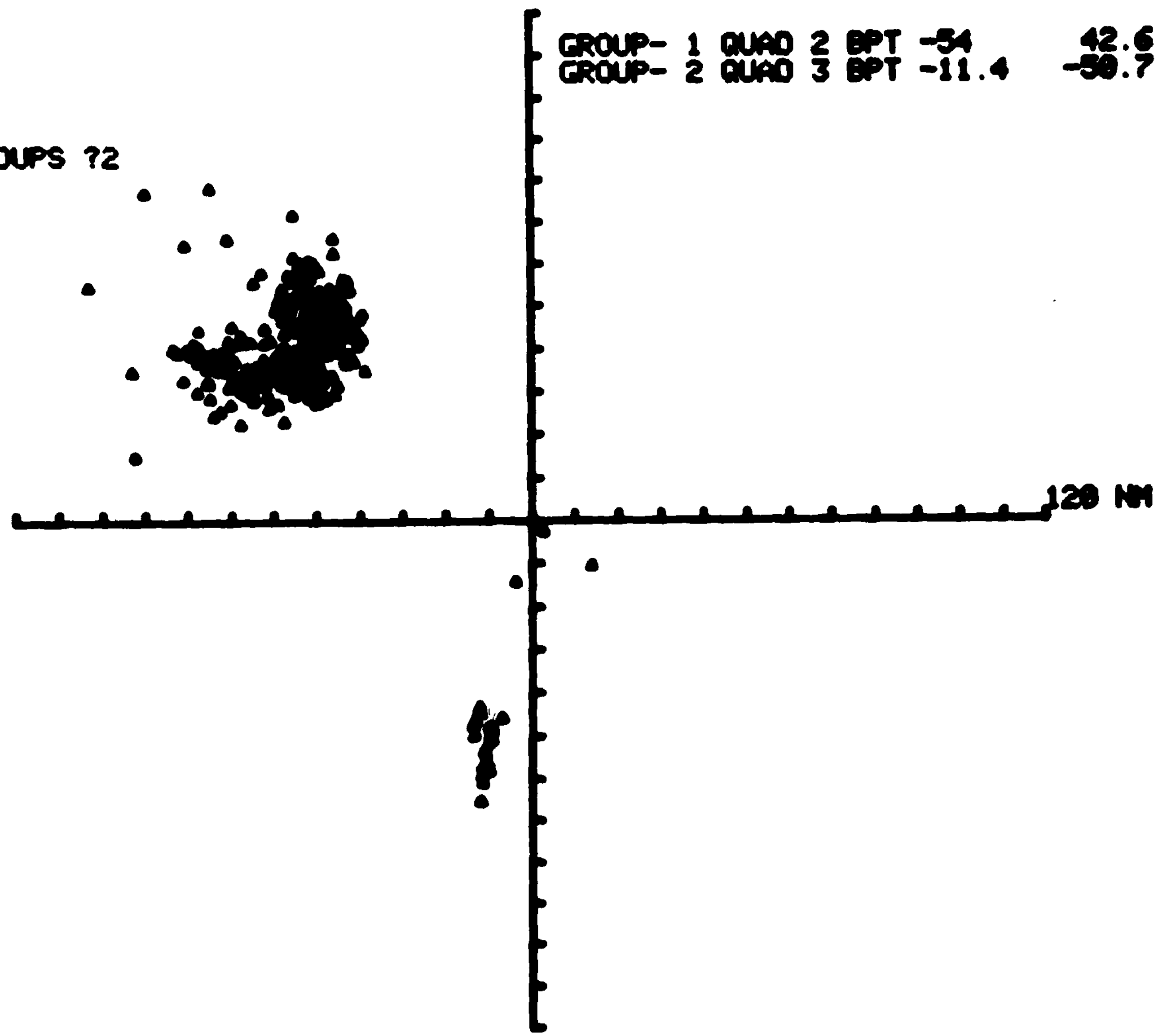

a. LDAR Electrical Activity

Figure B-6. Comparison of LDAR and Stormscope Electrical Activity, Run 2, 26 July 1978.

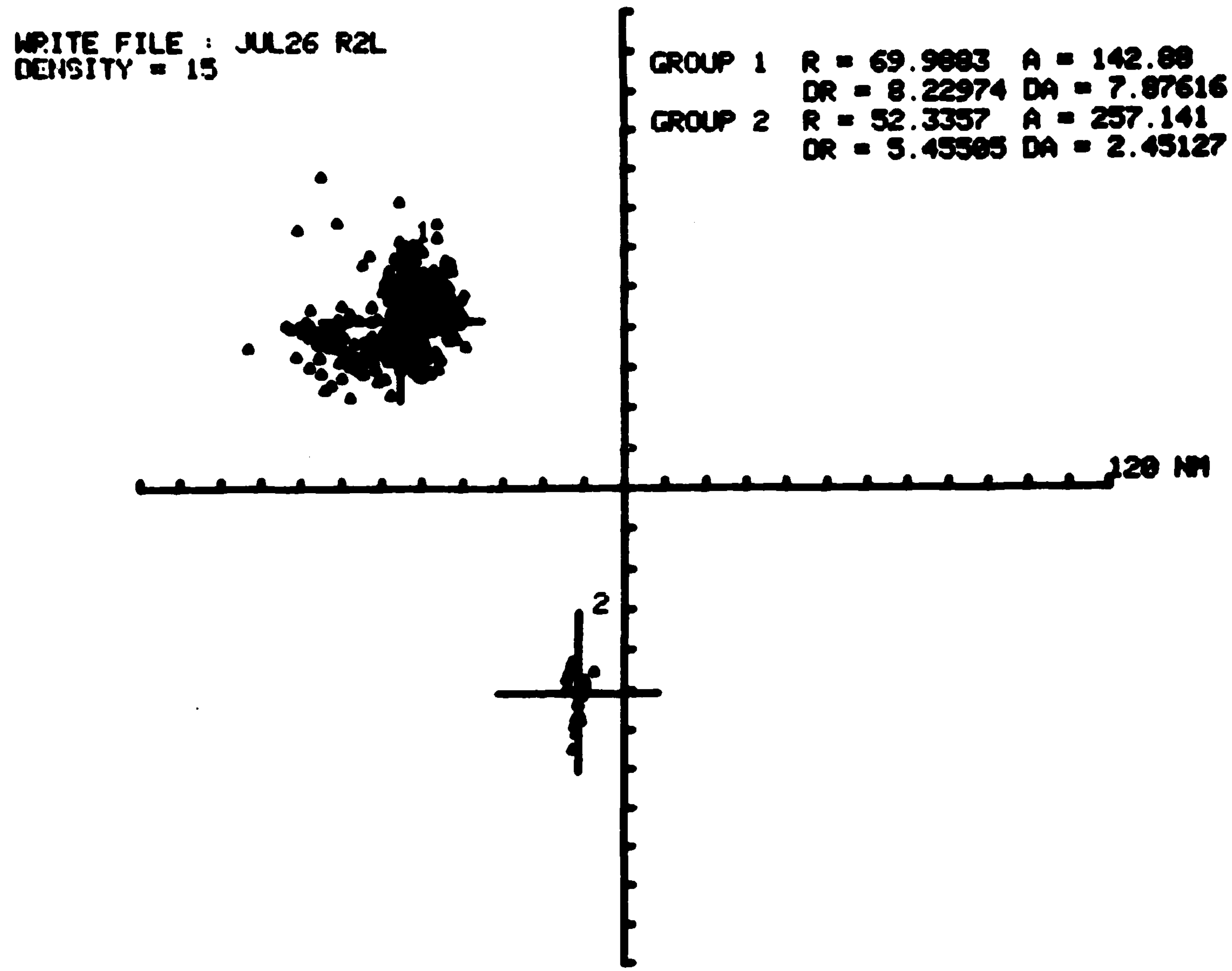

b. Centroids of LDAR Electrical Activity

Figure B-6. Comparison of LDAR and Stormscope Electrical Activity, Run 2, 26 July 1978.

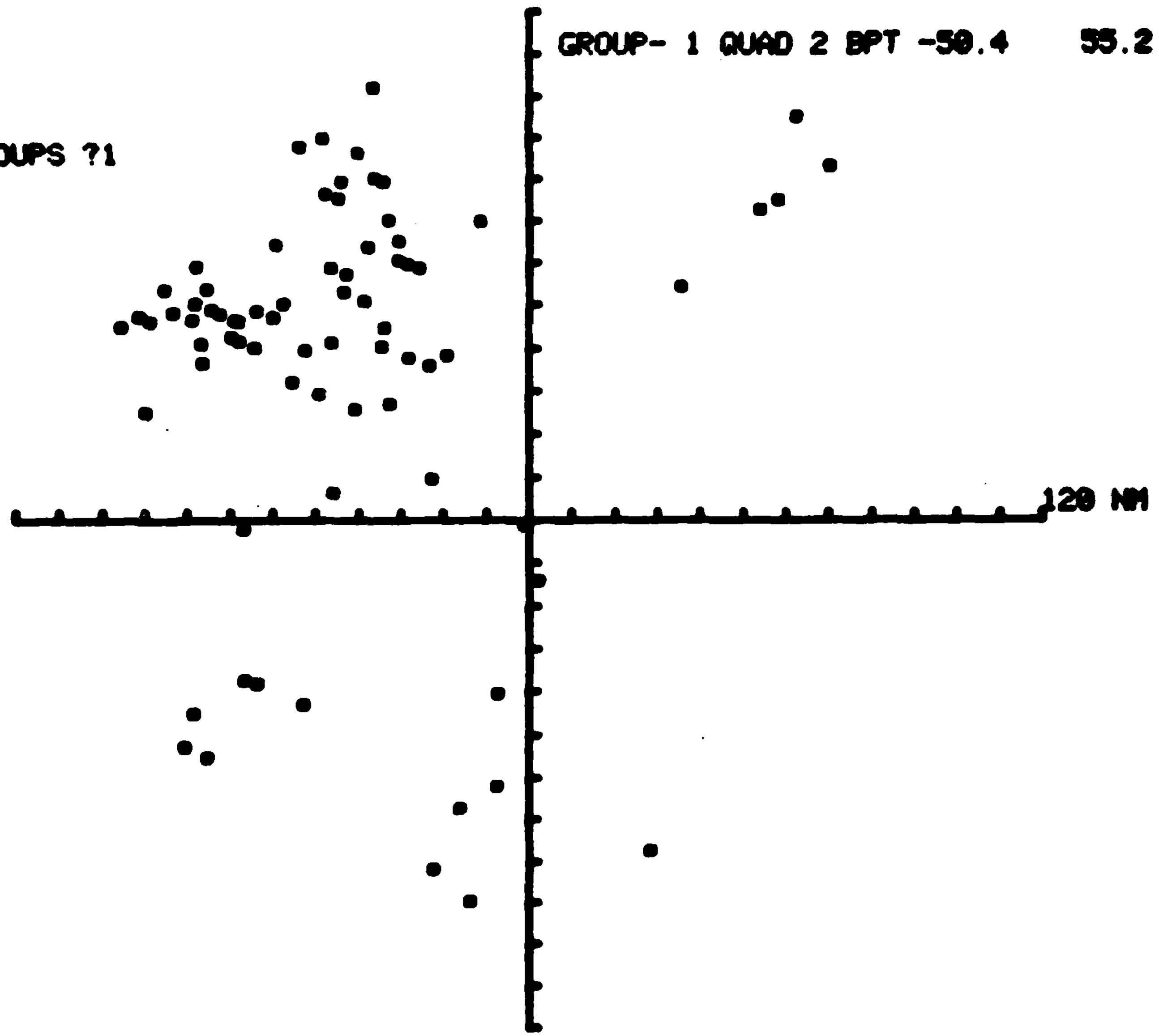

c. Stormscope Electrical Activity

Figure B-6. Comparison of LDAR and Stormscope Electrical Activity, Run 2, 26 July 1978.

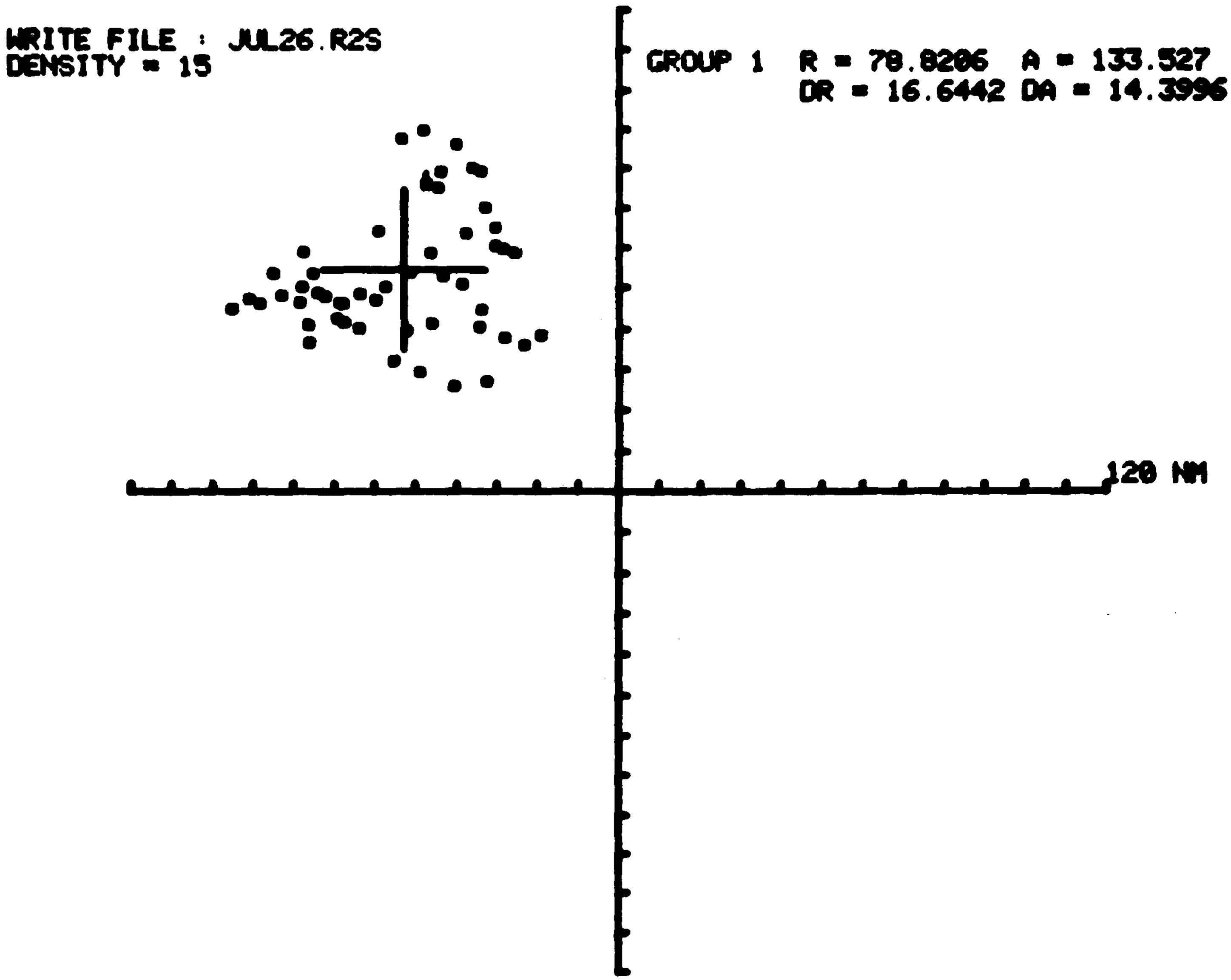

d. Centroids of Stormscope Electrical Activity

Figure B-6. Comparison of LDAR and Stormscope Electrical Activity, Run 2, 26 July 1978.

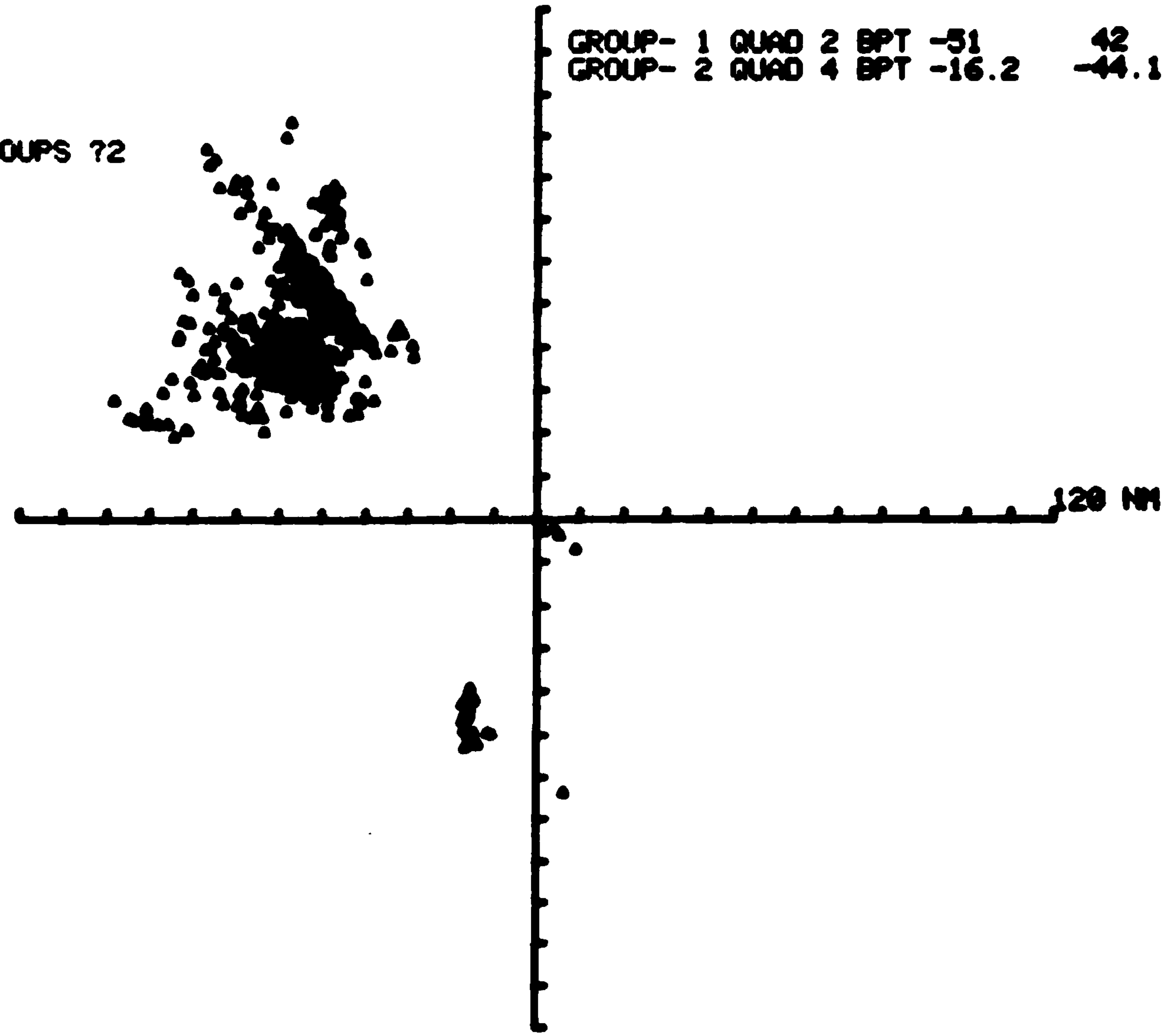

a. LDAR Electrical Activity

Figure B-7. Comparison of LDAR and Stormscope Electrical Activity, Run 3, 26 July 1978.

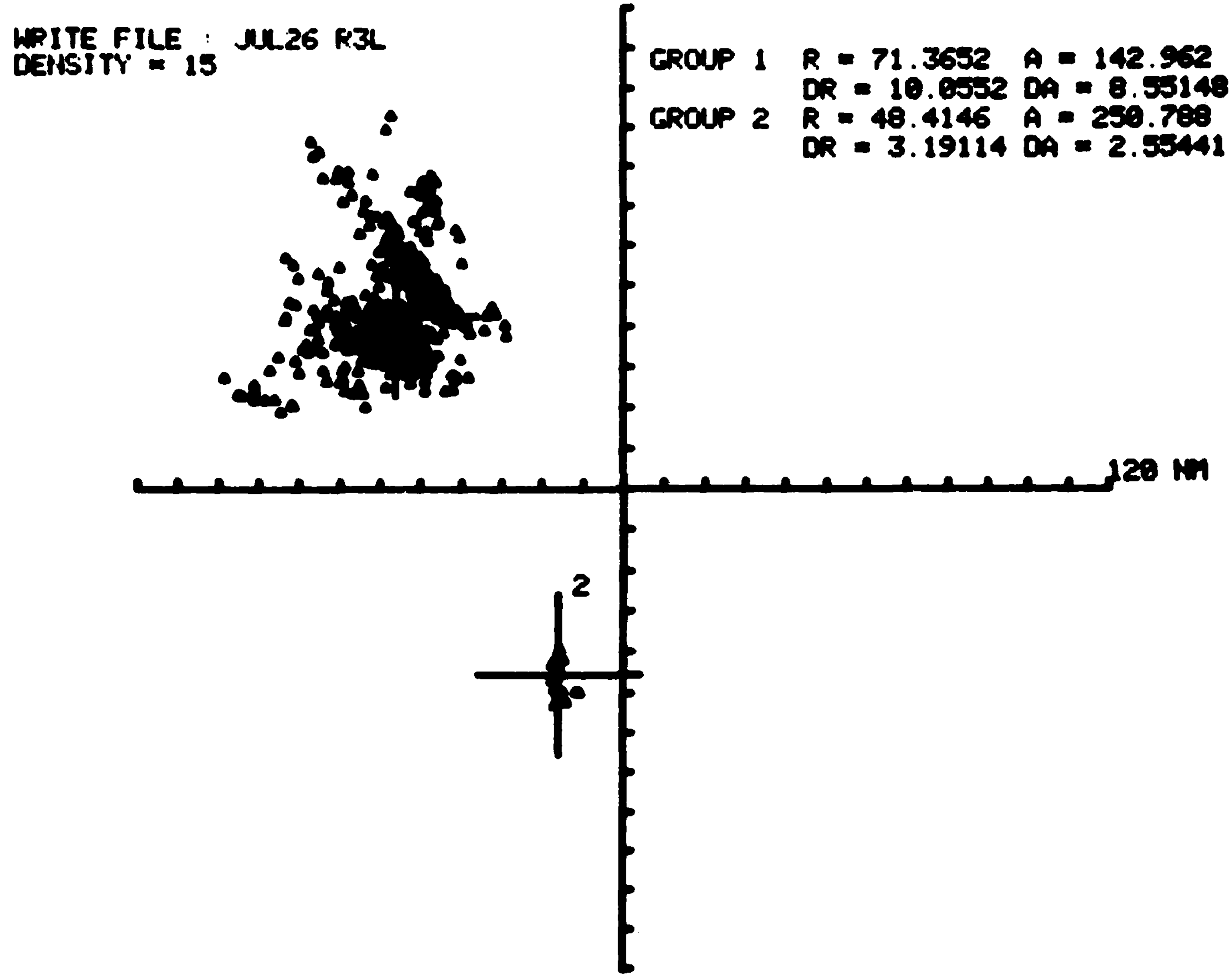

b. Centroids of LDAR Electrical Activity

Figure B-7. Comparison of LDAR and Stormscope Electrical Activity, Run 3, 26 July 1978.

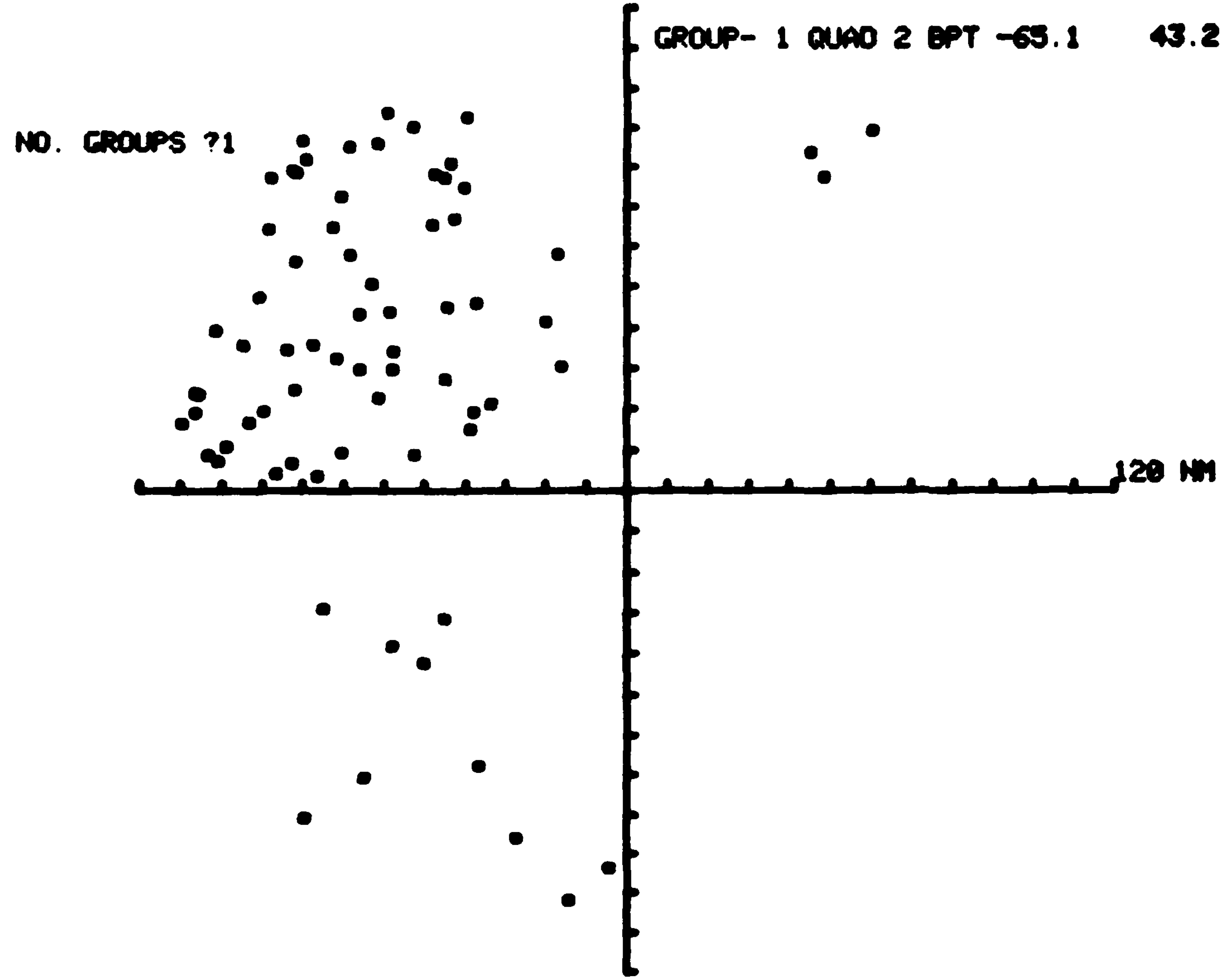

c. Stormscope Electrical Activity

Figure B-7. Comparison of LDAR and Stormscope Electrical Activity, Run 3, 26 July 1978.

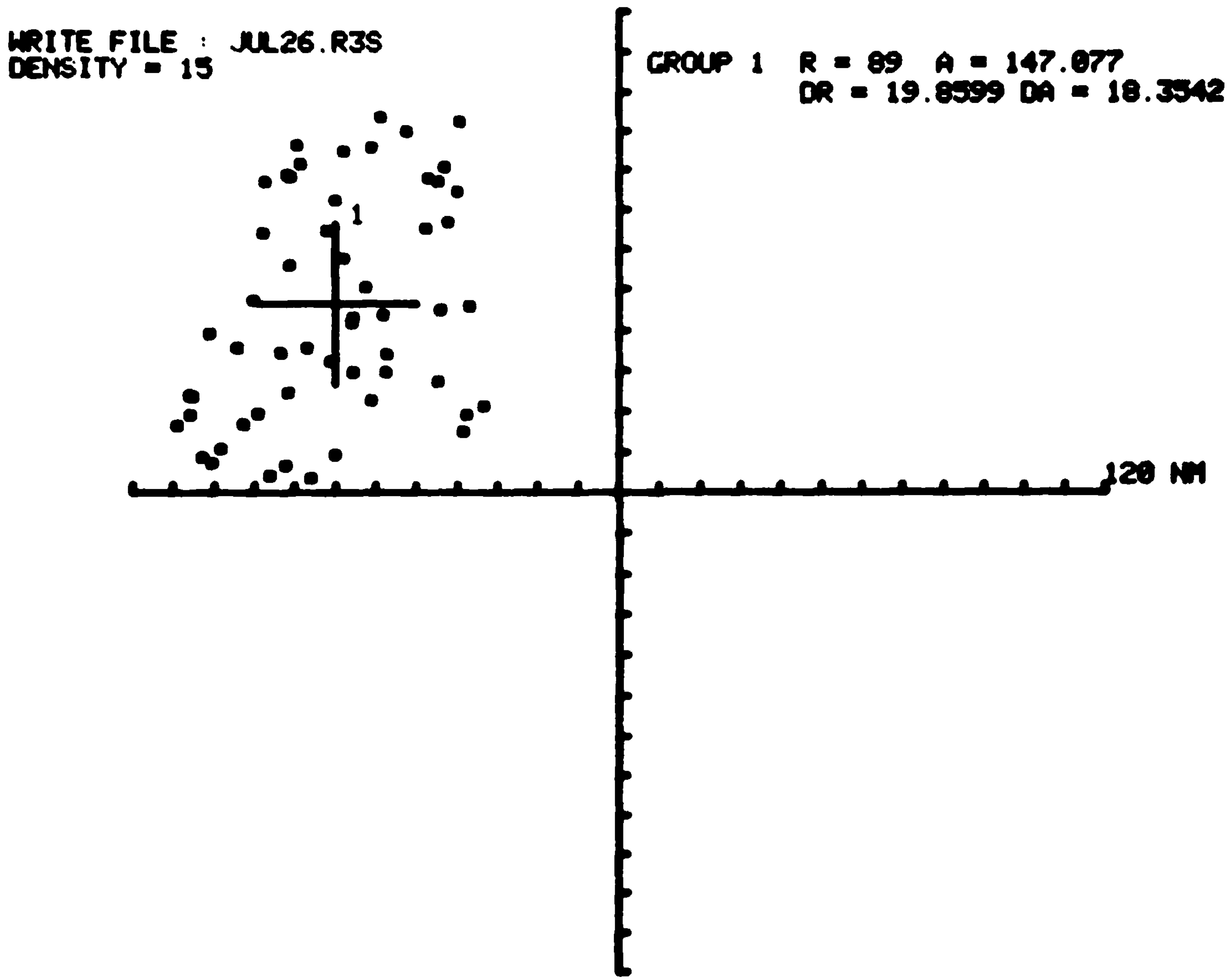

d. Centroids of Stormscope Electrical Activity

Figure B-7. Comparison of LDAR and Stormscope Electrical Activity, Run 3, 26 July 1978.

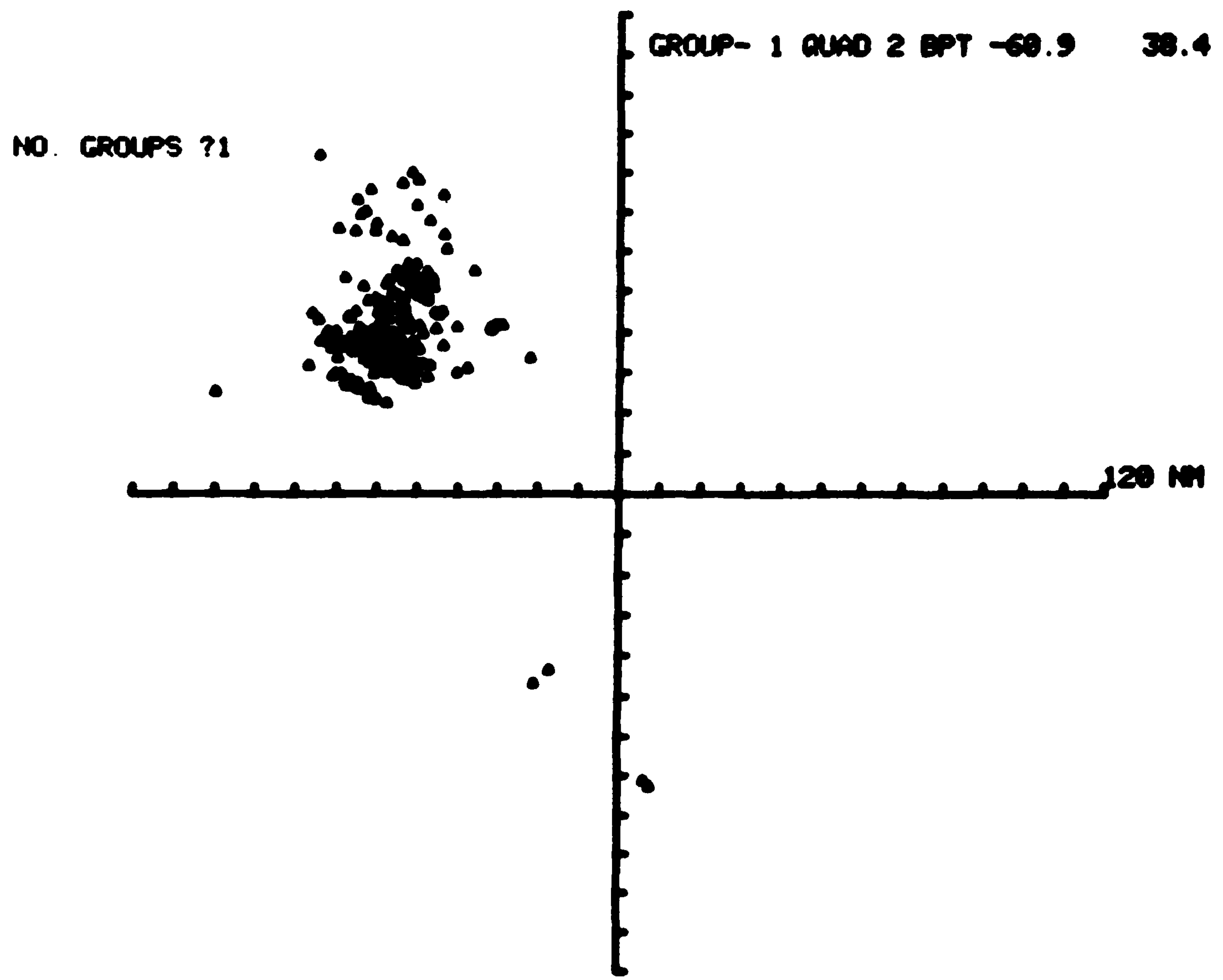

a. LDAR Electrical Activity

Figure B-8. Comparison of LDAR and Stormscope Electrical Activity, Run 4, 26 July 1978.

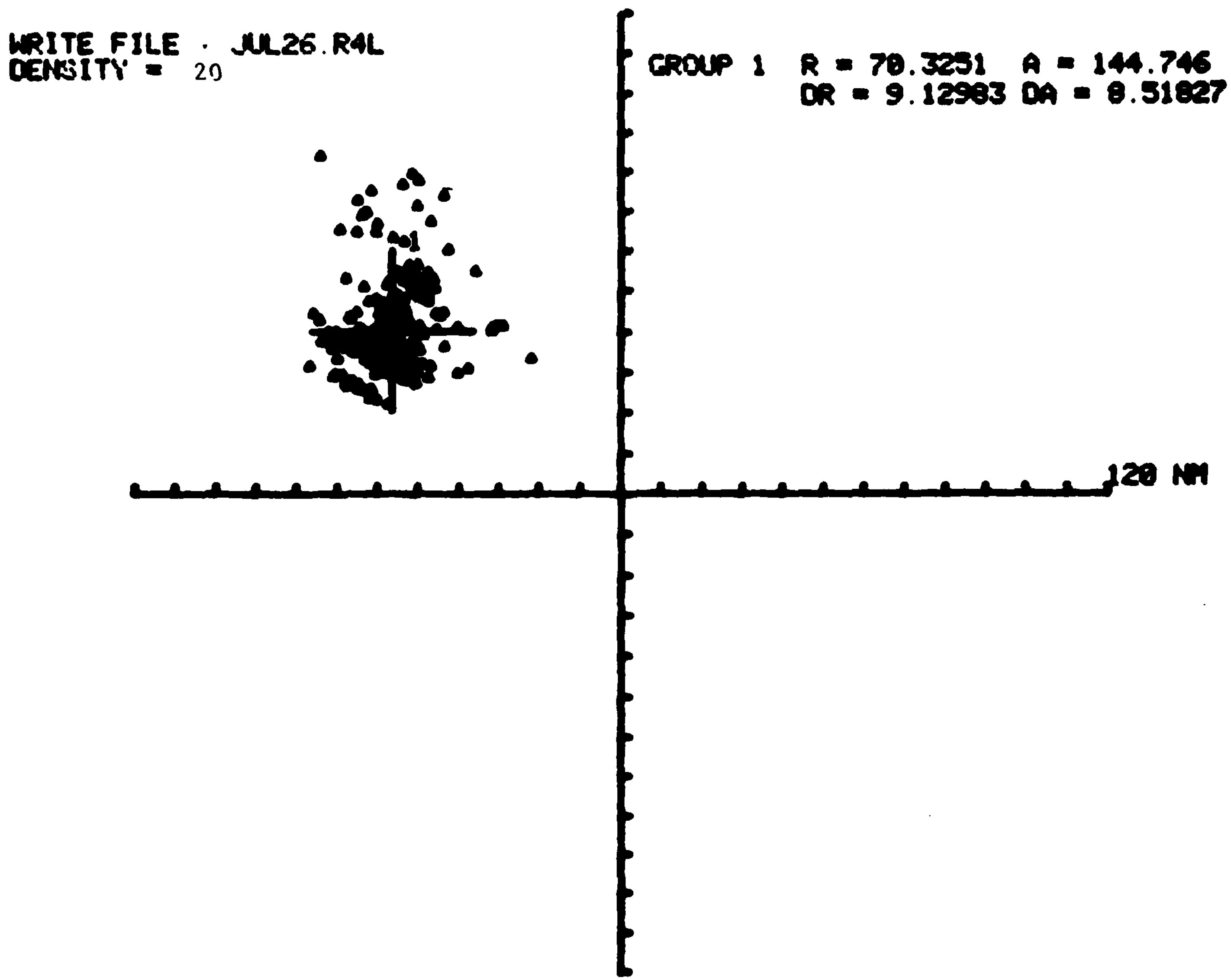

b. Centroids of LDAR Electrical Activity

Figure B-8. Comparison of LDAR and Stormscope Electrical Activity, Run 4, 26 July 1978.

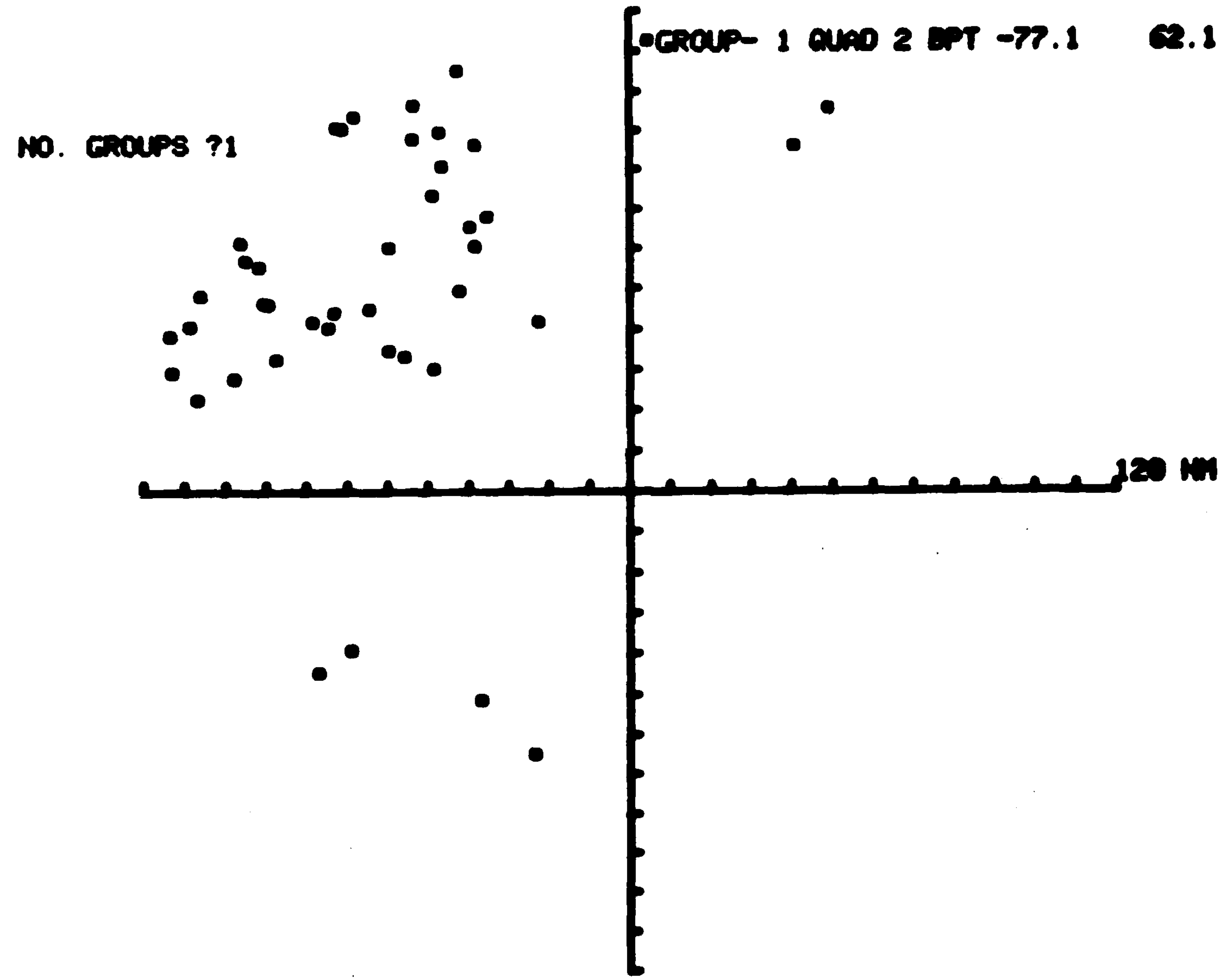

c. Stormscope Electrical Activity

Figure B-8. Comparison of LDAR and Stormscope Electrical Activity, Run 4, 26 July 1978.

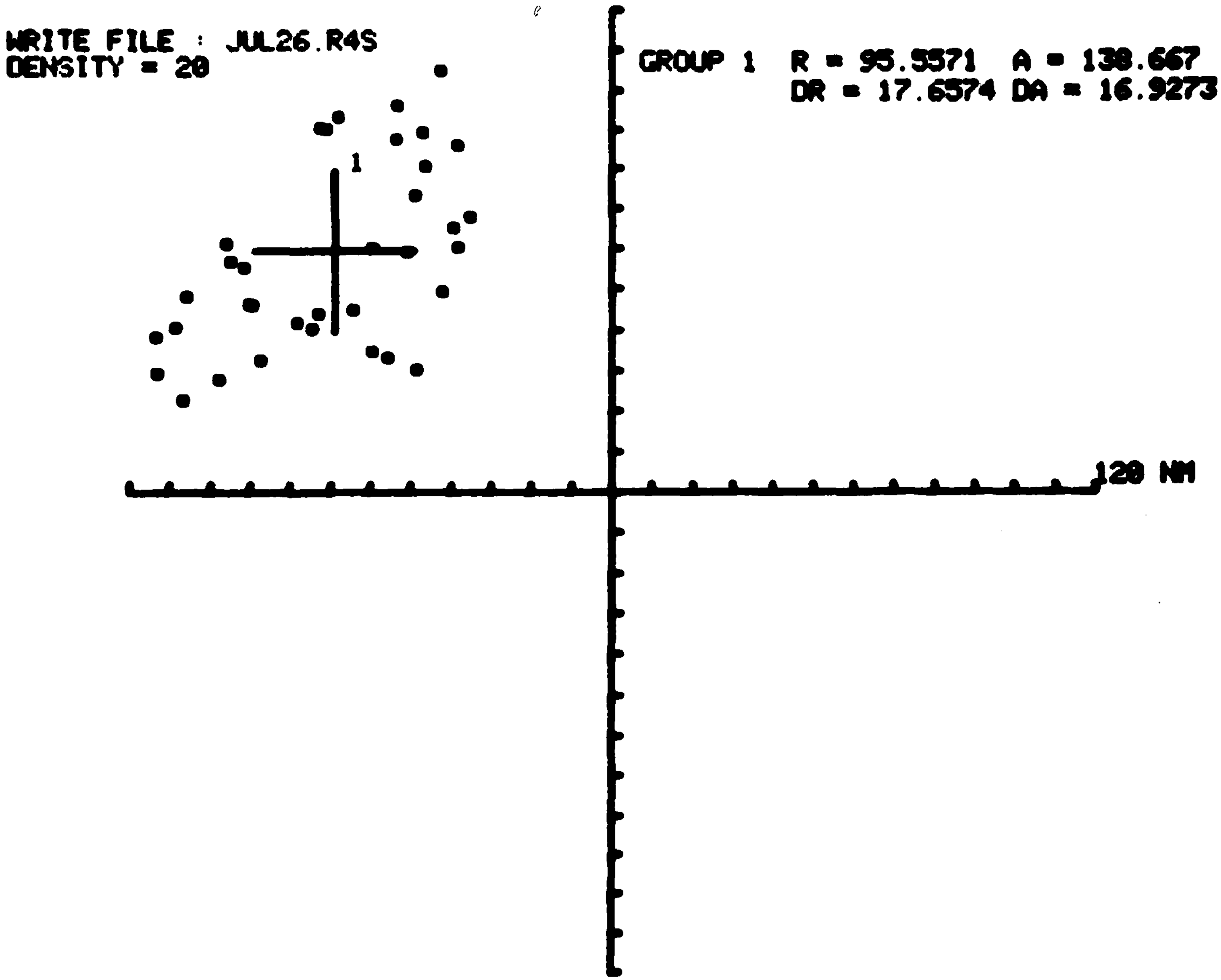

d. Centroids of Stormscope Electrical Activity

Figure B-8. Comparison of LDAR and Stormscope Electrical Activity, Run 4, 26 July 1978.

APPENDIX C

COMPARISON OF OVERLAP AREAS

LDAR VS STORMSCOPE

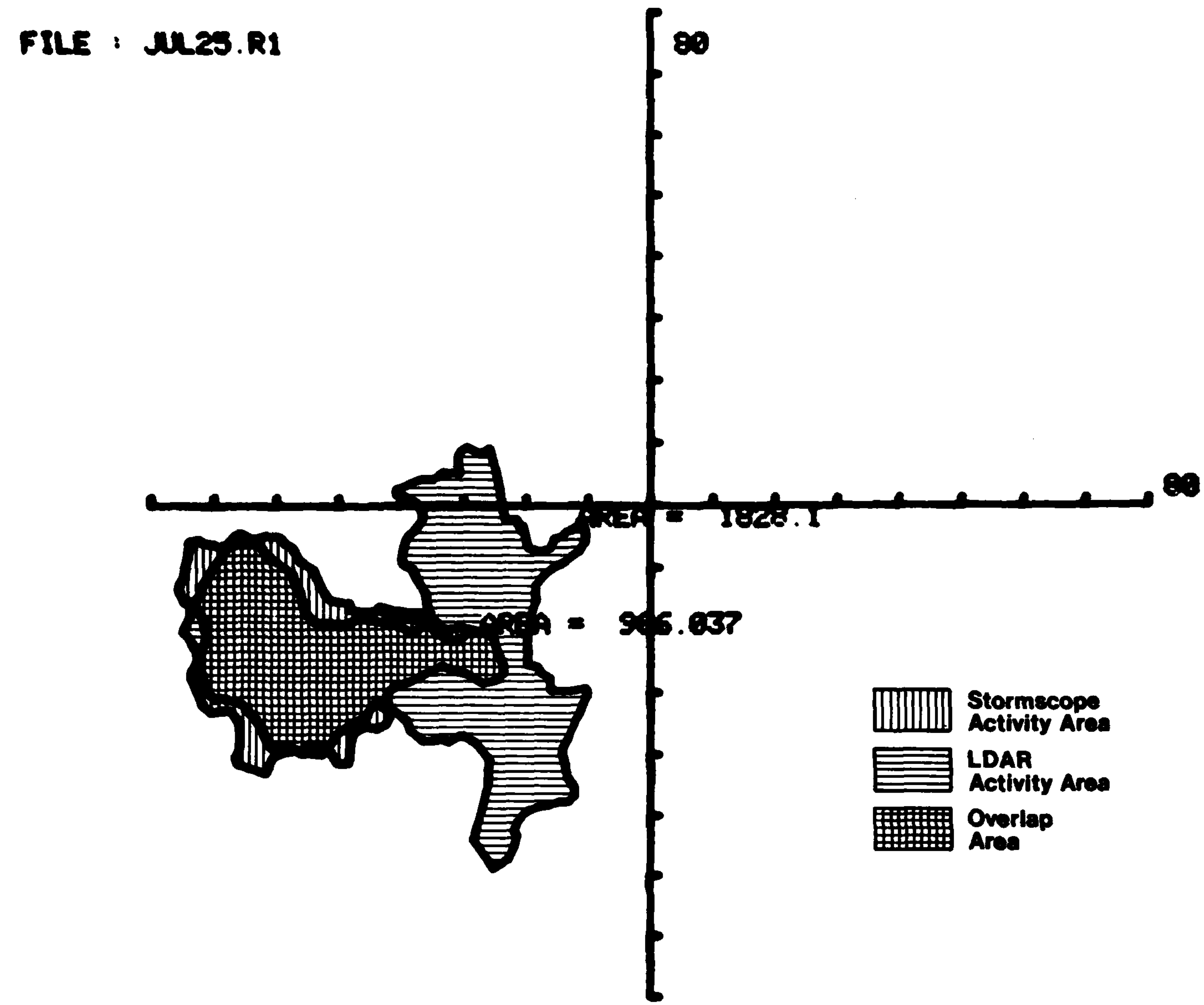

C-1. Overlap Areas - LDAR vs Stormscope
Run 1, 25 July 1978

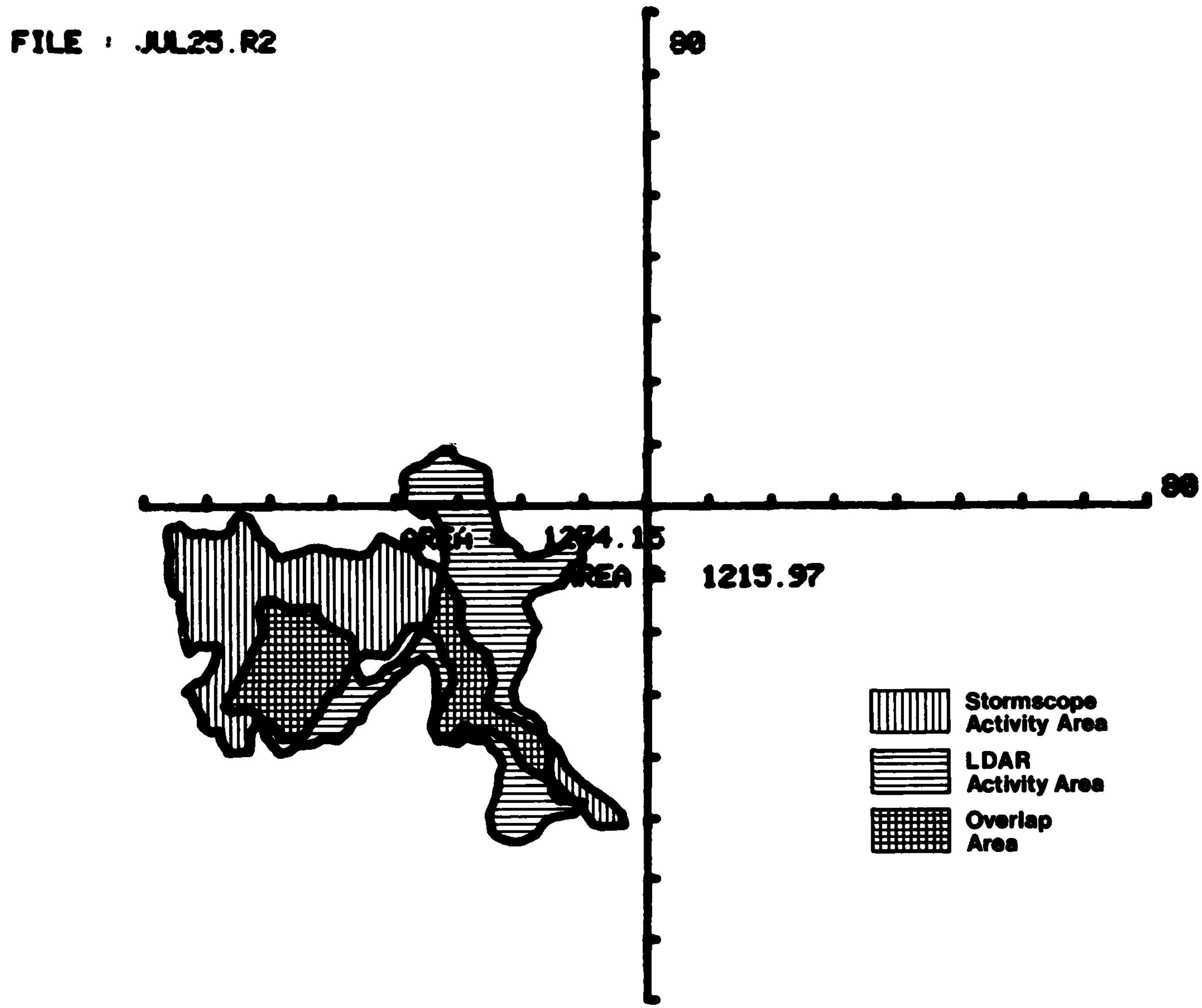

C-2. Overlap Areas - LDAR vs Stormscope
Run 2, 25 July 1978

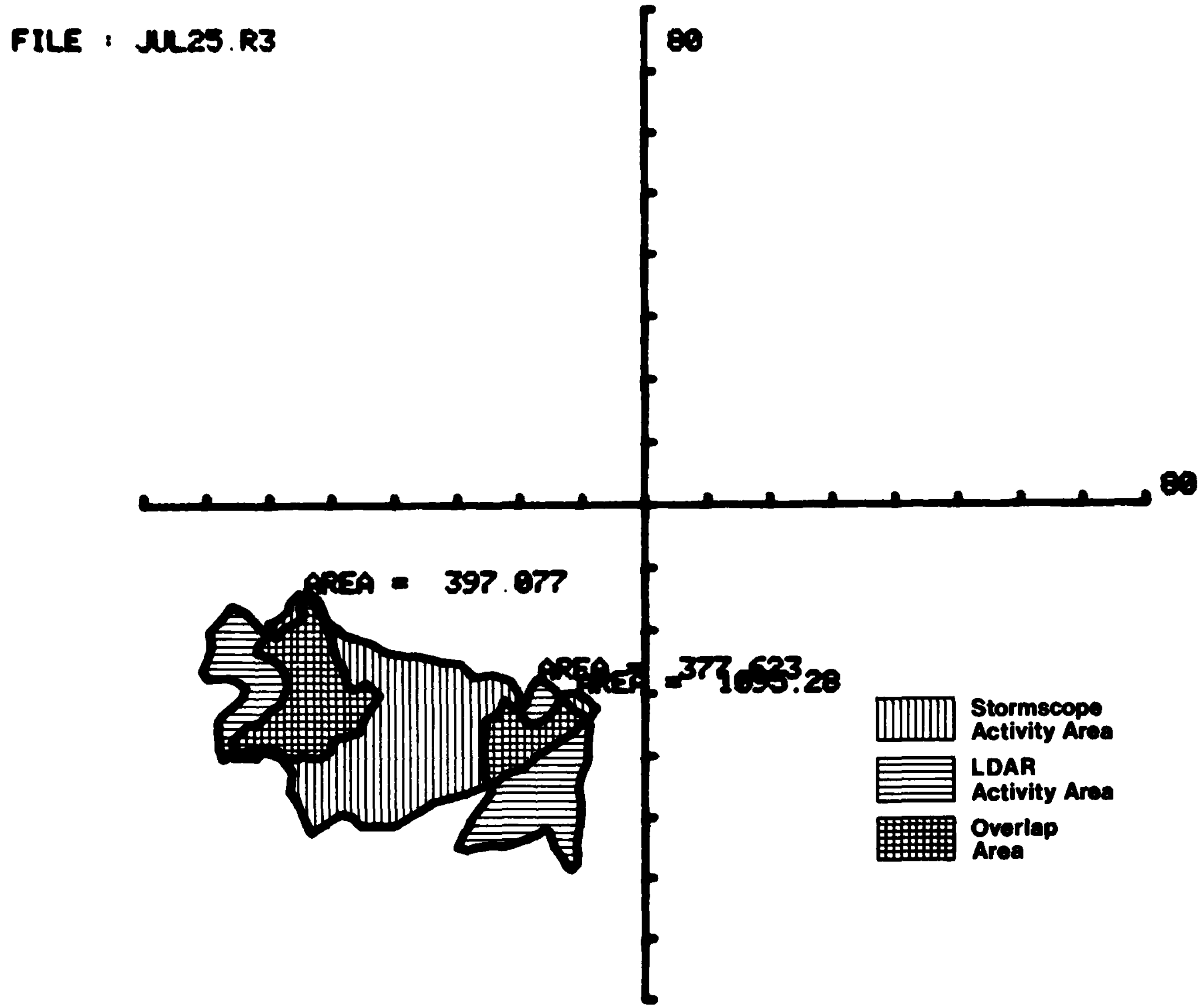

C-3. Overlap Areas - LDAR vs Stormscope
Run 3, 25 July 1978

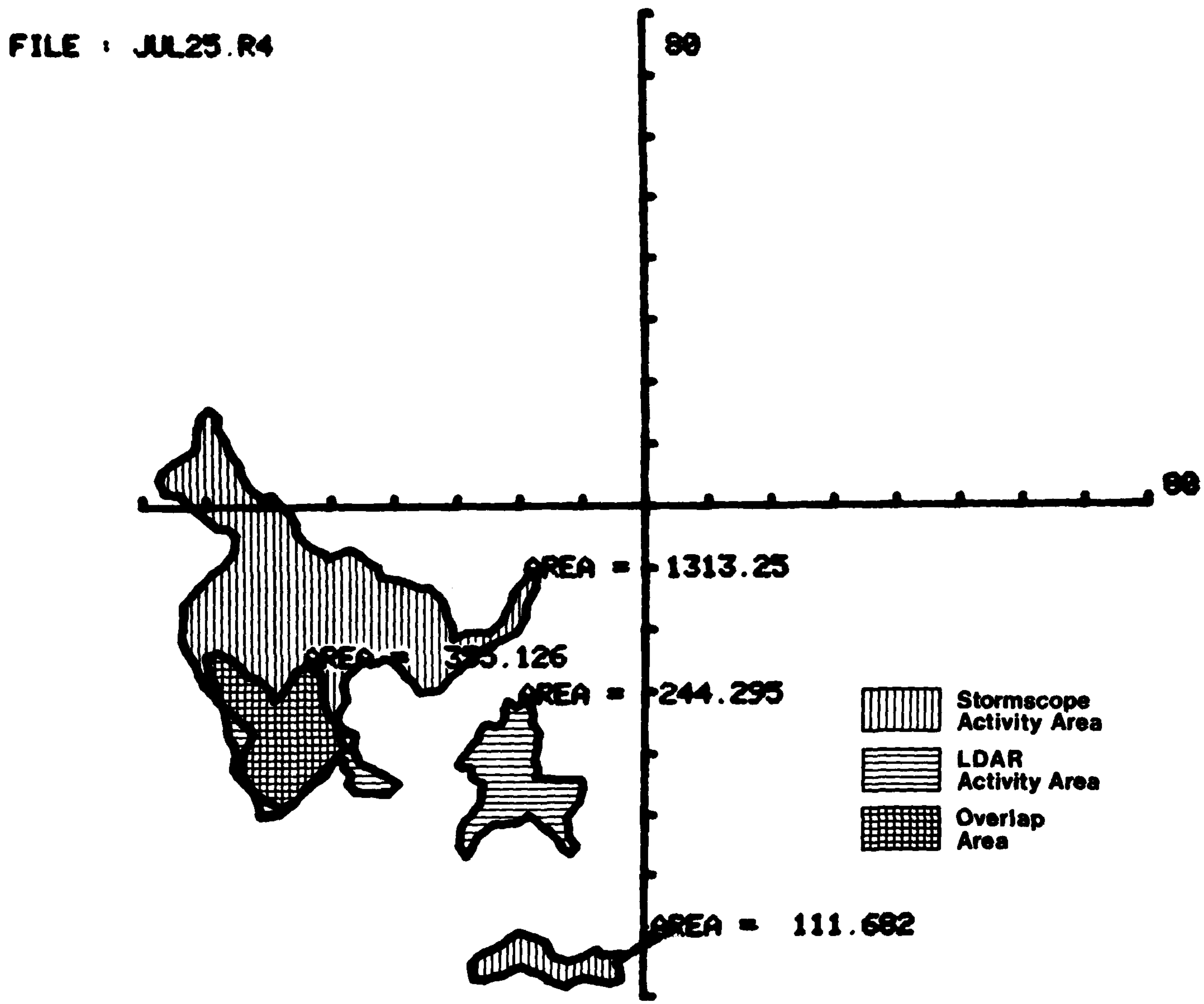

C-4. Overlap Areas - LDAR vs Stormscope
Run 4, 25 July 1978

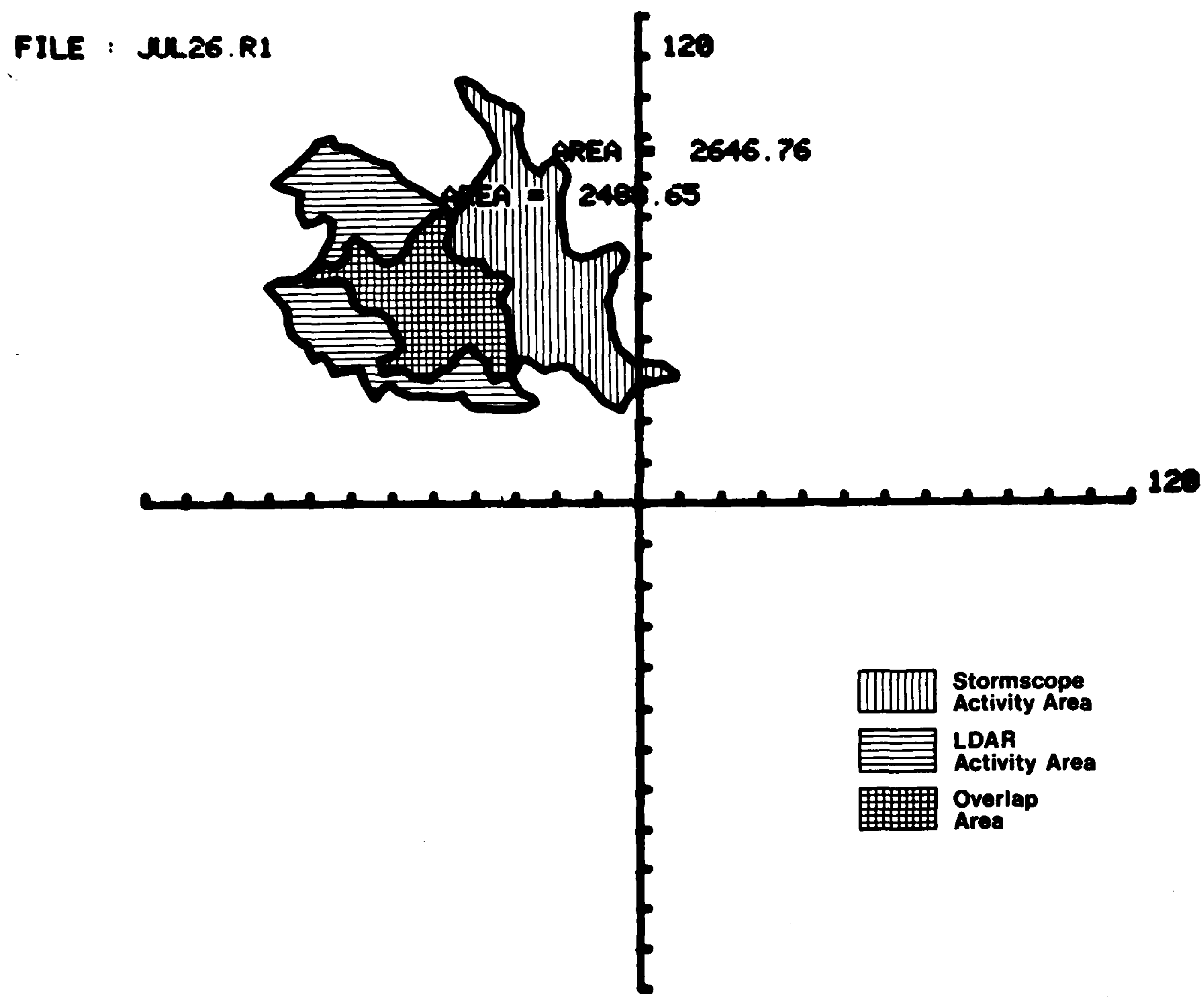

C-5. Overlap Areas - LDAR vs Stormscope
Run 1, 26 July 1978

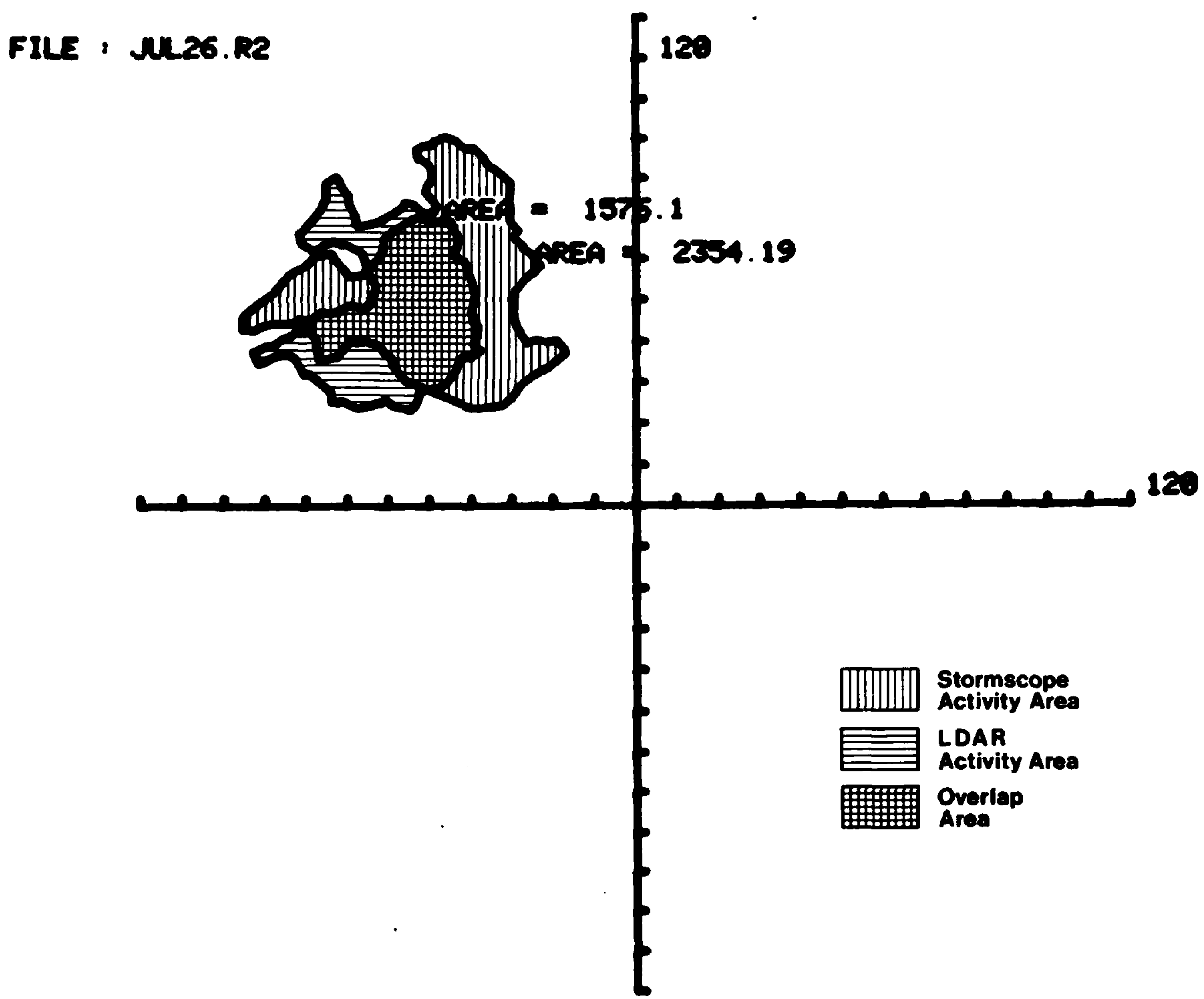

C-6. Overlap Areas - LDAR vs Stormscope
Run 2, 26 July 1978

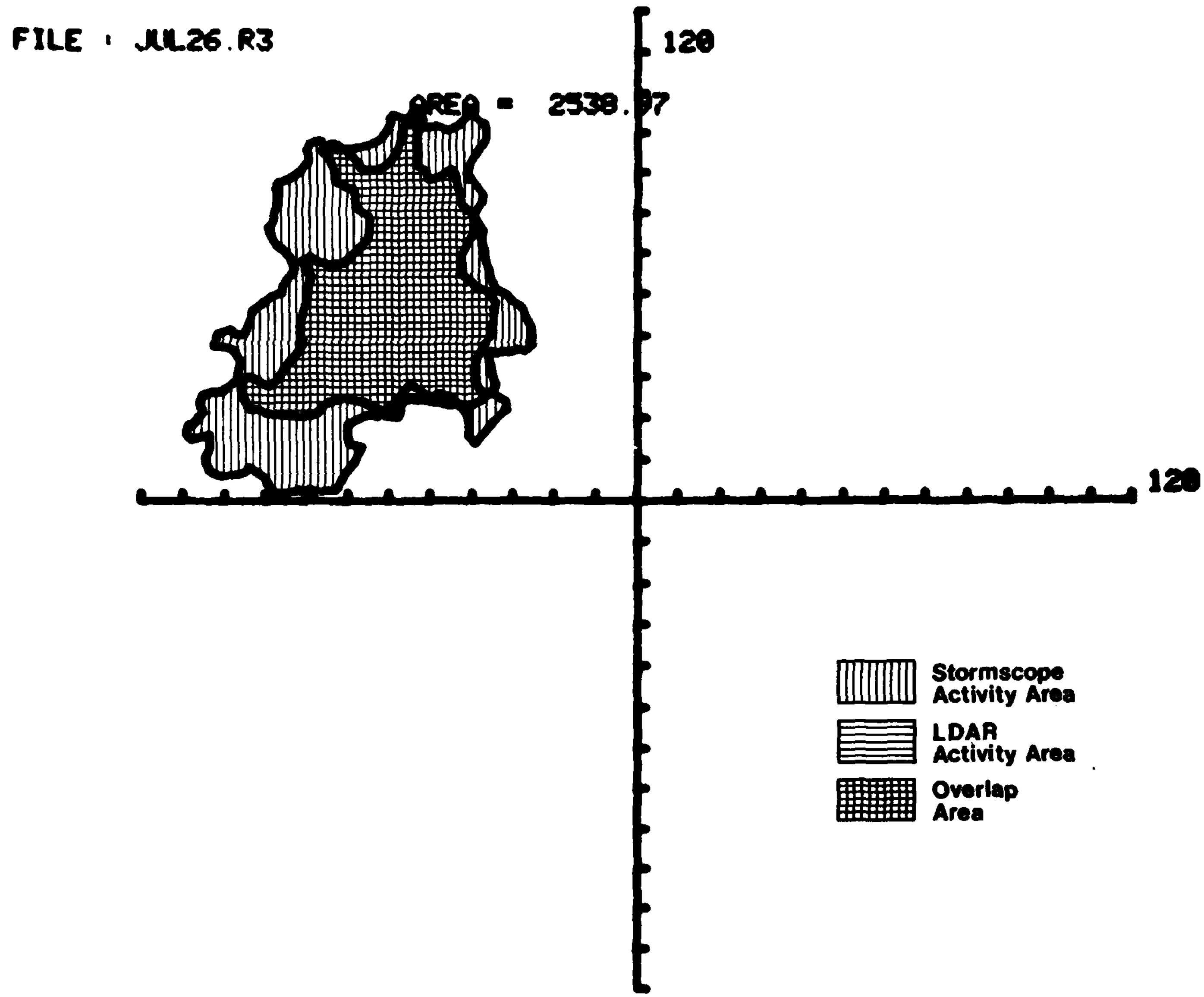

C-7. Overlap Areas - LDAR vs Stormscope
Run 3, 26 July 1978

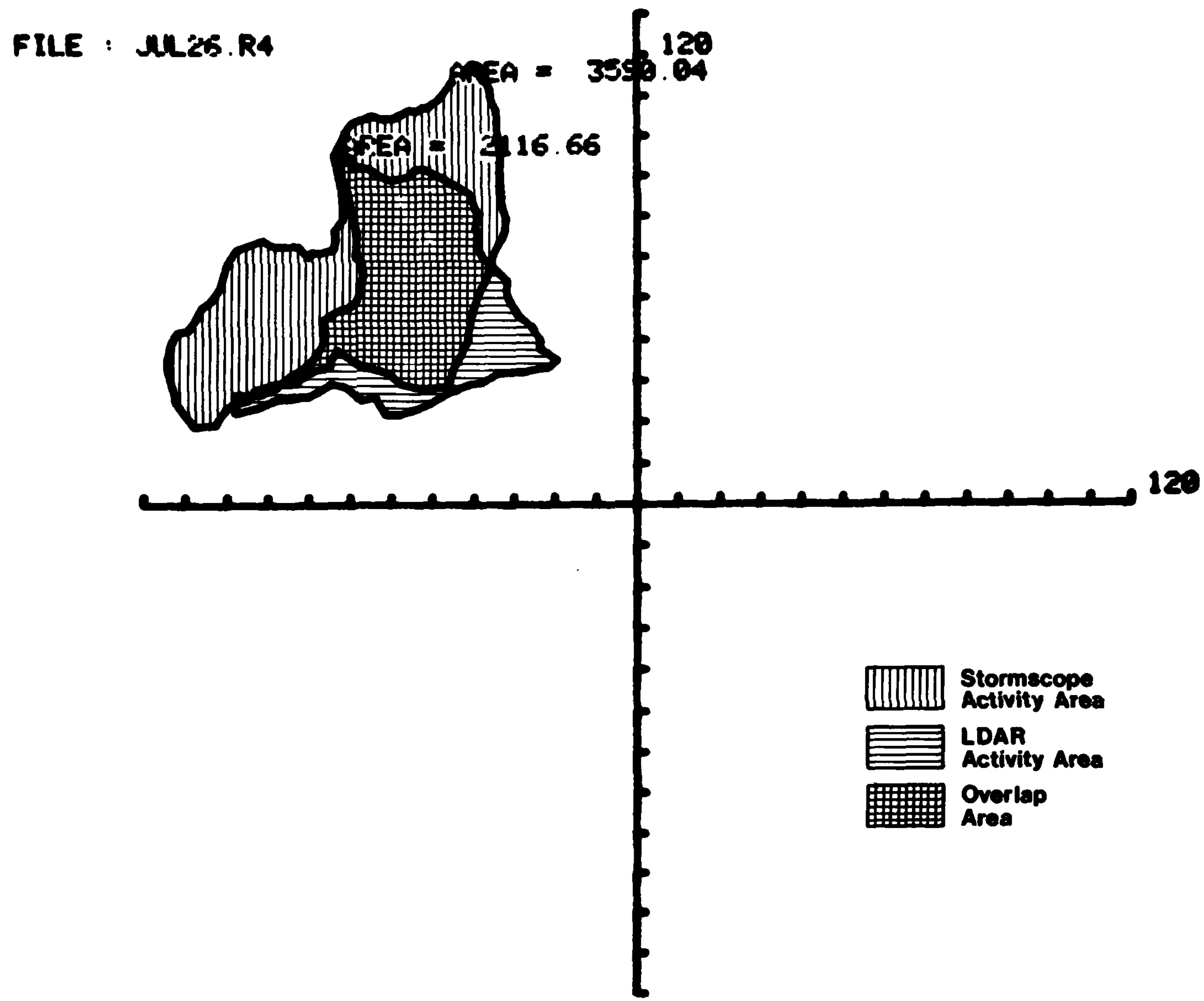

C-8. Overlap Areas - LDAR vs Stormscope
Run 4, 26 July 1978

ADDENDUM

On 27 July at approximately 15:28 EDT the instrumented T-39 aircraft described in this report was flown into a thin cloud layer at the freezing level to determine whether precipitation static would affect Stormscope's performance. The aircraft evidently went into corona during this time, causing an immediate loud squeal on the radio headset which impaired communications. The digital time code generator started counting backward and forward randomly, the digital radar display stopped functioning, the digital Stormscope display populated rapidly with a random display of dots and the digital PDP 11/05 computer stopped functioning and required reloading of all software before it would operate properly again. The corona condition lasted for approximately three minutes, during which time none of the above systems was operational.

Figure A below illustrates the Stormscope and radar displays just prior to the corona condition. Figures B, C and D show the effects of the corona on the Stormscope, radar and time code generator displays.

Figure A

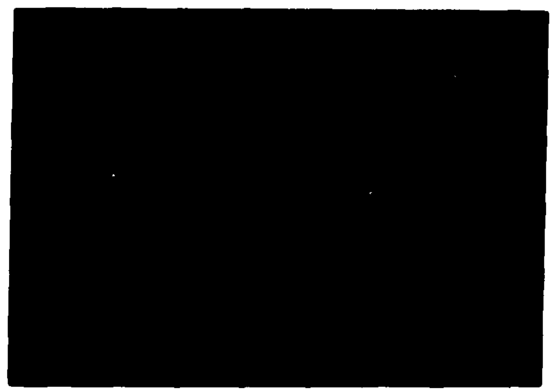

Figure B

Figure C

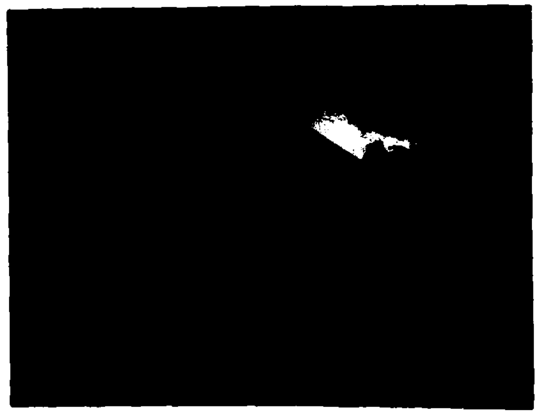

Figure D

An AR-700 recorder had also been installed on the aircraft. On reviewing the recorder data after landing, it was found that the recordings of aircraft heading, airspeed and altitude had been affected, even though coaxial lines ran from all the sensors to the recorder. A section of the Visicorder chart is shown in Figure E.

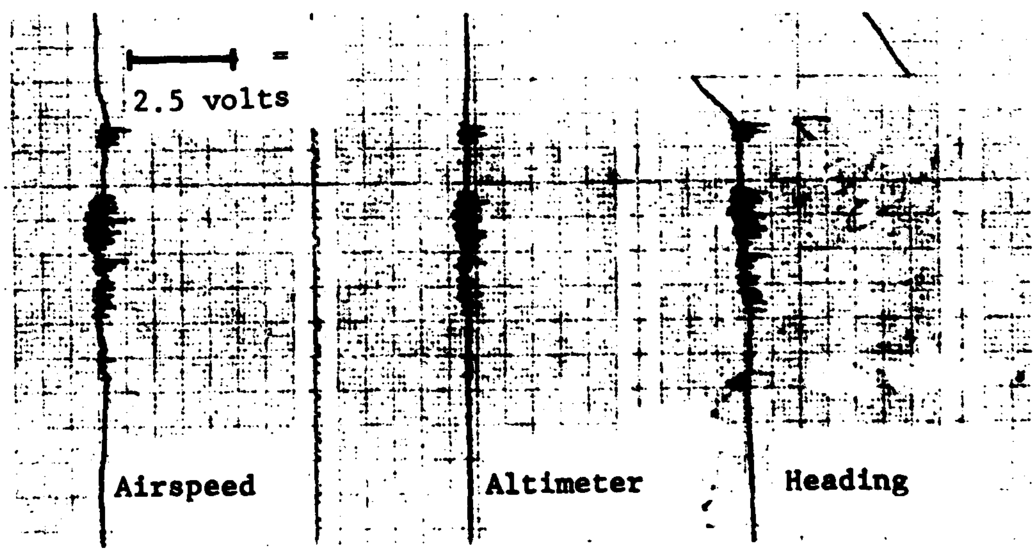

Figure E

REFERENCES

1. Corn, Philip B. Maj.(USAF), Lightning Hazards to Aircraft, Air Force Flight Dynamics Laboratory, Paper presented at the Second Annual Workshop on Meteorological and Environmental Inputs to Aviation Systems, March 28-30, 1978, University of Tennessee Space Institute, Sponsored by NASA, NOAA and FAA.

2. Poehler, H.A., A Preliminary Test of the Application of the Lightning Detection and Ranging System (LDAR) as a Thunderstorm Warning and Location Device for the FAA Including a Correlation with Updrafts, Turbulence, and Radar Precipitation Echoes, RCA Service Co., NASA Contractor Report CR-154629, December 1978.

3. Ryan Stormscope Weather Mapping System, How it Operates, Ryan Stormscope, 4800 Evanswood Dr., Columbus, Ohio, product leterature.

4. Mangold, V.L., Evaluation of Stormscope - Phase I, AFFDL/FES, January, 1978.

5. Poehler, H.A., An Accuracy Analysis of the LDAR System, Federal Electric Corporation, Report No. FEC-7146, March 1977.

6. Lennon, K., LDAR III - System Description and Performance Objectives, Federal Electric Corporation, RF Systems Branch, Kennedy Space Center, 26 April 77, (unpublished).

7. Uman, M.A., Lightning, McGraw Hill, Inc., 1969, pp. 104-106.

8. Beyer, W.H., Standard Mathematical Tables, 25th Edition, CRC Press, Inc., 1978, pp. 284, 506.

*U.S.Government Printing Office: 1980 — 657-084/770

E

D

FI

9

D